The 20S Proteasome from *Thermoplasma acidophilum*

by

Jose O. Nazario

Submitted in partial fulfillment of the requirements

for the degree of Doctor of Philosophy

Dissertation Advisor: Dr. Vernon E. Anderson

Department of Biochemistry

CASE WESTERN RESERVE UNIVERSITY

May, 2002

CASE WESTERN RESERVE UNIVERSITY

SCHOOL OF GRADUATE STUDIES

We hereby approve the thesis/dissertation of

_____

candidate for the _____ degree*.

(signed)_____

(chair of committee)

_____

_____

_____

_____

_____

_____

_____

(date)_____

*We also certify that written approval has been obtained for any proprietary material contained therein.

I grant to Case Western Reserve University the right to use this work, irrespective of any copyright, for the University's own purposes without cost to the University or its students, agents and employees. I further agree that the University may reproduce and provide single copies of the work, in any format that in or from microforms, to the public for the cost of reproduction.

(sign)

Dedication

This is dedicated, in part, to 'Milan', a sweetheart who, unlike so many of the other women in my life, hasn't left me. She's been there to cheer me up when I have been down, give me a reason to get out of bed, and a bright face when I come home at night.

The other person to whom this work is dedicated is my late grandfather, Ramon, a professor of botany. Despite my lateness in appreciating it, he taught me to enjoy the world around me and appreciate the role of science in my life. Thank you, I only wish you had been able to see this work's completion.

Contents

List of Tables

List of Figures

Acknowledgments

No one is alone in this world, and despite appearances, no graduate thesis can be done without a supporting cast. It's impossible to list everyone, so if you are missing, please know it is not intentional.

Most importantly, my mother and my father have been truly helpful for so many years. Their devotion to my education and their persistence in me completing this degree has made all the difference. Thank you, both of you, so very much.

Outside of work, friends like Beth Platt, Laura Wittenberg, Brandon Palmer, Paul Schneider, David Lukens, and Tod Detre have been welcome friends in an otherwise bleak place. Also, thanks to Chris Conneley, Ben Karas, Jeremy and Angela Anderson, Lynne Bremer, and everyone with who I have lived or kept as a roommate over the years. Thanks for the support, the beers, and the laughter when I needed it.

In the department, I have been graced by many, many friends over the years. Notably George Rogers, with whom I have gained numerous insights both inside and outside of the lab; Michael Strainic, with whom I have shared many laughs; John Clarkson, who helped ease my transition back home from Scotland with several nights of heavy scotch drinking; Mike Thompson, though despite being at Scripps in San Diego has managed to keep contributing to the beer and cigar fund, as well as helping me push the envelope in science; and Nancy Richter, always up for a good time. These are just some of the many people I have been fortunate enough to work with. The laboratories of Drs. Petier deHaseth, William Merrick, Richard Hanson, Ganesh Kumar, and Johnathan Leis are tremendous sources of help, assistance, friendship and humor, as are so many labs in the department.

been especially helpful during the last rounds of preparation of this thesis, and I thank them kindly for their time and hard work.

Lastly, the contributions of my thesis advisor, Prof. Vernon Anderson, is also noted. Of course, he has had the most influence and guide over this work, including proposing the topic to me. Though we didn't always see eye to eye, I grew beyond measure under his study, and find myself still learning from him.

This document was set in LaTeX, which was wise as it allowed for so much more control than Word or something similar would have given. I learned a lot of LaTeX in the process, assisted greatly by several friends: Natarajan Krishnaswarmi, Rick Wash and Sathaporn Laksanacharoen. Thank you all for the invaluable help and putting up with my pestering.

List of Abbreviations

Å	Angstroms (m^{-10})
Ac-	acetylated
AMC	7-amino 4-methyl coumarin
ATP	adenosine triphosphate
CAPSO	3-(cyclohexylamino)-2-hydroxy-1-propanesulfonic acid
CM-	carboxymethylated
ddH$_2$0	destilled, deionized water
DMF	N,N-dimethyl formamide
EDTA	(ethylenedinitrilo)tetraacetic acid
ER	endoplasmic reticulum
ES	enzyme substrate complex
ESI-MS	electrospray ionization mass spectrometry
GdnHCl	guanidine hydrochloride
HA	hemiacetal adduct
HEPES	N-[2-hydroxyethyl]piperazine-N'-[2-ethanesulfonic acid]
HIV	human immunodeficiency virus
IPTG	isopropyl β-D-thiogalactopyranoside
Mbp	mega (10^6) base pairs
MES	2-[N-morpholino]ethanesulphonic acid
MHC	major histocompatibility complex
MOPS	3-[N-morpholino]propanesulfonic acid
mV	millivolts
n.d.	not determined

NiNTA	nickel nitrilo-triacetic acid
OD_{600}	absorbance at 600 nm
PAGE	polyacrylamide gel electrophoresis
PAN	proteasome activating nucleosidase
PDB	Protein Data Bank
PEG	polyethylene glycol
PVP-10	polyvinylpyrrolidone, average molecular weight 10,000
SDS	sodium dodecyl sulfate
Suc-LLVY-AMC	*N*-succinyl-leucyl-leucyl-valyl-tyrosyl-aminomethylcoumarin
TAPS	*N*-tris[hydroxymethyl]methyl-3-aminopropanesulfonic acid
TEM	transmission electron microscopy
TS1	transition state 1
UV/Vis	ultraviolet-visible
V	volts
Z-LLLal	*N*-benzyloxycarbonyl-leucyl-leucyl-leucinal

The 20S Proteasome from *Thermoplasma acidophilum*

Abstract

by

JOSE O. NAZARIO

An *Escherichia coli* overexpression system for the 20S proteasome from the archaebacteria *Thermoplasma acidophilum* was obtained and purified recombinant enzyme was used to understand the mechanism of activation of the enzyme. Known activators include magnesium and other salts, and SDS and similar detergents. Two previously unknown activators, buffer ions and some proteins, have also been identified and their points of activation in the mechanism isolated.

Using the kinetics of a slow binding inhibitor, Z-LLLal, and measuring the remaining activity with the substrate Suc-LLVY-AMC, the steps affected by these activators have been identified. SDS, previously thought to enhance the rate of association between the enzyme and substrate, has been found to enhance the rate constant for release of product. Magnesium effects have been found to be largely due to ionic strength, and are due mainly to the stabilization of the tetrahedral intermediate. Activation by buffer ions has been demonstrated, representing a novel form of proteasome activation. It has been found that buffer ions promote the protonation of the first leaving group of the newly formed product, and this effect is pH and pK_a sensitive.

Secondly, evidence has been found that the 20S proteasome core particle can digest destabilized proteins at a biologically appreciable rate, similar to that of the proteases trypsin and chymotrypsin. This rate is significantly faster than the rate of digestion of the peptide Suc-LLVY-AMC and is due to the association of 14 active sites in close proximity. Only destabilized proteins

can be digested with any significant rate, as they must be able to enter the proteasome active site chamber. It is this step, substrate entry into the active site chamber, which has become the rate limiting step.

Lastly, cooperativity effects have been observed in the proteasome. Homotropic cooperativity has been observed in the presence of subsaturating amounts of the inhibitor peptide. Negative cooperativity has been observed with high substrate concentrations, leading to a depression of proteasome activity by approximately 30%.

These findings illustrate several key facets of the proteasome mechanism, and suggest an interlinked energy landscape for the hydrolysis reaction. Several suggestions for future experiments are also provided.

Chapter 1

Introduction

The 20S proteasome forms the core enzyme in the non-lysozomal protein degradation pathway. This large multimeric enzyme can cleave virtually any protein substrate, leaving peptides that are further digested by other enzymes. It lies at the heart of the cytosolic protein recycling pathway. In higher eukaryotes, it is involved in peptide antigen generation for the immune system, making the proteasome an attractive target for therapies for a number of conditions. However, for the enzyme to be an effective therapeutic target, detailed information about the chemical mechanism must be gathered.

Using the archaebacterial source for the enzyme, various facets of the chemistry of the 20S proteasome have been investigated. This form of the enzyme is more simple than the eukaryotic enzyme, containing only two different subunits as opposed to the eukaryotic form of the enzyme which contains 14 different subunits. Because of this simplicity, the *T. acidophilum* proteasome

makes a more attractive kinetic and biochemical subject for study than the eukaryotic proteasome. Much of the chemistry of the active site is conserved, as is the quaternary structure of the enzyme. The results from the studies shown here can be used to illuminate facets about the eukaryotic enzyme as well.

1.1   Structure

Both the tertiary and quaternary structure of the 20S proteasome have novel facets. For many years the structure of the 20S proteasome core particle was a mystery, generating several interesting theories. However, electron microscopy and later X-ray crystallography studies have since revealed interesting structural facets (Jap et al., 1993; Lowe et al., 1995; Groll et al., 1997).

The quaternary structure, first discerned by electron microscopic methods (Hegerl et al., 1991; Grziwa et al., 1994) and later at higher resolution in an X-ray crystal structure (Lowe et al., 1995), revealed a structure similar to that of the protein chaperone, GroEL. Four rings of proteins, each containing seven subunits, form a barrel structure. This is shown in Figure 1.1, showing both a proteasome molecule from *T. acidophilum* and from yeast. The catalytic chamber, formed by the β-subunits, has an entrance gated by a narrow pore formed by the α-subunits (Wenzel and Baumeister, 1995). This narrow pore, much smaller in the yeast 20S proteasome, is visible in Figure 1.2, where end on views of both the *T. acidophilum* and the yeast proteasomes are shown.

These catalytic and additional chambers are visible in Figure 1.3, showing a cutaway view of the interior of the proteasome barrel.

The proteasome is a rather large molecule. It measures some 148Å tall and approximately 113Å wide at the base (Lowe et al., 1995; Weissman et al., 1995). The central chamber forms a cavity approximately 500 nm^3 in volume (Baumeister et al., 1998; Lowe et al., 1995). This is big enough to hold a protein of approximately 30 kDa folded as a typical globular structure. However, the α-subunits define a narrow pore, restricting access to the proteasome active site chamber. As a result of this, only unfolded proteins can be threaded into this chamber for digestion (Wenzel and Baumeister, 1995).

This pore architecture differs between the *T. acidophilum* 20S proteasome structure and the yeast 20S proteasome structure (Groll et al., 1997). In archaeons, loop sequences from the α-subunits form a 13Å pore. The pore of the yeast 20S proteasome, however, is significantly more narrow and is effectively sealed. This occlusion is due mainly to the 7 *N*-terminal residues of subunit α-3, which form a tail structure that fills the area that would otherwise allow passage of a protein or peptide (Groll et al., 2000). This steric hindrance is alleviated by a structural rearrangement upon binding by a cap structure, such as the proteasome activating nucleosidase (PAN) (Groll et al., 2000; Whitby et al., 2000). This tail peptide rearranges to widen the α-subunits' pore significantly and allows unfolded polypeptide chains to pass freely. Interestingly, the same protein hydrolysis rates are observed in the absence of PAN and after

deletion of these N-terminal residues from the $\alpha 3$ subunit. Thus, the $\alpha 3$ amino terminus acts as a gate to the active site chamber in which the cap structure opens the doorways.

The formation of the heptameric ring structure of the intact enzyme is forced by the propensity of the α-subunits to form a heptameric structure. *In vitro* reassembly studies of the individual subunits of the *T. acidophilum* 20S proteasome found that the α-subunits are capable of forming stable heptameric rings, while the β-subunits formed aggregates lacking any regular oligomeric structure. Furthermore, the transition from monomers to a full 28-subunit complex appears to lack any discrete intermediates *in vivo* as no partial core particle structures have been isolated (Kruger et al., 2001).

The tertiary structures of the α- and β-subunits have unusual folds (Wlodawer, 1995; Lowe et al., 1995). Two beta sheets are surrounded by alpha helices, but packed with a tight 30° angle between each other (Figure 1.4) (Wlodawer, 1995). This gives an overall compactness of structure that is slightly higher than most alpha-beta sandwiches. Furthermore, at the end of the N-terminal β-strand of the β-subunit lies threonine 1, the catalytic nucleophile (Seemuller et al., 1995b). N-Terminal nucleophiles are a small emerging class of enzymes related in structure and their ability to catalyze acyl transfer reactions (Brannigan et al., 1995).

5
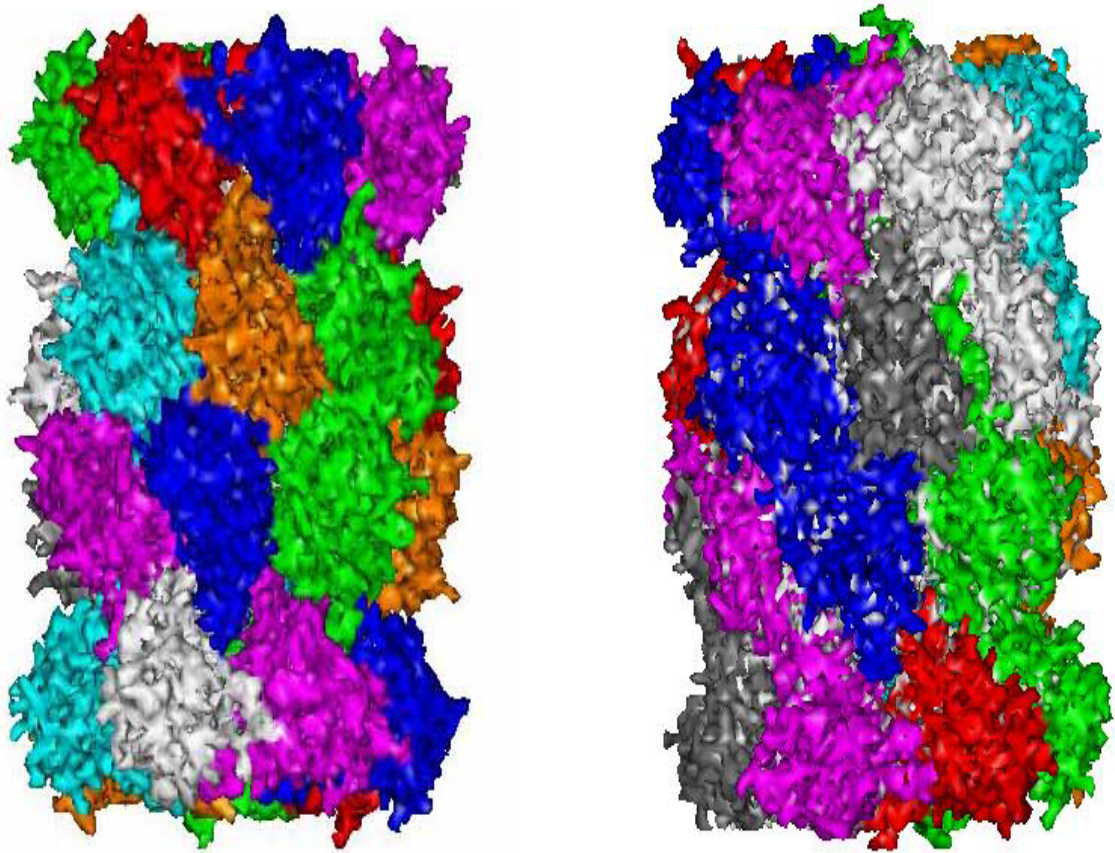
Figure 1.1: Quaternary Structure of Two Proteasomes

Two proteasome molecules, on the left from *T. acidophilum* and on the right from yeast, are shown here to illustrate their similar quaternary structure. The *T. acidophilum* structure file 1PMA from Lowe *et al.* (Lowe et al., 1995) and the yeast structure 1RYP from Groll *et al.* (Groll et al., 1997) were used. The coloration of the subunits is not indicative of uniqueness of the sequences, only to highlight the different chains.
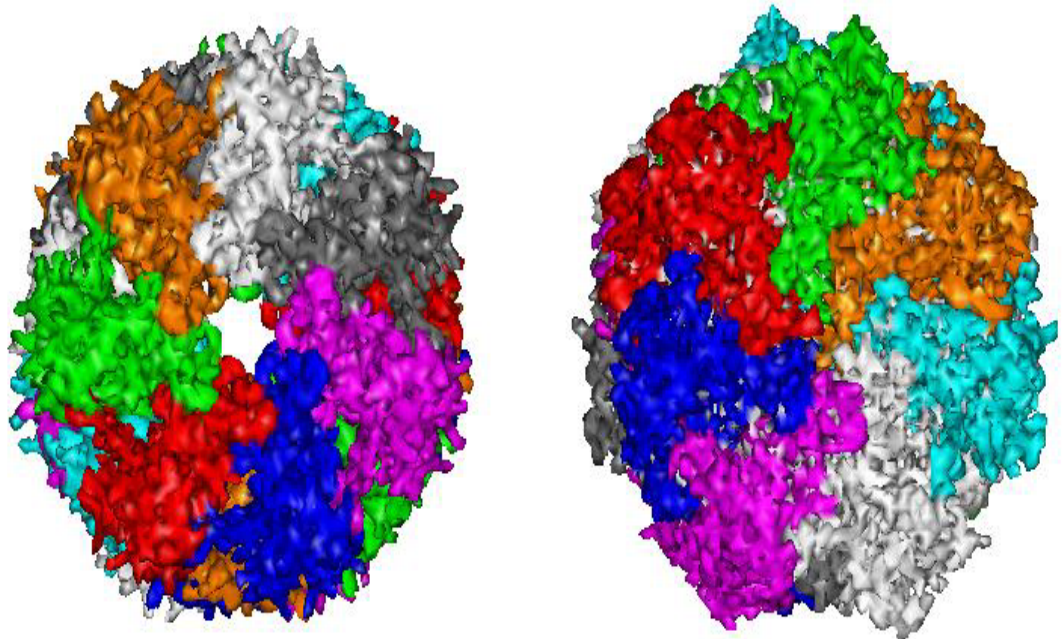
Figure 1.2: End On View of Two Proteasome Molecules

Two proteasome molecules contrasting the alpha subunit pores. On the left is the end on view of the *T. acidophilum* proteasome from PDB structure 1PMA (Lowe et al., 1995). On the right is a view down the end of the proteasome from yeast from PDB structure 1RYP (Groll et al., 1997). Immediately obvious is the difference in accessibility based on this pore.
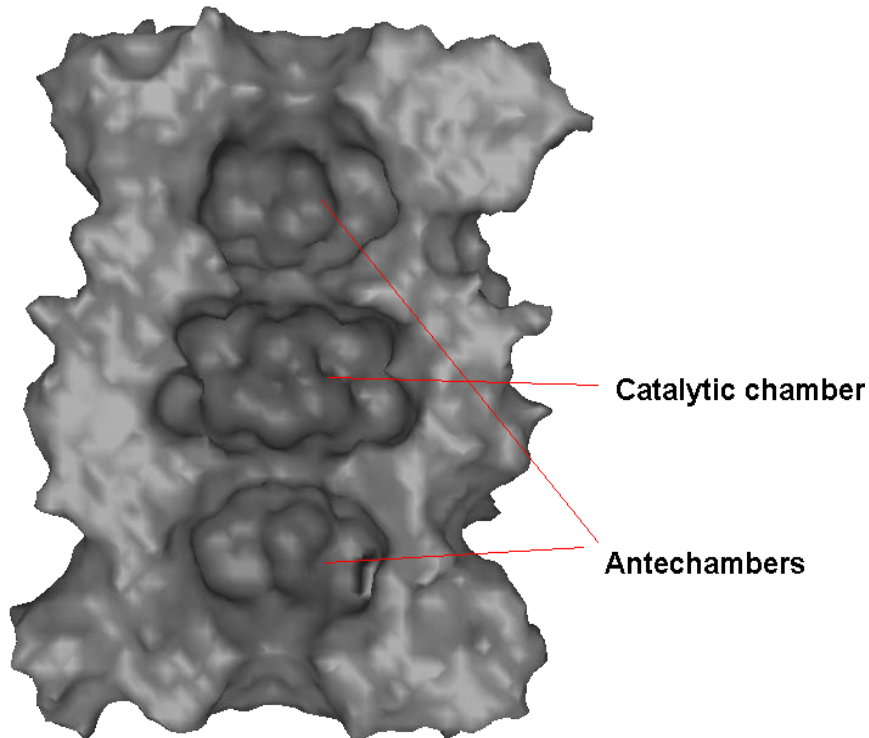
Figure 1.3: Cutaway View of the Proteasome Revealing Three Distinct Chambers

In this illustration, the crystal structure of the proteasome (PDB accession code 1PMA (Lowe et al., 1995)) was analyzed to produce a Connoley surface. One half of the structure was then removed to reveal the inside of the barrel structure. Indicated are the antechambers formed by the α-subunits and the large active site chamber formed by the β-subunits in the center.
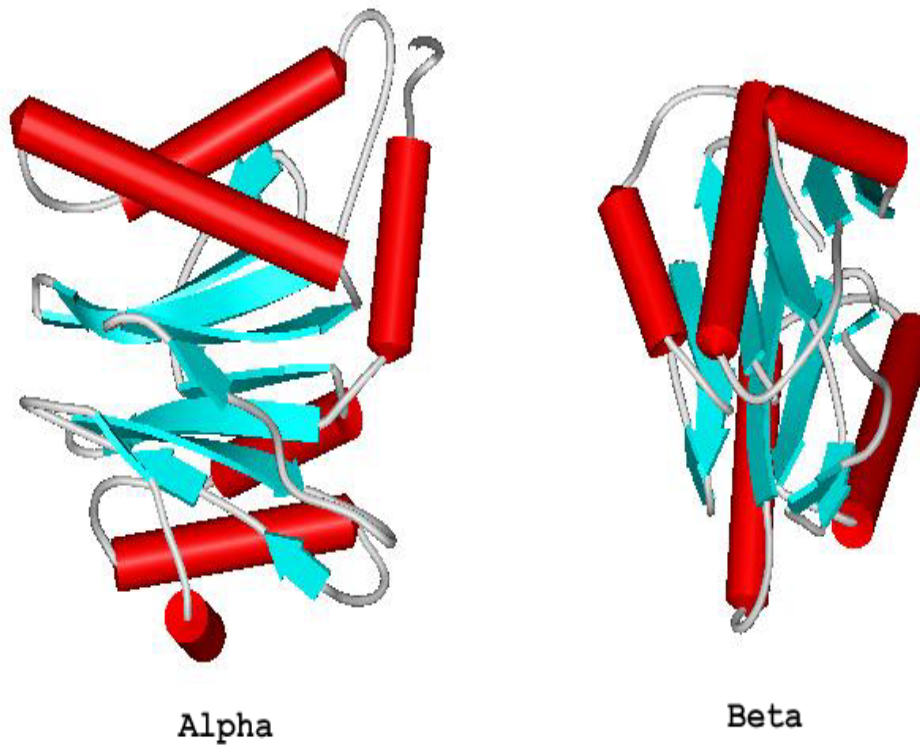
Figure 1.4: Secondary Structure of Proteasome Subunits

In this figure the schematic of the alpha- and beta-subunits of the 20S proteasome from *T. acidophilum* are shown, with beta strands shown as blue-green arrows and alpha helices as red tubes. These coordinates are from the 1995 crystal structure by Lowe *et al.* (Lowe et al., 1995) and was rendered using WebLab Viewer (MSI Software).

Because of its central role in cellular maintenance, the proteasome is found ubiquitously in all eukaryotic and non-prokaryotic life forms, including yeast (Dahlmann et al., 1989). Differences exist, though, in the forms of the enzymes, despite structural and sequence relatedness.

The eukaryotic forms of the 20S proteasome contain seven different isoforms each of the α- and β-subunits (Orlowski, 1990). This diversity gives the eukaryotic proteasome a high catalytic variety (Orlowski, 1993), enhanced in higher eukaryotes where subunits can be substituted in response to immunological signals such as interferon signaling (Tanahashi et al., 1993). A sequence alignment of the *T. acidophilum* β-subunit sequence and the β-7 subunit from yeast is shown in Figure 1.5. When measured using the BLAST tool (Altschul et al., 1997), a 21% identity between the two types of subunits exists for the core portions with approximately 40% homology in this section of the protein sequence.

In the archaebacterial and eukaryotic forms of the enzyme, the β-subunits are synthesized with an *N*-terminal precursor sequence (Kruger et al., 2001; Mayr et al., 1998; Seemuller et al., 1996). The -1 residue is consistently a glycine and is thought to be important for the structural requirements of cleavage of the propeptide sequence (Ditzel et al., 1998; Seemuller et al., 1996). After proper folding, the β-subunits self-process by cleaving the leader sequences to expose the *N*-terminal threonine of the active enzyme (Kruger et al., 2001). In the absence of processing, the enzyme remains inactive (Seemuller et al.,

1996).

1.2 Function

The central role of the 20S proteasome is as the core facility of the cytosolic
protein turnover machinery (Orlowski, 1990). Proteins are destined, through
some mechanism, to be fed into the proteasome where they are digested into
peptides (Wenzel and Baumeister, 1995). In higher eukaryotes, an additional
role of the proteasome is to generate antigens for the immune system (York
et al., 1999; Gaczynska et al., 1993).

In eukaryotes, proteins which are to be digested by the proteasome signal
this fate through the use of ubiquitin (Glickman and H., 2000). This 76
residue protein is highly conserved in eukaryotes and exists as a free monomer
in solution. However, it is covalently attached through a lysine residue on
the target protein by the actions of several accessory proteins involved in
ubiquitinylation. A well defined set of proteins identify targets and prepare
a ubiquitin tag (Hochstrasser et al., 1999; Rubin et al., 1997). Accessory
proteins to the 20S proteasome core particle, such as the 11S and 19S cap
structures, recognize this ubiquitin tag and remove it in an ATP-dependent
fashion (Tanahashi et al., 1999). Next, the target protein is unwound, also
through an ATP-dependent mechanism, and this resulting polypeptide is fed
to the 20S proteasome for hydrolysis (Sherman et al., 1996; Baumeister et al.,
1997; Navon and Goldberg, 2001).

```
                    10        20        30        40        50        60
                     .         .         .         .         .         .
  1                                           MNQTLETGTTTVGITLKDAVIMATE  thermoplas
  1  MSFLELTEVWGKPQKDIFFPSGSEVEESTDAPIQRTVQPIVTGSSVLALKFADGVMIAAD  20S_protea

                    70        80        90       100       110       120
                     .         .         .         .         .         .
 26  RRVTMENFIMHKNGKKLFQIDTYTGMTIAGLVGDAQVLVRYMK.AELELYRLQRRVNMPI  thermoplas
 61  NLASYGSLARFYDVERLTKVGDNLIVGAGGDISDYQQIQRLLEKLEIKEGNYGDGYALQP  20S_protea

                   130       140       150       160       170       180
                     .         .         .         .         .         .
 85  EAVATLLSNMLN..QVKYMPYMVQLLVGGLD...TAPHVFSIDAAGGSVEDIYASTGSGS  thermoplas
121  SYTHEYLSKVLYARRNKLDPYWNQLIVAGVDGENKEPYVAFADLRGTTYSAPAIATGFAM  20S_protea

                   190       200       210       220       230       240
                     .         .         .         .         .         .
140  PFVYGVLESQYS....EKMTVDEGVDLVIRAISAAKQRDSASGGMIDVAVITRKDGYVQL  thermoplas
181  HLALPMLRKATDDDRWKTLSKESARATIDECMRVLFYRDARSLNKFSVATITPEG...IEF  20S_protea

                   250       260
                     .         .
196  PTDQIESRIRKLGLIL            thermoplas
239  QTDQSVSSKWAFAEKQYGYGTQTV    20S_protea

      X   non conserved
      X   similar
      X   conserved
      X   all match
```

Figure 1.5: Alignment of β-subunits

Above are the aligned sequences of the *T. acidophilum* (listed as 'thermoplas' in the figure) and yeast (listed as '20S_protea' in the figure) β-subunits, specifically the sequence for the β-7 subunit from yeast. The catalytic threonine residue is located at position 44 in this Figure, including the propeptide which is cleaved before the enzyme is active. Note that the shown yeast β-subunit does not contain a similar residue at this position. The alignment was made using the CLUSTALW tool (Higgins et al., 1992; Thompson et al., 1994; Felsenstein, 1989) and the figure generated using TeXshade (Beitz, 2000)

Though the sequence conforming to the eukaryotic protein ubiquitin has been found in *T. acidophilum* in *N*-terminal peptide sequencing (Wolf et al., 1993), no such proteasome accessory proteins or ubiquitin-like system has been identified in the genome from the organism (Ruepp et al., 2000). Sequence analysis of the *T. acidophilum* genome has not detected any orthologs of the protein degradation signaling tags ubiquitin or SsrA(Roche et al., 1999). Likewise, any of the proteasome cap structures, including PA28, PA700, and the subunits of the 19S and 11S regulators have not had homologues identified in the *T. acidophilum* genome (Ruepp et al., 2000; Chu-Ping et al., 1994). Thus, if there is a proteasome targeting system for proteins in *T. acidophilum*, it has no identifiable orthologs either in bacteria, yeast, or higher eukaryotes (Glickman and H., 2000).

Proteins are believed to be targeted for degradation for a number of reasons. First, damaged proteins are obviously good candidates for proteasome based breakdown. In eukaryotes, an extensive system for the recognition of damaged protein exists, which utilizes ubiquitin to lead to the demise of damaged proteins (Matthews et al., 1989). The types of damage range from oxidative damage, misassembly of glycoslyation, or truncations by proteases (Schubert et al., 2000). Misfolded proteins are also targeted by the proteasome system for digestion (Glickman and H., 2000).

The size distribution of peptide products from the proteasome generally ranges from 7 to 12 amino acids (Kisselev et al., 1998a). This consistency

has led to the proposal of the "molecular ruler" hypothesis. The distance between adjacent active sites, approximately 25Å, is the distance of about 8 or 9 amino acids when extended (Wenzel et al., 1994). This is shown in Figure 1.6, where the distances between one active site and several of its neighbors are shown. This distance between active sites is the effective "molecular ruler". This product length distribution is not a strict rule (Kisselev et al., 1998a), however, but a general principle. Several experiments have shown that the length distribution of the product peptides is not as narrow as previously thought (Kisselev et al., 1998a; Kisselev et al., 1999b; Nussbaum et al., 1998).

One related hypothesis, the "bite and chew" proposal (Kisselev et al., 1999a), is based on the idea that initial nucleophilic attack by one active site is fast, while decomposition of the acyl enzyme intermediate is slow. Before the protein can dissociate from the enzyme, a second nucleophilic attack takes place at a nearby active site. If this scenario is correct, the distance between sites of attack becomes a function of the distance between the active sites. These distances, shown in Figure 1.6, would lead to various sized peptides with a minimal length of approximately 8 amino acids.
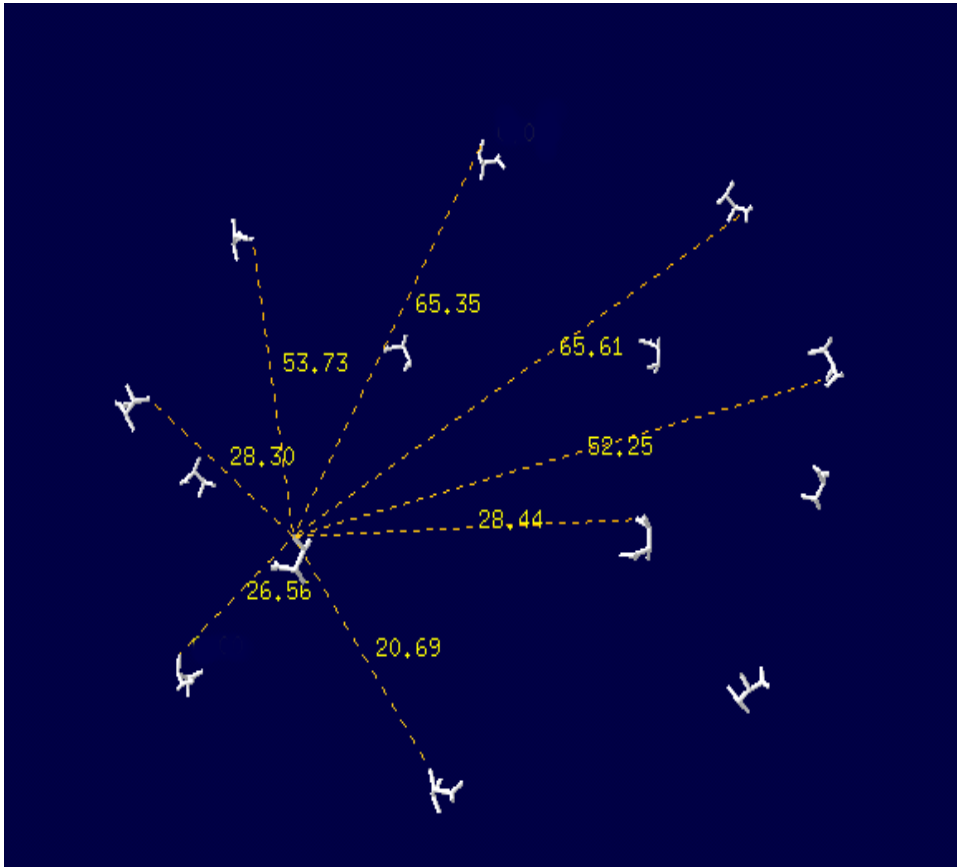
Figure 1.6: Active Site Geometry of the 20S Proteasome

The geometry of the active site of the *T. acidophilum* 20S proteasome was analyzed to find the distances from one active site to any eight of its neighbors. Six of these neighbors are in one ring and the other two are in the second ring of β-subunits. The distances are listed in Å. This figure was generated using the coordinates from the PDB file 1PMA (Lowe et al., 1995) and the program SwissPDB View (Guex et al., 1997).

The processivity of the proteasome has generated yet unresolved debates (Kisselev et al., 1998a; Kisselev et al., 1998b). Conflicting evidence either supports either a mechanism in which the proteasome breaks down an entire protein molecule before a second is started, and one whereby the enzyme releases large protein intermediates continually until they are entirely broken down into short peptides.

1.3 Distribution

The proteasome is found in the cytosol of every cell in eukaryotes and in non-prokaryotic life forms (Dahlmann et al., 1991a; Dahlmann et al., 1989). Prior to the characterization of the proteasome, the lysozome was thought to be the center of protein breakdown (Orlowski and Michaud, 1989). However, the proteasome is able to accomplish this feat in the cytosol of cells, utilizing control mechanisms such as ubiquitin tagging and recognition by auxiliary cap structures. Some studies have shown that up to 2% of total cellular protein is proteasome molecules, underscoring the central role of this enzyme (Dahlmann et al., 1989). In prokaryotes, other large multimeric proteases fulfill the proteasome's role in cytosolic protein turnover (Tamura et al., 1998; Tamura et al., 1996).

Immunolocalization studies have shown that the proteasome is nearly evenly distributed within mammalian cells (Kruger et al., 2001), but that there is, in

some cases, localization to the cell membrane (Kinoshita et al., 1990). The implications of this membrane localization remain unknown, however. In yeast, proteasome molecules are often associated with the ER membrane network (Kruger et al., 2001). The intracellular proteasome distribution includes the nucleus and perinuclear region in eukaryotic cells (McNaught et al., 2001).

1.4   Mechanism

From both crystallographic and mutagenesis studies, a novel proteolytic mechanism has emerged as shown in Figure 1.7 (Wlodawer, 1995). This mechanism is similar to the catalytic triad mechanism used in serine proteases, but involves four functional groups instead of three and a threonine replaces the serine nucleophile (Seemuller et al., 1995a; Seemuller et al., 1995b).

The N-terminal threonine with the β-hydroxyl group located on the β-subunit acts as the proteasome's nucleophile to attack the amide carbonyl carbon of the target peptide bond (Seemuller et al., 1995a). The neutral alpha-amino terminus accepts the acidic proton from the threonine, while lysine 33 and glutamate 17 help orient the nucleophile and may also be used in the stabilization of the anionic intermediates. After the formation of a tetrahedral intermediate, the C-terminal peptide or leaving group of the labile bond is lost, forming an acyl-enzyme intermediate. This intermediate is then hydrolyzed by an attack of a solvent water molecule, which is activated by hydrogen bonding to the unprotonated amino-terminus. Following formation of a second

tetrahedral intermediate, cleavage of the C-O bond results in the loss of the second peptide and regenerates the original form of the enzyme.

Several lines of evidence support the described mechanism. First, crystal structures of the enzyme with several bound inhibitors show a direct attack by the threonine nucleophile to form a hemiacetal intermediate (when reacted with an aldehyde inhibitor) (Lowe et al., 1995; Escherich et al., 1997; Groll et al., 2001). Second, the role of the alpha-amino terminus has been implicated in several studies showing that only mature, posttranslationally processed β-subunits are catalytically active (Ditzel et al., 1998; Groll et al., 1999). Without a free amino-terminus to act as a proton relay point, the enzyme is unable to begin the catalytic cycle. Third, the chemistry of the inhibitors is consistent with a role for the amino-terminus in the mechanism (Kim et al., 1999; Lee et al., 1998).
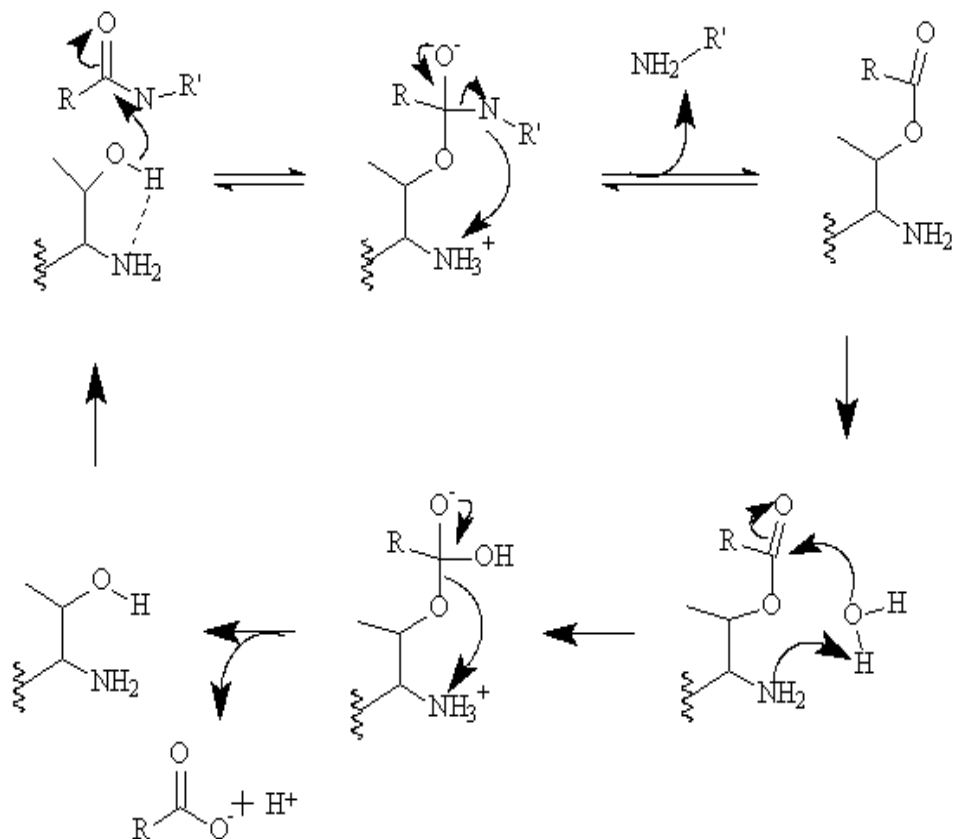
Figure 1.7: The Putative Catalytic Mechanism of the Proteasome

Based on mutagenesis, structural and additional data, a proposed mechanism of proteolysis by the 20S proteasome has emerged. The nucleophilic threonine is shown, but absent are the residues glutamic acid 33 and lysine 14. This figure is based on the description by Wlodawer (Wlodawer, 1995). After initial attack of the peptide bond carbonyl by the threonine nucleophile, the C-terminal portion of the substrate is released, leading to an acyl-enzyme intermediate. A water molecule then hydrolyzes the intermediate to generate the second product of the cleavage event and restores the free enzyme (see text).

1.5 Inhibition of the Proteasome

The proteasome is an especially attractive therapeutic target for inhibitor design for a variety of reasons (Rivett et al., 2000). First, due to the necessity of the enzyme for cells to survive, the selective inhibition of the enzyme would make an attractive therapy for diseases such as cancer (Adams et al., 2000; Kanayama et al., 1991). Secondly, for treatments which may require the suppression of the immune system, inactivation or suppression of the proteasome could be useful in suppressing the presentation of peptide antigens in the MHC system (Michalek et al., 1993; Niedermann et al., 1999). Such treatments include tissue and organ transplants where downregulation of proteasome activity might limit rejection of the transplanted tissue by the immune system.

To successfully and specifically inactivate the proteasome, a detailed understanding of its mechanism needs to be obtained (Murray et al., 2000). Furthermore, inhibitors may reveal facets about the chemistry of the mechanism. These differences between the proteasome mechanism and the chemistry of other enzymes can be exploited to provide specificity against the proteasome. Currently, while we have been able to inhibit the proteasome, many of these inhibitors are non-specific and affect several enzymes. This reflects the limited understanding we currently have of the proteasome mechanism.

The selective inactivation of the proteasome is of interest as an emerging treatment for cancers and autoimmune disorders (Teicher et al., 1999; Adams

et al., 2000). However, this has so far been hindered by the finding of inactivator molecules which are selective for the proteasome and can be synthesized readily. Proteasome inhibitor molecules so far identified are either difficult to synthesize in large quantities, or it has been shown that they affect a range of protease enzymes.

Many of the reversible inhibitors of proteasome function are other, previously characterized protease inhibitors. Commonly used *in vitro* and *in vivo* inhibitors include peptide aldehydes (McCormack et al., 1998; Vinitsky et al., 1994), such as various forms of the calpain inhibitors, alpha keto-peptides (Chatterjee et al., 1999), peptide benzamide derivatives (Myung et al., 2001a), and boronic esters (Teicher et al., 1999). These classes of inhibitors are known to inhibit a variety of serine proteases by forming stable adducts with the enzyme (Muszkat et al., 1983). Their specificity and affinity is usually determined by their peptide composition. Furthermore, through the use of multivalency, lower inhibition constants and tighter binding can be achieved (Loidl et al., 1999).

Vinyl sulfones are a class of irreversible synthetic inactivators that lead to an ether adduct with the proteasome (Bogyo et al., 1997; Cormack et al., 1997). However, they also inactivate a number of cellular cysteine proteases, making them less attractive as *in vivo* proteasome inactivators (Schmidtke et al., 1999).

Several additional classes of proteasome inhibitors have been found, some

of which are natural products (Li et al., 1991; Gao et al., 2000). Beta-lactones are one of the major natural product proteasome inhibitors that have been found, β-lactacystin, for example, was originally isolated from the organism *Streptomyces lactaysinaeus* (McCormack et al., 1998; Dick et al., 1997). Nucleophilic attack on the β-lactone results in the formation of an ester adduct with the proteasome, which is inefficiently hydrolyzed and effectively inhibits the enzyme (Dick et al., 1996; Cormack et al., 1997). However, β-lactacystin has been found to also interfere with other cellular proteases (Lee et al., 1998), revealing that it as less enzyme specific than previously thought.

High proteasome specificity has been found with the natural product family of α', β'-epoxyketone peptides (Elofsson et al., 1999). These microbial metabolites lead to a 6 membered morpholino adduct with the threonine active site of the 20S proteasome. Furthermore, unlike beta-lactones, α', β'-epoxyketone peptides are relatively easy to synthesize in the laboratory. As such, these are a promising line of therapeutic proteasome inhibitors (Lee et al., 1998).

However, because the proteasome is a peptidase, the inhibition of other proteases could interfere with normal cellular function. The promiscuity of the active site, together with the the novel active site chemistry, means that new considerations arise when designing therapeutics that may interfere with the proteasome. One example of this cross reactivity is the HIV protease inhibitor, Ratinovir (Schmidtke et al., 1999). Recent evidence has shown that the length and composition distribution of peptide antigens generated by the

20S proteasome is affected by the interference of Ratinovir with proteasome function (Schmidtke et al., 1999).

1.6   Kinetic Studies

The 20S proteasome, from both archaebacterial and eukaryotic sources, has received some kinetic analysis by other groups. Most of the attention has been focused on the eukaryotic enzyme, but these investigations have been hampered by the catalytic, and hence kinetic, variability in the enzyme. However, most of the assays have focused on enzyme activity and not kinetic parameters. As such, these studies have not been as definitive as is needed to characterize the mechanism of the enzyme.

Several groups have successfully measured inhibition kinetic constants of both the *T. acidophilum* and yeast proteasomes. K_i values for peptide aldehyde inhibitors (Escherich et al., 1997) and association parameters for vinyl sulfones (Bogyo et al., 1997) have been obtained. Another commonly obtained value is the IC$_{50}$, the concentration of inhibitor which gives 50% of the control activity (Loidl et al., 1999). These values are then used in evaluation of substrates, inhibitors, and modulators of proteasome activity.

Unfortunately, the complexity of the kinetics of the 20S proteasome have often been ignored. The traditional enzyme kinetic parameters of K_m and k_{cat} assume simple bi-molecular associations between the enzyme and the substrate which are not likely to occur in an enzyme with 14 active sites per molecule.

These parameters have been obtained with proteins (Dolenc et al., 1998) and peptides (Seemuller et al., 1995a; Seemuller et al., 1995b) as substrates. In these published studies, the analysis of the data has assumed what is likely to be an incorrect kinetic model, meaning that the values obtained are incorrect or misleading.

Most of the studies to day on the 20S proteasome have focused on using activity as a measurement. This has been used to test various substrates (Dahlmann et al., 1991b; Tamura et al., 1995), the effects of various activators (Akopian et al., 1997; Pereira et al., 1992), and mutations (Seemuller et al., 1996). The effects are then described as percent increases or decreases from the activity under basal conditions. This approach has had limited success in isolating the mechanism of various activators.

Very few studies have rigorously examined the kinetics of the proteasome and its activators. The complexity, and the differentiation, of SDS and Triton X-100 activation of the rat liver 20S proteasome has been studied (Arribas et al., 1990). By using several different substrates and measuring the kinetic parameters, different modes of activation by Triton X-100 and SDS were shown. Furthermore, each of the substrates showed different kinetic behavior with the enzyme, suggesting preferential interactions with the various active sites and the resulting cooperativity. The values obtained, though, are likely to be due to a mixture of effects from the diversity of active sites.

The kinetic analysis of SDS on the activation of the proteasome was further

examined by specifically focusing on the chymotryptic activity of the rabbit muscle 20S proteasome (Stein et al., 1996). This set of experiments highlighted the kinetic complexity of the proteasome, showing interconversion between a latent and an active form of the enzyme, substrate inhibition, and the effect of SDS on the lag phase of activation. One consequence of this examination is that the previous studies assumed Michaelis-Menten kinetics. As a result, they are now clearly limited in validity for interpretation of the data.

The kinetic effects of the immune system interferon signaling molecules have also been investigated (Kuckelkorn et al., 1995). Catalytic variability in the eukaryotic proteasome in mammals has been known for several years (Groettrup and Schmidtke, 1999), providing a diversity of proteolytic activities. These effects appear to affect the V_{max} or K_m parameters, depending on the subunits exchanged, and clearly indicate the diversity of catalytic subunits available to the proteasome.

Unfortunately, few studies have focused on the simpler proteasome from *T. acidophilum*, leaving ambiguous kinetic results more often than clear findings. As such, more detailed experiments are required to obtain this level of mechanistic information.

1.7 Substrate Preferences

The central role of the proteasome is protein hydrolysis, which requires that it be able to cleave virtually any peptide bond (Orlowski, 1993). As such, a

broad substrate utilization is required with minimal specificity requirements. However, each subunit displays tendencies towards different cleavage sites.

Eukaryotic proteasomes utilize several different β-subunits to provide a diversity of proteolytic preferences (Orlowski and Michaud, 1989). Five different proteolytic activities have been identified, with each activity being specific to a particular subunit (Orlowski and Wilk, 2000). These activities were described on the basis of their activity against traditional protease substrates (Orlowski and Michaud, 1989). Each of these subunits can be specifically inactivated via different specific inhibitors or mutated to inactive forms to assay their contributions to the overall proteolytic activity (Myung et al., 2001b).

Archaebacterial proteasomes, such as the 20S proteasome from *T. acidophilum*, have only one catalytically active subunit type, but 14 copies in each 20S proteasome particle (Dahlmann et al., 1989). This activity, termed "chymotrypsin-like" due to the nature of the preferred substrates used to test for activity, is similar to the eukaryotic proteasome subunit with which it shares a high sequence similarity (Orlowski and Michaud, 1989).

For both the complex eukaryotic proteasome and the simpler archaebacterial proteasome, proline residues are rarely found in the P_1 position (Shimbara et al., 1998; Cardozo et al., 1994). This is most likely due to the geometric constraints that arise from the unusual structure of the proline residue (Stein et al., 1996; Cardozo et al., 1994).

A minimal length dependence is also observed for both types of 20S proteasomes. A peptide of at least three residues in length is required to serve as a substrate. This requirement is presumably due to the binding interactions of the peptide in the active site of the enzyme.

1.8   The Role in Immunity

In higher eukaryotes, an additional role of the proteasome is to generate MHC Class I peptide antigens (Tanaka et al., 1997). Furthermore, interferon expression induces an exchange of three of the catalytic proteasome subunits (Akiyama et al., 1994) which alters the proteolytic products (Gaczynska et al., 1996). This exchange causes the limited proteolysis of both self and non-self proteins, and their import into the MHC Class I antigen presentation system. Under normal immunological responses, T-cells ignore self peptides. As described below, however, the proteasome's processing of self peptides can lead to autoimmune diseases.

1.9   The Proteasome and Disease

Because the proteasome is involved in housekeeping and protein level regulation, it seems obvious that disruptions in the ubiquitin/proteasome pathway could lead to disease. These diseases differ in their pathology due to the nature of the genetic abnormality leading to disease (Vu et al., 2000). There are

complex paths leading both to and from the proteasome as a protein turnover center. Any of these can fail and cause disease, described below.

Because of the close association of the proteasome with the ubiquitin tagging system in eukaryotes, defects in ubiquitinylation cause problems in protein turnover catalyzed by the proteasome. These defects can arise from any one of the enzymes that recognize and affix ubiquitin tags to proteins, or from changes to ubiquitin itself (Vu et al., 2000). Diseases that might be linked to problems with the ubiquitin tagging system include cystic fibrosis, Angelman's syndrome, Parkinson's disease (through problems in ubiquitin ligation) and Liddle syndrome (Vu et al., 2000; Schwartz et al., 1999). At the cellular level, each of these diseases is caused by elevated levels of various proteins that are otherwise kept in check by the proteasome system. A frame shift in the gene encoding ubiquitin-B has been linked to the late onset, non-familial form of Alzheimer's disease. In this disease, proteins accumulate to abnormally high levels and then aggregate, leading to the pathology of protein plaques. The ubiquitinylation system fails to properly tag proteins that should be degraded by the proteasome, leading to their accumulation (Johnston et al., 1998).

The opposite problem, excessive ubiqutinylation, leads to accelerated protein degradation. This is the chief cause of muscle wasting caused by defects in the ubiquitin-proteasome system such as increased proteasome activity or ubiquitinylation. Proteins that are hypertagged with ubiquitin and digested by the proteasome, leading to a rapid net loss of protein mass. The cellular

machinery unable to synthesize replacement proteins fast enough (Kumamoto et al., 2000; Mitch et al., 1996).

Genetic abnormalities upstream of the ubiquitin tagging system can lead to malignancies through disruption of the levels of the tumor suppressor protein p53. Due to excessive ubiquitin production, and the subsequent attachment of these tags on proteins, increased protein degradation follows. This leads to decreases in p53 levels and its efficacy as a tumor suppressor (Moretti et al., 2000; Magae et al., 1997).

Another point of involvement of the proteasome in disease is in the interaction with protein aggregates within cells, particularly neurons. A number of neurodegenerative diseases are caused by protein plaques which result from the aggregation of misfolded or damaged proteins. This includes the accumulation of Lewy bodies in Parkinson's disease and Alzheimer's disease (Bennett et al., 1999; Ii et al., 1997).

Two mechanisms can lead to the development of protein aggregates, which, because proteins must be threaded into the active site chamber, are indigestable by the proteasome (Kopito et al., 2000; Johnston et al., 1998). The first is an increased rate of misfolded or damaged protein production. This can arise either from genetic mutations or from environmental factors such as exposure to oxidative stress. This reaction of the protein and environmental stresses can lead to altered chemical identities of the sidechains, cross linked protein chains, and truncations. The second, a slowdown of the proteasome

proteolytic system, can result from a variety of causes. Lower proteasome levels would effect a slowdown of the entire proteasome centric protein turnover system. Problems in the ubiquitin tagging system could also interfere with the entrance of proteins into the proteasome degradation pathway. In either case, the rate of protein aggregation outpaces that of the proteasome pathway for breakdown.

This imbalance in the production of misfolded or damaged proteins and their digestion by the proteasome system can lead to formation of Russel bodies, which are accumulations of protein aggregates in the ER lumen or cytosol. These protein aggregates have been implicated in many diseases including neurodegenerative diseases.

For these reasons, the proteasome makes an attractive target for therapeutic investigations both for the inhibition of the enzyme as well as an increase in its function. Early experiments indicate it is a promising target for the treatment of certain cancers and immune diseases (Adams et al., 2000).

1.10 *Thermoplasma acidophilum* Biology

The source of the enzyme for the experiments in this thesis, the archaebacteria *Thermoplasma acidophilum*, is an interesting organism. As a member of the thermophilic eubacteria within the archae kingdom, it thrives best in acidic and warm conditions (Darland et al., 1970). Originally isolated from coal slag, *T. acidophilum* has optimal growth conditions at approximately pH 1-2 and

temperatures between 55 and 60^oC (Ruepp et al., 2000; Darland et al., 1970). Although the organism thrives in an acidic environment, a nearly neutral cytosolic pH is maintained without the use of a rigid cell wall (Langworthy et al., 1972).

The lipid composition of *T. acidophilum* has been the subject of several investigations. This work has revealed the presence of large polar lipids, often glycosylated with glucose, mannose and gulose, phosphorylated, or both, forming phosphoglycolipids (Shimada et al., 2002). These lipds are typically large, often C_{20} or C_{40}, isopranoid chains, sometimes containing up to three cyclopentane rings or branches (Shimada et al., 2002; Langworthy and A., 1977; Langworthy et al., 1972). These unusual lipid compositions help the organism survive under these otherwise harsh conditions of temperature and pH by restricting proton flow across the membrane more efficiently than non-branched lipids (Baba et al., 2001).

The genome of *T. acidophilum*, a 1.5 Mbp circular plasmid, reveals a considerable amount of gene shuffling with related archaebacteria (Ruepp et al., 2000). Approximately 1500 open reading frames have been identified, many of which are putatively identified as proteases. These are presumably involved in cellular metabolism to provide a pathway for the metabolic utility of scavenged peptides which appear to be the primary source of nutrients for *T. acidophilum*.

1.11   Specific Aims

The experiments detailed below were aimed at evaluating the contribution of the quaternary structure of the proteasome to its function. The 20S proteasome from *T. acidophilum* was chosen because of the seven-fold rotational symmetry for both the α-and β-subunits (Lowe et al., 1995). This structural feature greatly simplifies kinetic and structural analyses. The conservation of the major structural features as well as the high sequence homology between the catalytic β-subunit and one of the eukaryotic β-subunits (Dahlmann et al., 1989) allows us to extend our analysis beyond the archaebacterial enzyme and further our understanding of the eukaryotic form of the enzyme. Furthermore, these experiments are designed to dissect the proteolytic mechanism of the 20S proteasome which is common between the archaebacterial and the eukaryotic forms of the enzyme (Wlodawer, 1995).

The project described herein had several goals which could be readily approached using the *T. acidophilum* 20S proteasome, yet should also have some relevance to the eukaryotic 20S proteasome which is more clinically relavent. These experiments include the determination of the optimal conditions for enzyme activity. These conditions include metal ions, detergents, temperature, and substrate concentrations. The results of these studies would be useful in understanding the chemical mechanism of the enzyme. These activation factors would then have to be mapped into their points of action within the proteolytic mechanism to identify at what steps they act. This requires a

minimal kinetic mechanism to be developed.

Additional goals of the project included the determination of the number of active sites per particle in solution. Each enzyme partical has up to 14 active sites, all of which may not be active at any one time. This concentration of active sites could lead to significant rate enhancements if they are all active. Secondly, the project aimed to understand any cooperativity between the subunits which affect the overall kinetics and mechanism of the enzyme. The close contact between the subunits is expected to lead to communications through conformational changes between the active subunits, to cause either negative or positive cooperativity.

Chapter 2

Mechanism of Activation of Peptide Hydrolysis by Sodium Dodecyl Sulfate and Magnesium Chloride

2.1 Abstract

The 20S proteasome is a ubiquitously distributed cytosolic proteolytic enzyme found in archaeons and eukaryotes and is composed of four heptameric rings defining three chambers. Active site reactivity was probed using a slow binding inhibitor, *N*-benzyloxycarbonyl-leucyl-leucyl-leucinal (Z-LLLal), to investigate the effects of exogenous activators on *Thermoplasma acidophilum* proteasome activity. Enzyme activity was monitored with fluorescence spectroscopy using the peptide substrate, *N*-succinyl-leucyl-leucyl-valyl-tyrosyl-7-amido-4-methyl

coumarin (Suc-LLVY-AMC). It has been postulated that sodium dodecyl sulfate (SDS) causes stimulation of activity by enhancing access to the proteolytic chamber (Baumeister et al., 1998). If SDS were facilitating access to the active site chamber, similar increases in the rate constant for binding of the inhibitor would be expected. No significant changes in the apparent K_i is found, k_{on}, or k_{inact} parameters for inhibitor binding upon the addition of SDS. Instead, an increase in the rate constant for release of the inhibitor, k_{off}, is found with added SDS. An additional activator, $MgCl_2$, has been shown to provide an approximate ten-fold activation of the pre-steady state activity against Suc-LLVY-AMC. Upon addition of magnesium, the K_i increases, and both k_{on} and k_{off} for inhibitor binding increase as well. These data suggest that accessibility of the active site does not increase with added SDS, but that it is the ionic strength contribution that increases the reactivity of the nucleophile.

2.2   Introduction

The 20S proteasome is a large cylindrical macromolecular protease that is distributed from archaeons to all eukaryotes (Dahlmann et al., 1989; Tanaka and Ichihara, 1988). This molecule is responsible for most of the non-lysozomal protein turnover within the cell (Orlowski, 1990). An additional role is for the generation of Class II MHC peptide antigens in higher life forms (Dick et al., 1994). Because of the involvement of the proteasome in important cellular events, understanding its mechanism is of potential value in the development

of therapeutic agents.

The 20S proteasome from the archaeon *Thermoplasma acidophilum* provides a highly symmetrical model to study the role of quaternary structure on enzyme mechanism. The archael form and the eukaryotic form of the enzyme share nearly identical quaternary structure and high sequence homology (Dahlmann et al., 1989; Groll et al., 1997). Four stacked rings, containing 7 polypeptides each, form a barrel structure with the α-subunits forming the two outer rings and the 14 β subunits, which contain the active sites, forming the inner rings. The presence of a symmetrical number of active sites and seven-fold symmetry simplify the potential kinetic analysis when compared to the eukaryotic enzyme (Lowe et al., 1995). The yeast and human forms of the enzyme have seven different active subunits (Orlowski, 1990).

In vitro, the 20S proteasome is commonly activated by different treatments, e.g. the addition of fatty acids or detergents such as SDS (Yamada et al., 1998; Stein et al., 1996; Dahlmann, 1985). It remains unclear as to the physiological role played by lipids although it has been reported that a significant amount of proteasome is associated with the cell membrane in erythrocytes (Kinoshita et al., 1990). Furthermore, Mg^{2+} is a well known activator of proteasome activity, showing dramatic enhancements of proteolysis rates against peptide substrates, as is guanidinium (Akopian et al., 1997). However, the biochemical mechanisms of activation of the peptide hydrolysis activity of the proteasome remain unclear.

It has been proposed that SDS activates 20S proteasome function by facilitating access to the active site chamber by increasing the size of the pore formed by the α-subunits (Baumeister et al., 1998). To test this hypothesis, kinetics of inactivation by Z-LLLal were monitored as a function of activator concentrations. This peptide is a slow binding inhibitor of proteolytic function which permits the direct measurement of the association and dissociation rate constants (Morrison et al., 1988). The kinetic behavior of inhibition is expected to mimic that of early steps of proteolysis for small peptide substrates. The ability to directly measure the rates of association and dissociation of an active site-directed ligand has permitted us to determine whether the activators function by increasing the accessibility of the active site, or other steps in the reaction mechanism.

2.3 Materials and Methods

2.3.1 Materials

E. coli BL21 (DE3) cells containing the plasmid pRSET5a with the genes for the processed α- and β-subunits of the 20S proteasome from *Thermoplasma acidophilum* with a histidine affinity tag (Dolenc et al., 1998) were a generous gift of Dr. W. Baumeister (Department of Molecular Structural Biology, Max-Planck-Institute for Biochemistry Germany). Suc-LLVY-AMC was obtained from Bachem, USA, and used without further purification. Z-LLLal

was obtained from Sigma and used without further purification. Fatty acids were obtained as solids from Alltech/Applied Science and solubilized in DMF. All other reagents were at least enzyme grade and were obtained from Sigma or Fischer Scientific.

2.3.2 Proteasome Purification

E. coli cells containing the pRSET5a plasmid expressing mature *Thermoplasma acidophilum* proteasome with a C-terminal histidine affinity tag were grown in SOB media (Sambrook and Russell, 2001) containing 0.4% glucose at 37°C to an of OD_{600} of 0.6. At this point, 50 mM IPTG was added to induce overexpression of proteasome subunits and the cells were grown for another 4-6 hours. Cells were then pelleted via centrifugation at 10,000g, collected and stored frozen at -80°C until thawed for proteasome purification.

Pelleted cells were solubilized in 5 ml of sonication buffer (50 mM sodium phosphate, pH 8.0, 300 mM NaCl) per gram of cell pellet. Lysozyme was added (1 μl ml^{-1}) and the mixture was placed on ice for 45 min. Protease inhibitors, leupeptin and aprotinin, were added to a final concentration of 1 μg ml^{-1} and the mixture subjected to sonication with six cycles of 30 s blasts and 30 s on ice. RNase and DNase I were added to 1 μg ml^{-1} and the mixture left at room temperature for 1 h. Cell debris was then pelleted by centrifugation at 10,000g (4°C, 30 min). This supernatant was batch loaded to a 5 ml bed volume NiNTA affinity column (QIAGEN) for 1 h on ice. The column was

washed at a flow of 12 ml h^{-1} for six h with sonication buffer, six h with wash buffer (50 mM sodium phosphate, pH 6.0, 10% glycerol, 300 mM NaCl) with a one h gradient between the two buffers. Recombinant 20S proteasome was eluted either using a three h gradient from 0 to 0.5 M imidazole in wash buffer or by isocratic elution at 0.25 M imidazole in wash buffer. Proteasome fractions were identified by proteolytic activity against the substrate Suc-LLVY-AMC and assayed for purity by SDS-PAGE methods. Pure (as assayed to be at least 90% proteasome specific bands on an SDS-PAGE gel), high concentration fractions were pooled and dialyzed against wash buffer to remove imidazole. Samples were then aliquotted into 200 μl fractions and stored at -80°C for further use. Under these conditions, activity remained constant for at least 8 mos.

2.3.3   Electron Microscopy

Purified enzyme was passed through a Sephadex G10 desalting column equilibrated with ddH$_2$O (Penefsky and S., 1977) to remove any salts and buffers, absorbed at a concentration of 0.5 mg ml^{-1} onto a 600 mesh copper grid for 30 seconds and negatively stained with 2% ammonium molybdate (pH 7.8) for 1 minute. Micrographs were taken at 60,000 times magnification using a Jeol JEM 600 model TEM instrument, with a beam current of 80 mA and an acceleration voltage of 80V,

2.3.4 Mass Spectrometry

Purified enzyme (400 μg) in storage buffer was dialyzed (4°C, with stirring) against 500 ml buffer containing 100 mM NaCl and 50 mM Na-phosphate (pH 6.0) for six hours, then buffer containing 50 mM Na-phosphate (pH 6.0) overnight, then buffer containing 10 mM Na-phosphate (pH 6.0) for at least six hours before passage over a Sephadex G10 column (1 cm x 8 cm) equilibrated with distilled water. Fractions (0.5 ml) were collected, analyzed by UV/Vis spectroscopy and a small aliquot was analyzed by the method of Bradford (Bradford and M., 1976). Purified, desalted samples were diluted 1:2 with methanol, acetic acid and water (1:1:10, vol/vol/vol), and infused at a flow rate of 5.0 μl min^{-1} through an electrospray ionization source.

2.3.5 Proteolytic Assays

Hydrolysis of Suc-LLVY-AMC solubilized in DMF (final concentration not more than 0.1% DMF) was measured in TAPS buffer (25 mM, pH 8.1 at 45°C, titrated using NaOH or NH$_4$OH) using an Applied Photophysics SX18 stopped flow fluorimeter; substrate and enzyme concentration were as listed. Unless otherwise noted, NaCl was added to a final concentration of 100 mM, EDTA to a final concentration of 250 μM, SDS to a concentration of 0.008% (w/v), and substrate concentrations were typically at 20 μM. This concentration of substrate was chosen as the approximate K_m for the substrate Suc-LLVY-AMC (Figure 5.1) (Stein et al., 1996). At concentrations above 40 μM,

substrate inhibition occurs, as shown in Figure 5.1. To monitor activity with the substrate Suc-LLVY-AMC, free AMC production was monitored using an excitation wavelength of 340 nm and emission above 350 nm was monitored via a cut-on filter (Oriel, Stratford, CA, catalog number 51260) used with the emission detection photomultiplier. Unless otherwise noted, enzyme concentrations were approximately 20 nM. This is illustrated in Figure 2.1 showing the hydrolysis of the peptide Suc-LLVY-AMC to yield the free AMC product.

2.3.6   Inhibitor Studies

Inhibition of the proteasome was done using the peptide aldehyde inhibitor, Z-LLLal (illustrated in Figure 2.2) solubilized in DMF (final concentration less than 0.1%). Enzyme activity was followed by monitoring the activity as a function of time using the substrate Suc-LLVY-AMC. To measure the rate constant for binding, k_{on}, enzyme in buffer was reacted against a solution containing both substrate and inhibitor. The unimolecular dissociation rate constant k_{off} was measured using the following methods. First preincubating enzyme and inhibitor at 45°C overnight to form the enzyme-inhibitor adduct. The proteasome-inhibitor complex was then diluted 10:1 into excess substrate in buffer. To measure the inactivation parameter, k_{inact}, substrate was reacted with enzyme plus inhibitor and aliquots were taken at short time intervals to measure the activity against the substrate Suc-LLVY-AMC.
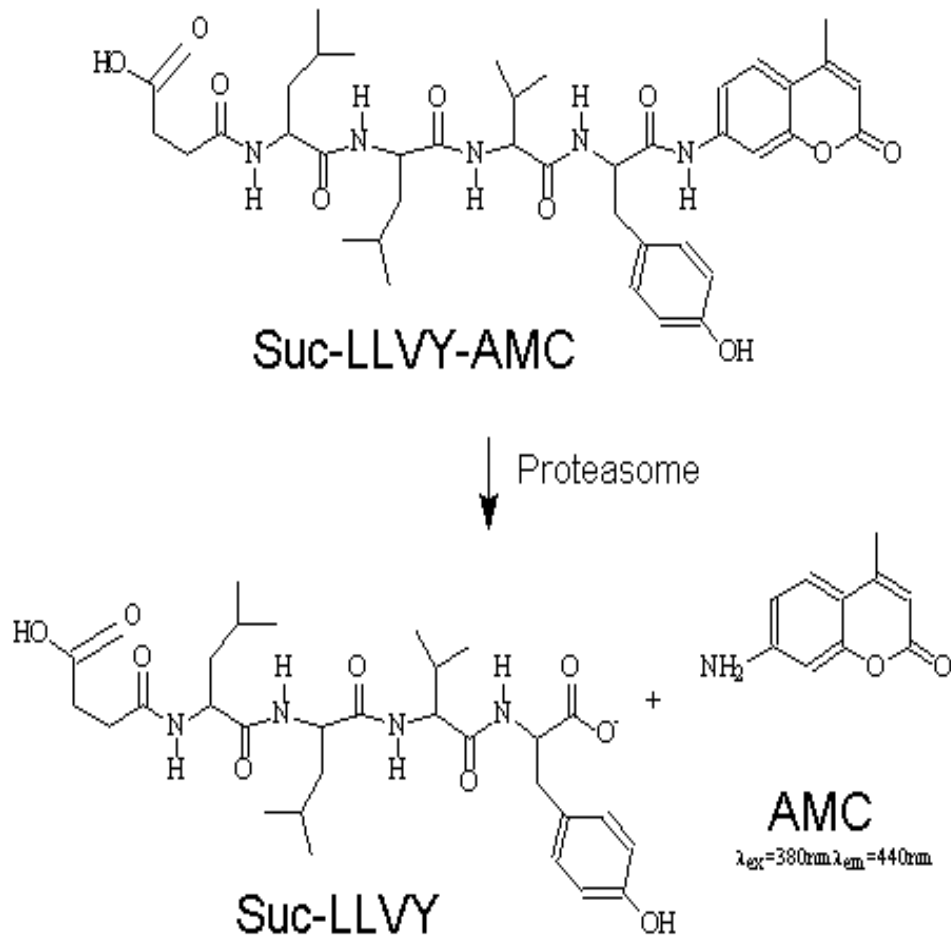
Figure 2.1: Substrate Peptide Suc-LLVY-AMC and Products
Schematic showing the intact substrate peptide Suc-LLVY-AMC and the products generated by cleavage of the tyrosyl-AMC bond. It is only this event that is detected when the production of free AMC is measured.
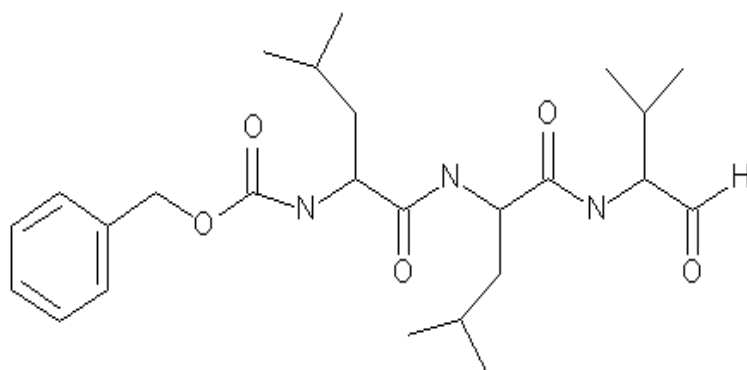
Figure 2.2: Structure of Z-LLLal Inhibitor

The tripeptide aldehyde inhibitor attaches itself to the enzyme's active site through the C-terminal aldehyde functional group. For the sake of clarity, only the terminal hydrogen is shown.

2.3.7 Data Analysis

Fluorescent voltages were converted to concentration by generating a standard curve each day of known free AMC concentrations. Both initial (when distinct) and steady state rates were calculated from linear fits to portions of the data. Initial rates were calculated from a linear fit to the first 200 seconds of the data; steady state velocity was calculated from the last 200 seconds of the data (1000 seconds total collected). Inhibition kinetics were fit by the method of Morrison and Walsh (Morrison et al., 1988) to describe a slow binding inhibitor. The time courses in the presence of inhibitor were fit to Equation 2.1 to obtain the observed binding rates of the inhibitor molecule.

$$P = P_0 + \frac{(v_i - v_f)}{k_{obs}} + \frac{(v_f - v_i)e^{-k_{obs}t}}{k_{obs}} + v_f t \tag{2.1}$$

In this equation, k_{obs} is the pseudo-first order rate constant for the change in velocity, P is the amount of product at time t, P_0 is the amount of product present initially, and v_i and v_f are the initial and final velocities, respectively. The association and dissociation rate constants, k_{on} and k_{off}, were obtained from the linear fit of k_{obs} as a function of inhibitor concentrations (Equation 2.2)

$$k_{obs} = k_{on}[I] + k_{off} \tag{2.2}$$

K_i, the inhibition constant, was measured using the equation

$$\frac{v_{obs}}{v_c} = \frac{1}{1 + \frac{I}{K_i}} \tag{2.3}$$

where v_{obs} is the observed steady state activity in the presence of inhibitor, and v_c is the control velocity in the absence of inhibitor. The inactivation parameter, k_{inact}, was measured by monitoring the initial activity as a function of time and fit using the equation

$$\ln(\frac{v_{obs}}{v_c}) = -k_{inact}[I]t \qquad (2.4)$$

which describes an exponential decay of activity.

Thermodynamic analyses on the transition state and the tetrahedral intermediate state were done using Equations 2.5 and 2.6, respectively.

$$\Delta\Delta G = -RTln(\frac{K_i^0}{K_i^{MgCl_2}}) \qquad (2.5)$$

$$\Delta\Delta G = -RTln(\frac{k_{on}^0}{k_{on}^{MgCl_2}}) \qquad (2.6)$$

K_i^0 is the value of K_i in no added magnesium, and $K_i^{MgCl_2}$ is the value of K_i in the presence of added magnesium. Similarly, k_{on}^0 is the value of k_{on} in the absence of magnesium and $k_{on}^{MgCl_2}$ is the value of k_{on} in increasing concentrations of magnesium.

Nonlinear least squares analyses were performed using Grafit 3.01 (Eritha-cus Software, Ltd.).

2.4 Results

2.4.1 Expression and Assembly of Recombinant Enzyme

Both ESI-MS and TEM analysis was performed to assess the correct expression of recombinant 20S proteasome, as well as to assess the assembly of functional, intact particles. ESI-MS analysis gave three major peaks, one at 23,100 m/z, one at 25,417 m/z and one at 25,805 m/z, with relative peak heights of 1:1:3. The peaks at 23,100 and 25,805 correspond to the mature, processed β-subunit with a C-terminal His$_6$ affinity label and the α-subunit, respectively. The peak at 25,417 m/z could correspond to an N-terminally truncated α-subunit, suggesting the loss of the first three residues of this subunit (MQQ). This truncation is not expected to interfere with enzyme activity on the basis of structural analysis which shows that the N-terminus of the α-subunit is distal from the active site or end pore of the cylinder (Lowe et al., 1995).

Analysis via TEM showed that overexpressed, purified enzyme was correctly assembled into cylindrical oligomers. At 60,000-fold magnification, our results were comparable with those published previously (Puhler et al., 1992). Visible were several proteasome assemblies on their sides with a small number visible standing on their ends. The pore is clearly visible in the standing proteasomes analyzed while the four rings are visible in the proteasomes existing on their sides.

These results, together with those of other groups (Akopian et al., 1997)

who are working with the same recombinant expression system, suggest to us that proteasome assembly is correct in the *E. coli* overexpression system.

2.4.2 Z-LLLal is a Reversible, Slow Binding Inhibitor

Various serine protease inhibitors act against the activity of the 20S proteasome from *T. acidophilum*, including peptide aldehyde inhibitors (Akopian et al., 1997; Seemuller et al., 1995a). Shown in Figure 2.3 are the progress curves of proteolytic activity against the substrate Suc-LLVY-AMC in the presence of varying concentrations of the inhibitor Z-LLLal. The onset of inhibition is slow, with the observed half life being between 1 and 5 min., typical of slow binding inhibitors (Morrison et al., 1988). As shown in Figure 2.4, this inhibition is dependent upon the concentration of the inhibitor present. The reversibility of the inhibition is shown in Figure 2.5 in which enzyme equilibrated with Z-LLLal is diluted into substrate in buffer. The slow recovery of proteolytic activity against the substrate Suc-LLVY-AMC demonstrates the reversibility of inhibition by the peptide aldehyde Z-LLLal, as noted previously (Williams et al., 1979).
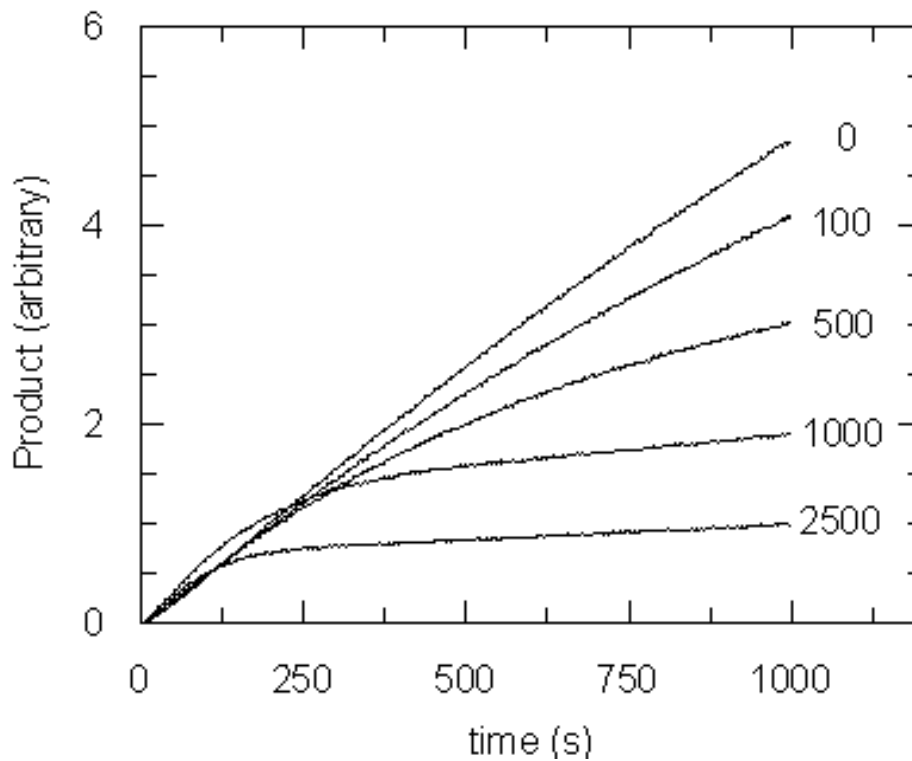
Figure 2.3: Effect of Peptide Aldehyde Z-LLLal on Proteasome Activity
The progress curves of proteasome activity with the substrate Suc-LLVY-AMC
in the presence of the peptide aldehyde inhibitor Z-LLLal are shown with the
nanomolar concentrations of inhibitor marked in the figure. The slow approach
to a steady state activity is a common trait of a slow acting inhibitor. The
product axis is shown in the fluorescence voltages detected.
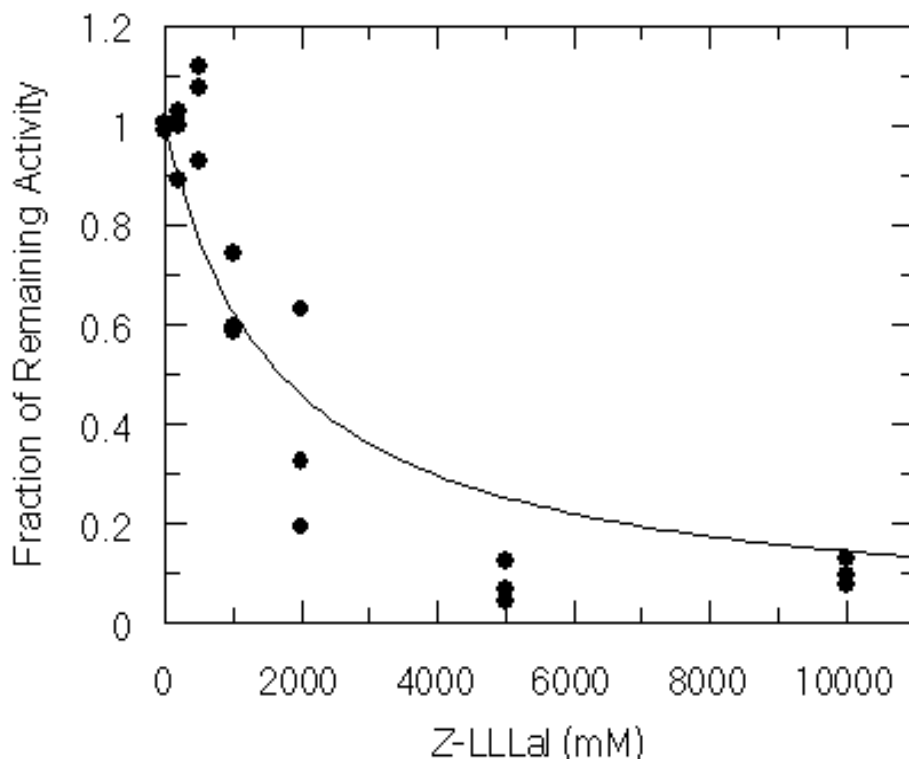
Figure 2.4: Fraction of Remaining Activity vs Inhibitor Concentration
To calculate the inhibition constant K_i, enzyme and substrate were reacted in varying concentrations of the inhibitor Z-LLLal and the activity measured. Plotting the fraction of remaining activity, defined in Equation 2.3, against the inhibitor concentration allows for the calculation of the constant K_i. In this experiment purified recombinant 20S proteasome from *T. acidophilum* (50 nM) was reacted with 20 μM substrate in buffer (100 mM NaCl, 25 mM TAPS, pH 8.1, 250 μM EDTA, 0.010% SDS, 50 mM MgCl$_2$) at 45°C. When analyzed using this equation, this data yields a K_i value of 730 $\pm$160 nM.
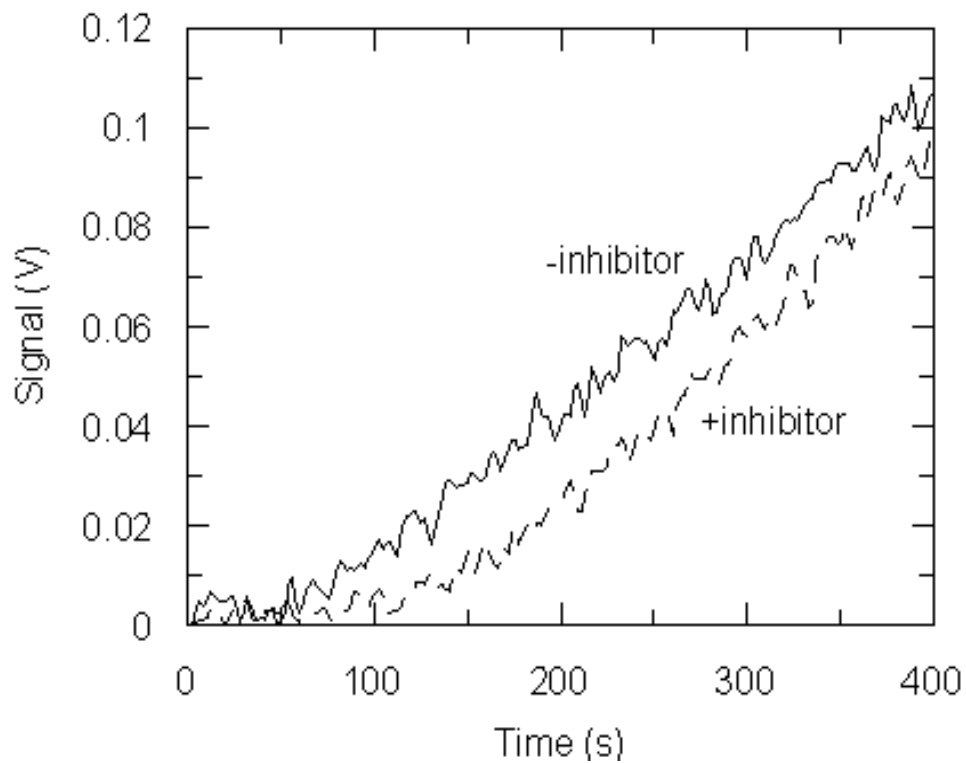
Figure 2.5: Recovery of Activity After Dilution

Enzyme and peptide aldehyde inhibitor Z-LLLal were incubated in buffer at 45°C overnight to form the enzyme-inhibitor adduct. This was then diluted ten-fold into a pool of substrate Suc-LLVY-AMC in buffer and the activity measured. The slow recovery of activity demonstrates the reversibility of inhibition by Z-LLLal. Shown in this Figure are representative traces in the presence and absence of inhibitor.

From these progress curves, both the rate constants for the association and dissociation rate constants of the inhibitor from the proteasome active site, k_{on} and k_{off}, can be obtained as described in *Methods* (Figure 2.6). In Figure 2.7, proteasome was reacted with varying concentrations of inhibitor, aliquots were taken at time intervals and the pre-steady state activity against the peptide substrate Suc-LLVY-AMC was measured. The observed slow loss of enzyme activity is consistent with that seen before for peptide aldehyde inhibitor on proteasome function (Akopian et al., 1997). The exponential decay of activity was analyzed as described in *Methods* to determine the rate constant of inactivation, k_{inact}, as illustrated in Figure 2.8.

2.4.3 Effect of SDS on Inhibitor Binding Constants

Activation of the 20S proteasome by SDS has been observed by several groups before (Stein et al., 1996; Baumeister et al., 1998). This activation has been shown to be biphasic, showing a brief increase in activity at low concentrations of SDS, followed by a decrease in activity with increased SDS concentrations. Shown in Figure 2.9 is a typical time trace showing the increased rate of production of free AMC from the substrate Suc-LLVY-AMC in the presence of 0.050% SDS, when compared to the activity in the absence of SDS. This is also displayed in Figure 2.10, which shows the biphasic effect of SDS on enzyme activity, ie. stimulation followed by a marked inhibition of proteolytic activity. These results are similar to those reported by other groups studying

proteasome activation by SDS (Stein et al., 1996; Dahlmann et al., 1993).

The most direct manner in which SDS could enhance peptide hydrolysis activity is by increasing the forward rate constants of early steps of the mechanism. Possible actions include facilitated access for the substrate to the catalytic chamber (Baumeister et al., 1998) and an increased reactivity of the nucleophilic threonine side chain. As described above, these parameters can be directly measured by monitoring the inhibition rate constants for the small peptide inhibitor as a function of SDS concentrations. As depicted in Figure 2.11, enzyme and substrate with varying concentrations of inhibitor were reacted in buffer while the concentration of SDS was varied. This rate constant, k_{on}, measures the reactivity of the nucleophile in response to added detergent. Figure 2.10 shows the peptide hydrolysis activity as a function of SDS concentration, which is consistent with data from other groups (Dahlmann, 1985). In Figure 2.12, enzyme was reacted with differing concentrations of inhibitor in buffer and aliquots were taken at time intervals and the activity measured with the substrate Suc-LLVY-AMC, measuring the parameter k_{inact}. This parameter is a measurement of the accessibility of the active site to the small peptides used in the experiment.
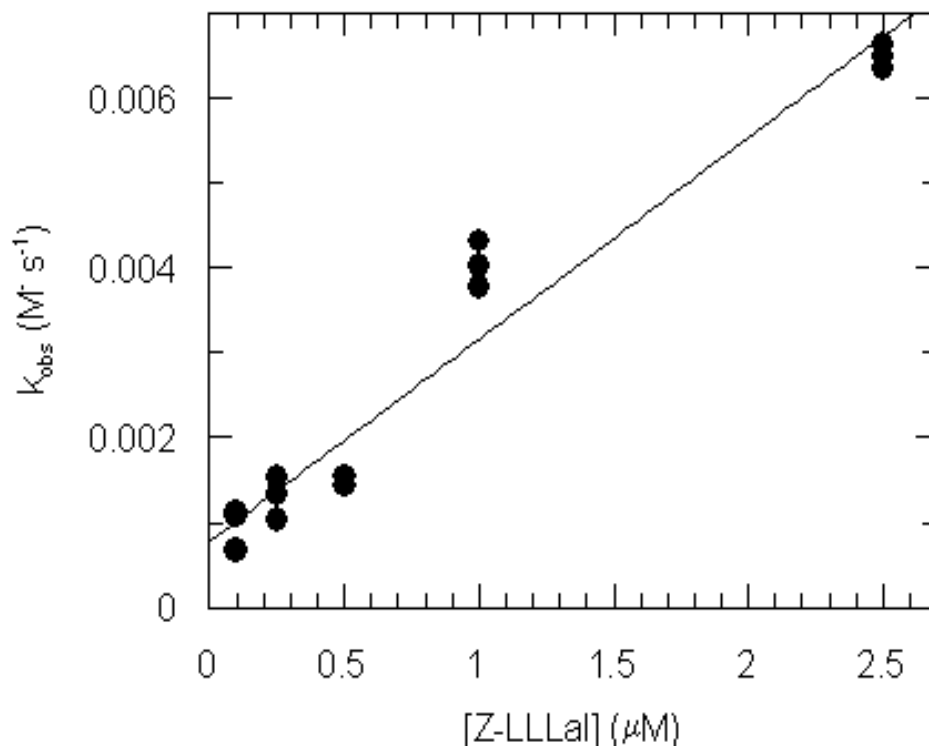
Figure 2.6: Calculation of Inhibitor Binding Constant

To calculate the inhibitor binding constant, data such as that in Figure 2.3 was fit to Equation 2.1 to obtain the value k_{obs}. This was then plotted as a function of inhibitor concentration and analyzed using Equation 2.2 to obtain the binding constants k_{on} and k_{off}. Conditions were the same as those in Figure 2.4. When analyzed, the data shown above yields a value for k_{on} of 2378 $M^{-1}s^{-1}$ and for k_{off} a value of 0.0008 s^{-1}.
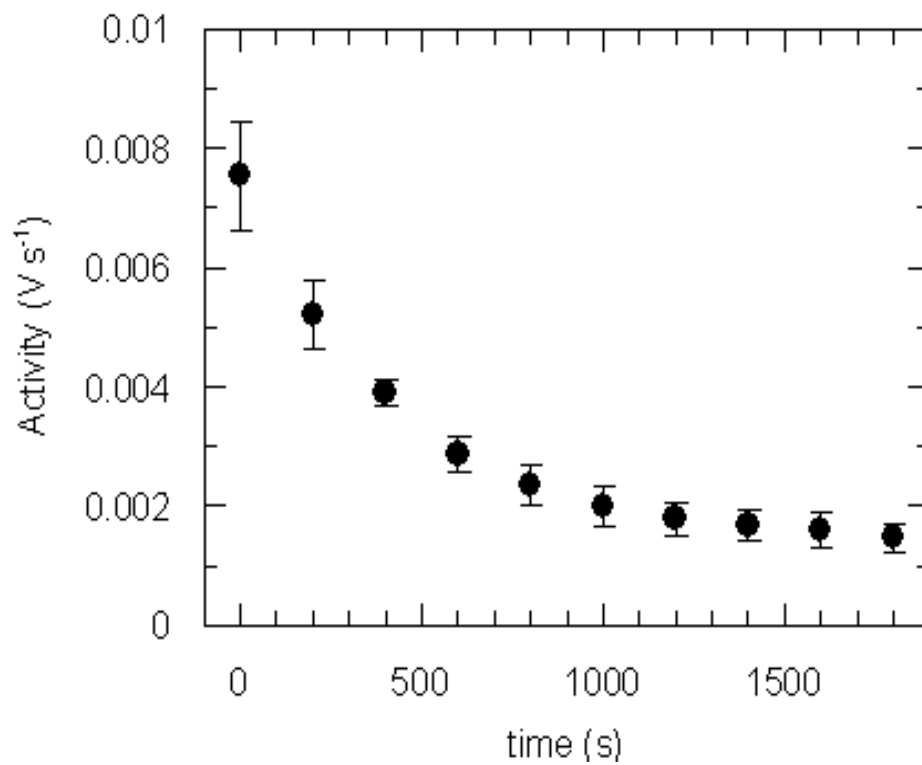
Figure 2.7: Time-Dependent Inactivation of the Proteasome by Z-LLLal
As described in *Methods*, enzyme and inhibitor were mixed together in buffer and reacted every 200 seconds with substrate, Suc-LLVY-AMC, and the activity measured. The kinetics of inactivation were best characterized by a first order process, explified by Equation 2.4 describing a single exponential fit. This method was used later to calculate inactivation parameters in varying concentrations of SDS.
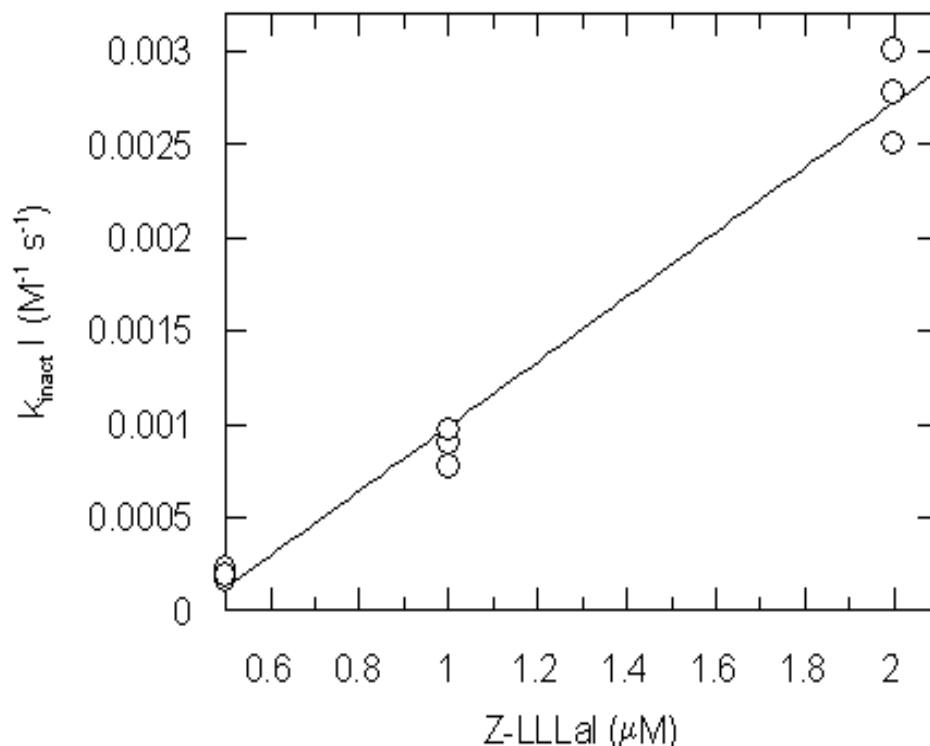
Figure 2.8: Calculation of k_{inact}

Data from the time course of inactivation of the 20S proteasome were analyzed using Equation 2.4 to yield the parameter $k_{inact}I$, the inactivation parameter dependent on the concentration of inactivator. This was then analyzed as shown in this figure to yield the constant k_{inact}. The data in this experiment was collected using TAPS buffer with 0.004% SDS under the standard assay conditions. When analyzed as described in *Methods*, this data yields a value of $k_{inact}I$ of 1732 $\pm$90 s^{-1}.

2.4.4   Effect of Other Detergents

To test the generalizability of this SDS activation, PEG and Triton X-100 were examined to test their ability to activate the proteasome. As shown in Figure 2.13, Triton X-100 is capable of moderate amounts of enzyme activation. Triton X-100, a non-ionic polyethoxy polymer, doesn't stimulate activity as much as SDS does although there is a detectable amount. PEG molecules between 2000 and 8000 Da are also capable of enzyme activation (data not shown). Both PEG and Triton X-100 are non-ionic polymers with carbon and oxygen linked backbone chains. Because of this they are likely to interact with the proteasome in a similar fashion, and modulate activity in a similar manner, as well.

Immediately observable in theses Figures (2.11-2.12) is the lack of a trend similar to that observed for substrate hydrolysis (Figure 2.10). There is no increase in the rate constants of inhibition by this small peptide aldehyde over the range of SDS that increases proteolytic activity against the tetrapeptide substrate, suggesting no change in the reactivity of the nucleophilic base or the access to the active site chamber as detergent is added.
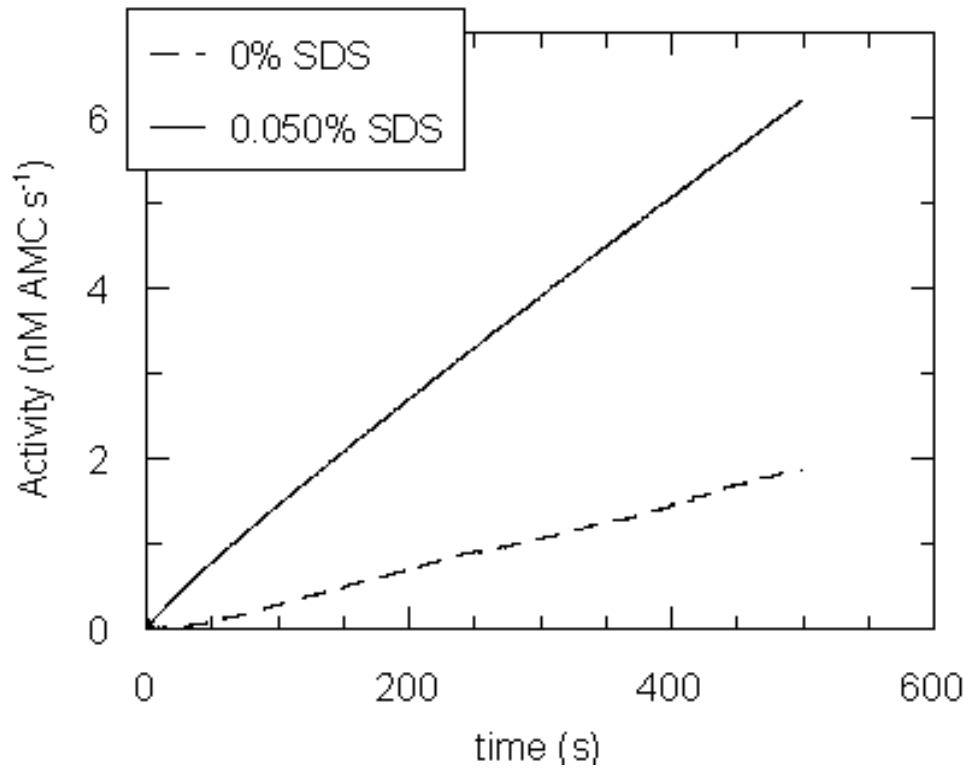
Figure 2.9: Effect of SDS on AMC Production

SDS was added to the reaction mixture between proteasome and substrate peptide, Suc-LLVY-AMC, and the activity measured as described in *Methods*. The time traces of AMC production are shown for both 0% SDS and 0.050% SDS (wt vol^{-1} %). In this experiment, the enzyme concentration was approximately 0.12 μM.
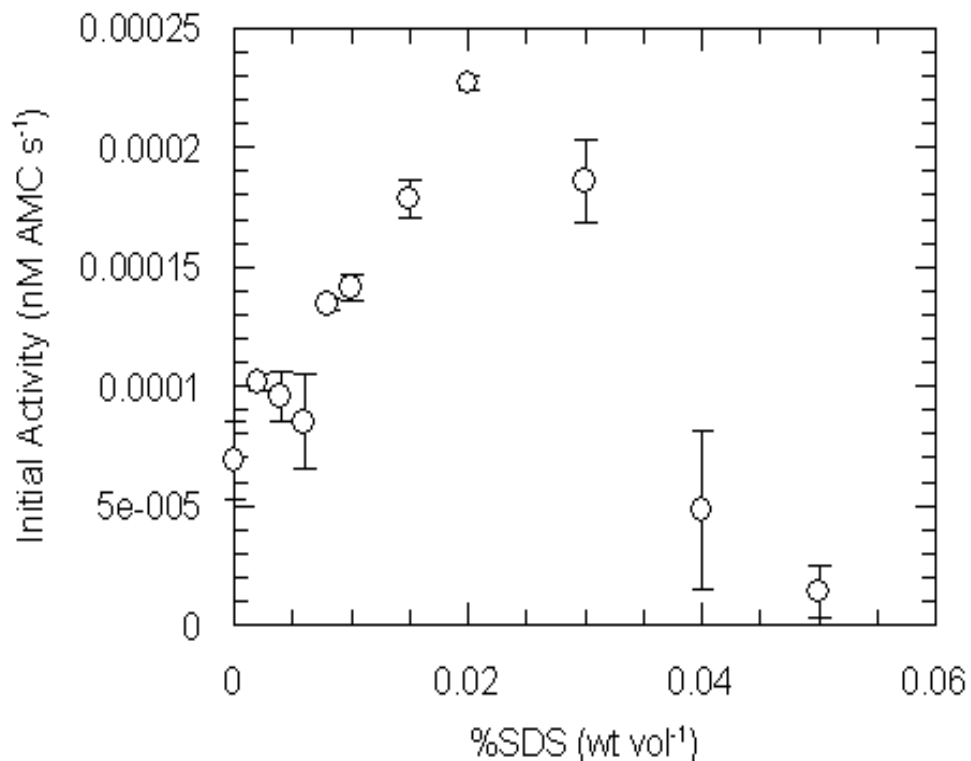
Figure 2.10: Effect of SDS on Peptidase Activity

The steady state enzyme activity was measured as a function of SDS concentrations (wt vol^{-1} %) using the peptide substrate Suc-LLVY-AMC. The average of at least three measurements are shown with the standard error indicated. The peak activity occurs under these conditions (25 mM TAPS buffer, pH 8.1, 100 mM NaCl, 45°C) is 0.020% SDS, with an enzyme concentration of approximately 0.05 μM.
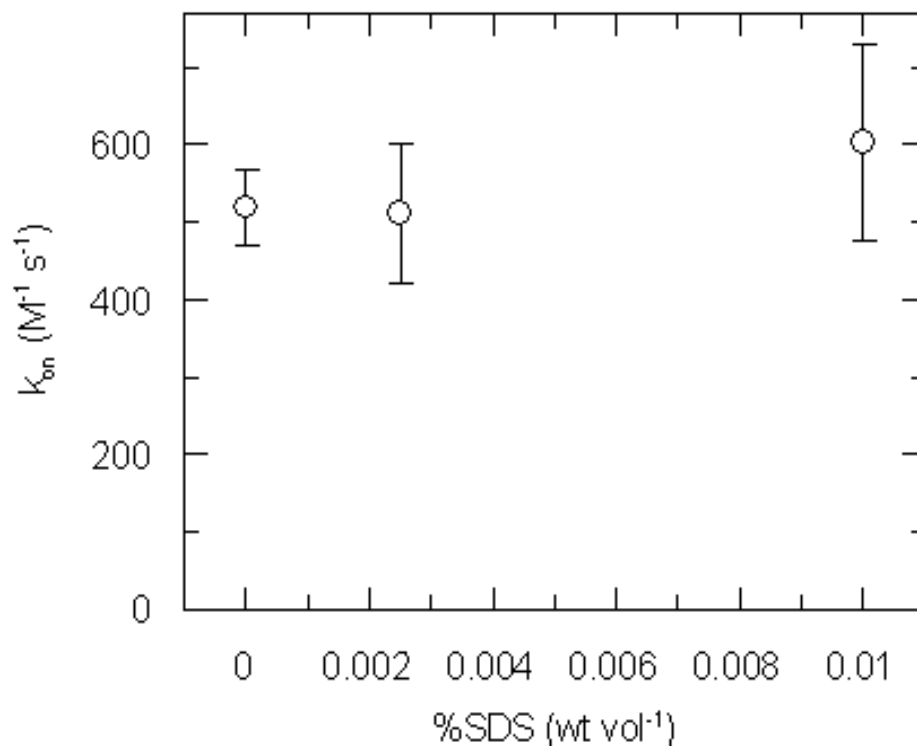
Figure 2.11: Effect of SDS on Inhibitor Binding Rate

To examine the role of SDS in early proteolytic events, the rate of inhibitor binding was measured at varying concentrations of SDS. Over this concentration range a strong increase in proteolytic activity is seen, yet no effect on inhibitor binding rate is observed. This suggests that activation by SDS is occurring sometime after the initial nucleophilic attack.
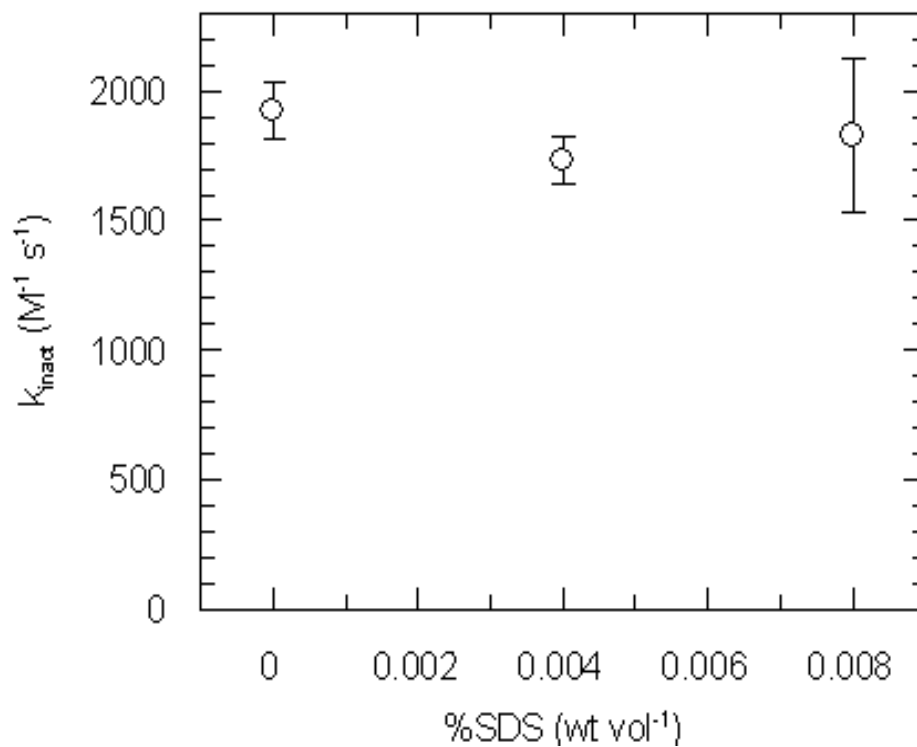
Figure 2.12: Enzyme Inactivation Rate Response to SDS

The rate of inactivation kinact was measured as a function of SDS concentration as described in *Methods* to examine the change in access to the active site chamber. The lack of an increase in k_{inact} over this range differs significantly from the enzyme activity in these conditions, where strong increase in the rate of proteolysis of Suc-LLVY-AMC is observed. This suggests that it is not access to the active site chamber that is being enhanced, rather some other step.

2.4.5 Effect of Fatty Acids

The *in vivo* proteasome activation experiments described above and in the preceeding literature have focused on SDS or other non-natural molecules. These are often thought to mimic the effects of fatty acids or other natural long chain polymers found *in vivo*. To investigate the validity of this assumption, fatty acid chains of a variety of lengths, from 12 to 20 carbon atoms, were tested for their ability to enhance proteasome specific peptidase activity. This size range was chosen to mimic the size of SDS (12 carbons) as well as the size range of some of the naturally occurring fatty acids found in *T. acidophilum* (Shimada et al., 2002; Langworthy and A., 1977; Langworthy et al., 1972).

Only one of the tested fatty acid moleculess, *cis*-5 C_{12}, provided any measurable amount of enzyme activation, which was approximately two-fold above basal (0% fatty acid) levels of activity. The other lipid molecules tested either failed to enhance activity over a reasonable concentration range (0-0.1% wt vol^{-1}), or actually provided a modest level of inhibition (up to 50% inhibition, data not shown).
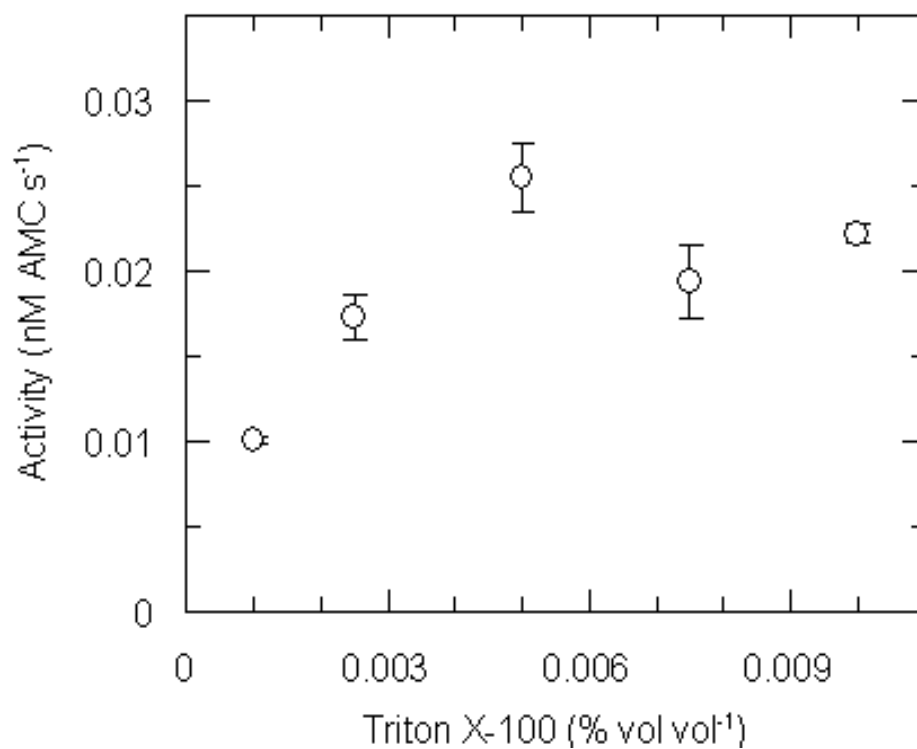
Figure 2.13: Effect of Triton X-100 on Enzyme Activity

To test the effect of the non-ionic detergent Triton X-100 on enzyme activity, increasing amounts were added to the reaction between the enzyme and substrate peptide Suc-LLVY-AMC. The average of three data points, with standard errors indicated, are shown for the pre-steady state activity.

2.4.6 SDS Enhances the Rate of Inhibitor Release

The dissociation rate constant, k_{off}, for Z-LLLal was determined by diluting the enzyme-inhibitor adduct into a pool of excess substrate in buffer. The first order rate constant for inhibitor release from the enzyme in the presence of SDS is shown in Figure 2.14. The data indicate that increasing SDS concentrations increase the rate constant for the dissociation of the inhibitor Z-LLLal from the proteasome active site.
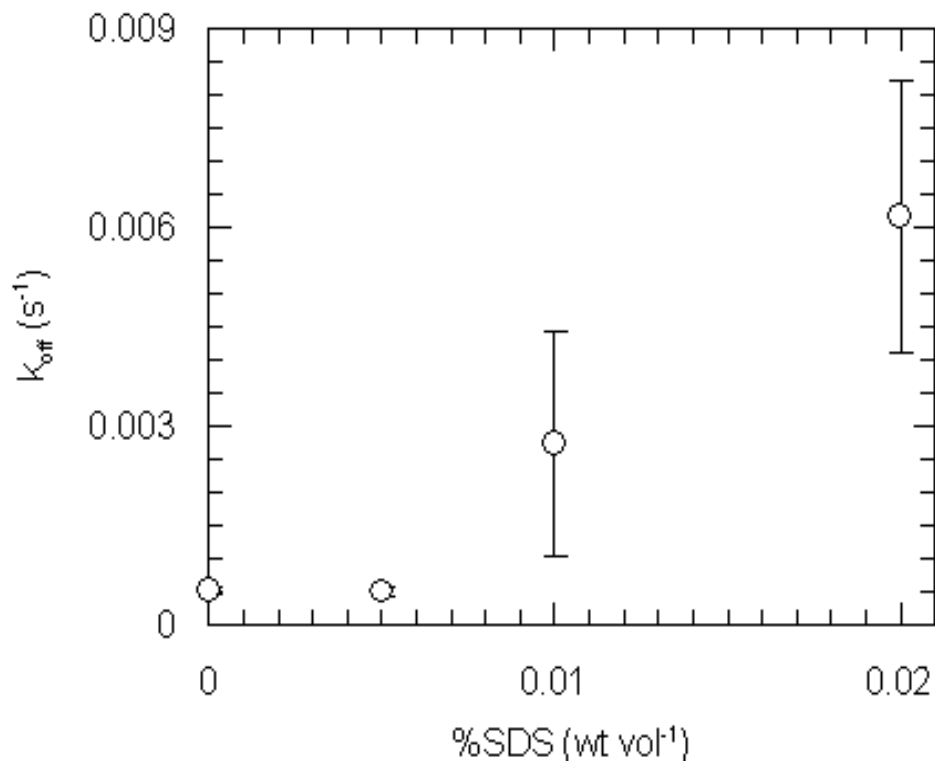
Figure 2.14: Effect of SDS on Inhibitor Release Constant

Purified proteasome and peptide aldehyde inhibitor Z-LLLal were incubated at 45°C in buffer overnight at various SDS concentrations. This was then diluted 10:1 into a pool of substrate in buffer and the rate of activity recovery measured. The increase in the rate constant for inhibitor release from the proteasome active site suggests the effect of SDS is at the stage of acyl enzyme decomposition, which would lead to an increase in activity.

2.4.7 Mg^{2+} Enhances the Rate of Proteolytic Attack

The rate constant of inhibition by the peptide aldehyde was measured as a function of increasing concentrations of magnesium chloride. In the concentration range from 0 - 0.5M, there is approximately a six-fold increase in proteolytic activity against the tetrapeptide Suc-LLVY-AMC, analogous to the enhancement found by Aikopain et al. (Akopian et al., 1997). This effect is shown in two time traces measuring the production of free AMC from the peptide Suc-LLVY-AMC in the absence and presence of 0.5 M magnesium (Figure 2.15). This effect is pronounced with both calcium (Figure 2.16) and magnesium (Figure 2.17) showing similar levels of activation over the same concentration range.

As shown in Figure 2.18, k_{on} for the inhibitor increases linearly with increasing magnesium chloride from 20 to 500 mM. Maximal observed stimulation of the pre-steady state activity of the enzyme against this substrate over this range is an 8-fold increase. A similar effect is observed with the release rate constant, k_{off}, as shown in Figure 2.19. A biphasic effect is found, with a maximal value observed at 100 mM magnesium. When analyzed more closely, the effect of magnesium on the inhibition constant, K_i, show a marked increase over this concentration range tested here, with a cumulative effect on both k_{on} and k_{off}. This is shown in Figure 2.20.
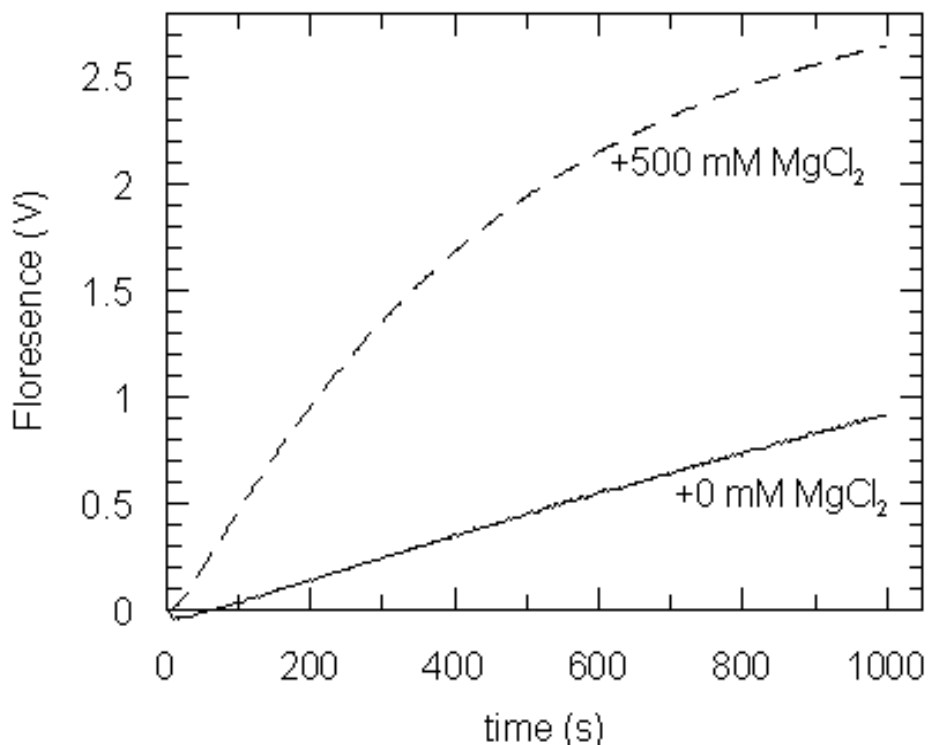
Figure 2.15: Effect of Magnesium on Enzyme Activity Profile

The effect of the activator magnesium was tested on the hydrolysis of the substrate peptide Suc-LLVY-AMC by the 20S proteasome. Both the pre-steady state and the steady state activities are affected by the presence of magnesium. In this experiment, purified enzyme (50 nM) was reacted with 20 μM substrate in buffer (100 mM $MgCl_2$, 25 mM TAPS, pH 8.1, 250 μM EDTA, 0.010% SDS) at 45°C. In this plot the signal due to the released AMC in volts is plotted as a function of time. This signal was converted to the concentration of AMC for analysis by using a standard curve.
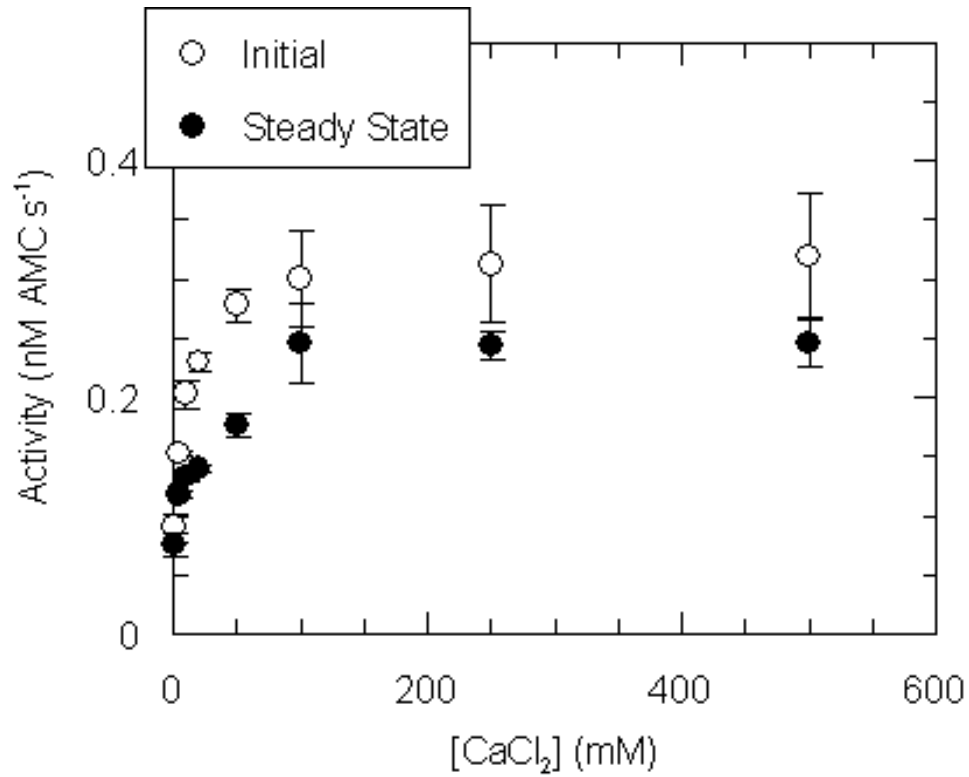
Figure 2.16: Effect of Calcium on Activity

To examine the effect of the divalent metal ion calcium on the peptidase activity of the proteasome, the activity against the substrate peptide Suc-LLVY-AMC was measured in increasing amounts of $CaCl_2$. Both the pre-steady state (open symbols) and the steady state (filled symbols) activity values were measured.
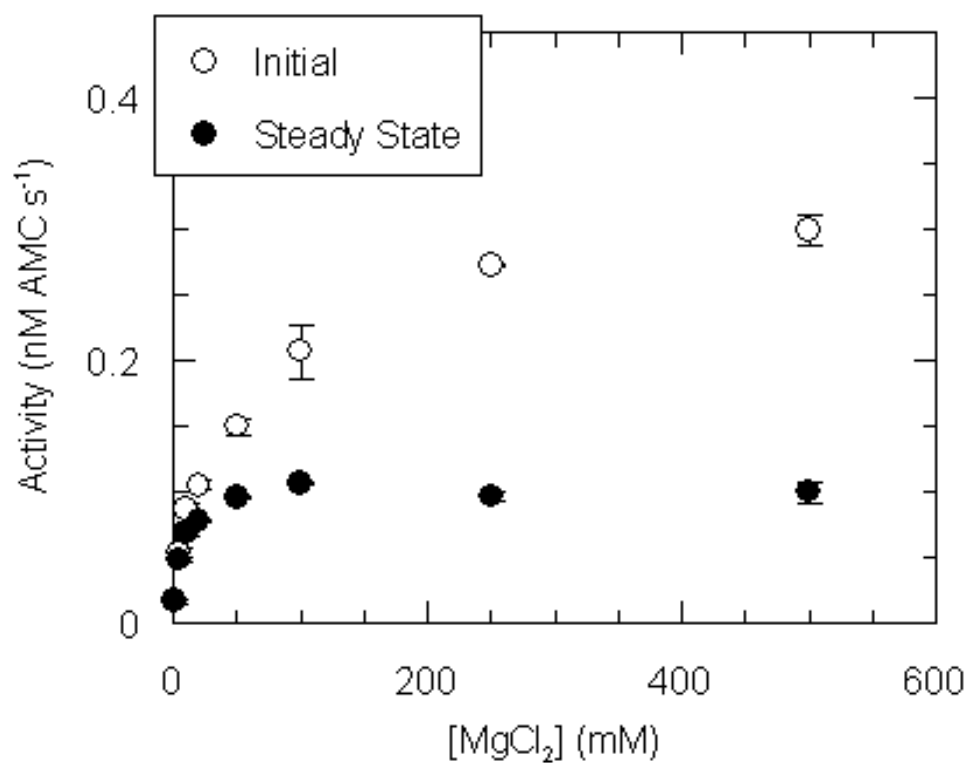
Figure 2.17: Effect of Magnesium on Activity

The response of the peptidase activity of the proteasome was measured as a function of $MgCl_2$ concentration. Both the initial (open symbols) and steady state (filled symbols) activities were measured as described in *Methods*.
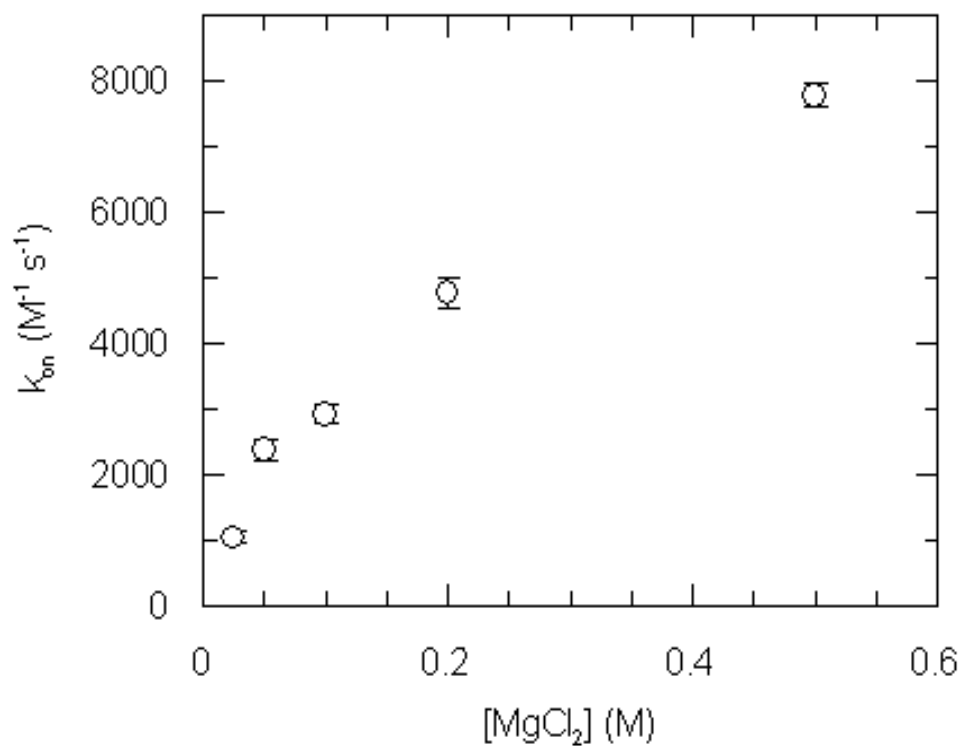
Figure 2.18: Effect of Magnesium on Inhibitor Binding Rate

The peptide aldehyde inhibitor Z-LLLal was reacted with 20S proteasome in varying concentrations of magnesium chloride and the rate constant of inhibition, k_{on}, was measured. The inhibition rate increases with increasing concentrations of magnesium, suggesting the effect is at an early stage in the mechanism, possibly the initial nucleophilic attack.
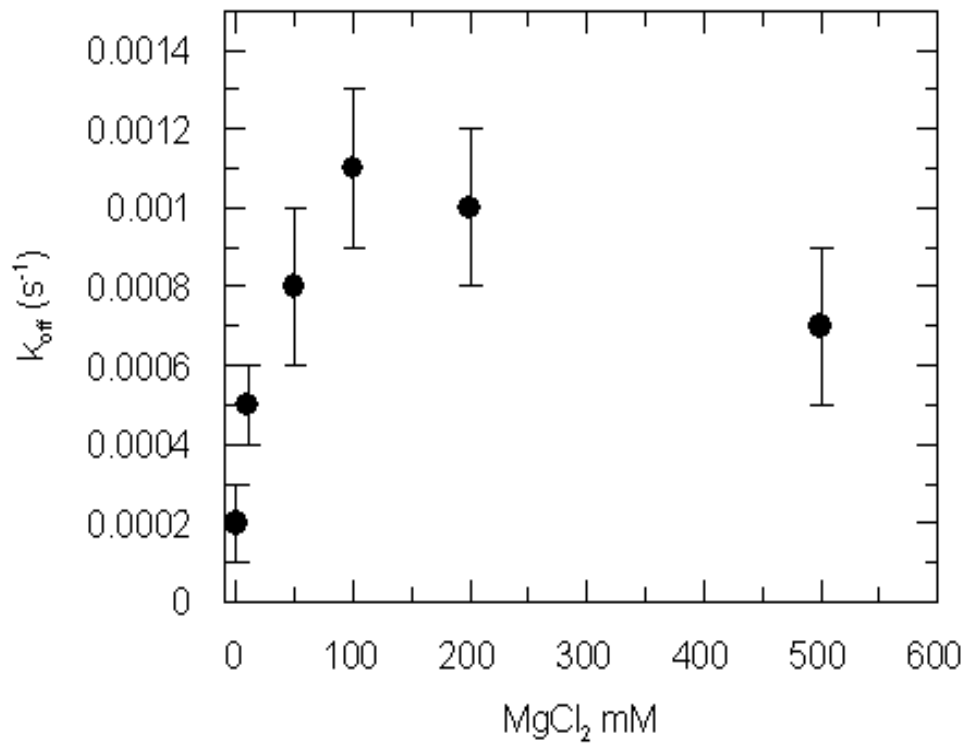
Figure 2.19: Effect of Magnesium on Release Rate of Inhibitor

The inactivation parameter, k_{off}, was measured as described in *Methods* and Equation 2.2 in response to an increase in the concentration of Mg^{2+}. After an initial increase of approximately four-fold, a maximal value is reached at approximately 100 mM magnesium, with a slight decrease as the concentration approaches 500 mM magnesium.
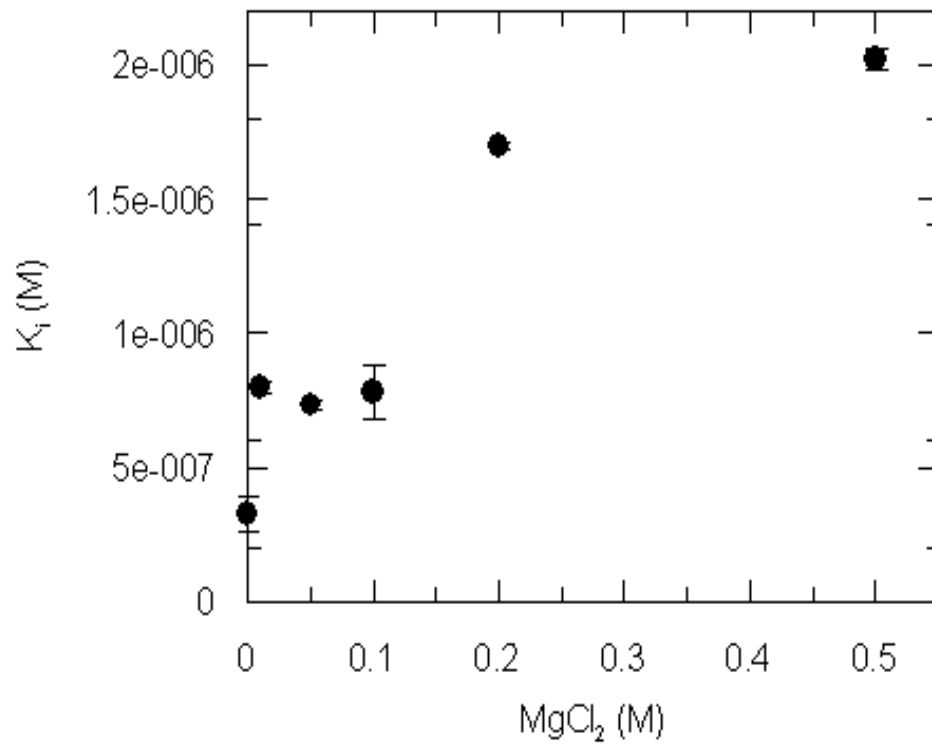
Figure 2.20: Effect of Magnesium on Inhibition Constant K_i

Inactivation data such as that shown in Figure 2.3 was analyzed to obtain the inactivation constat K_i as described in Equation 2.3. This parameter was analyzed as a function of Mg^{2+} concentration, and shows a hyperbolic dependence of K_i on magnesium concentration.

2.4.8 Salt Induced Activation is Largely Due to Ionic Strength

One of the issues that is often overlooked in studying magnesium chloride activation of the proteasome is the effect of ionic strength as opposed to a specific metal ion effect. To test if there is an effect specific to Mg^{2+}, various salts were added to concentrations to maintain 1.5 M ionic strength. As shown in Figure 2.21, KCl, NaCl, Na-acetate, and LiCl all provide similar amounts of activation as $MgCl_2$ at 1.5 M ionic strength. This strongly suggests that the activation may be largely due to ionic strength.

To further examine the specific role of magnesium in activation, the ionic strength was kept constant at 1.5 M by compensating with potassium chloride and the rate of inhibitor binding was measured. As shown in Figure 2.22, at low concentrations there is a noticeable effect specific from magnesium. Above 100 mM magnesium there is no is appreciable proteolytic activation observed. From this it can be seen that the enhanced activity seen with added magnesium is largely due to the increase in ionic strength.
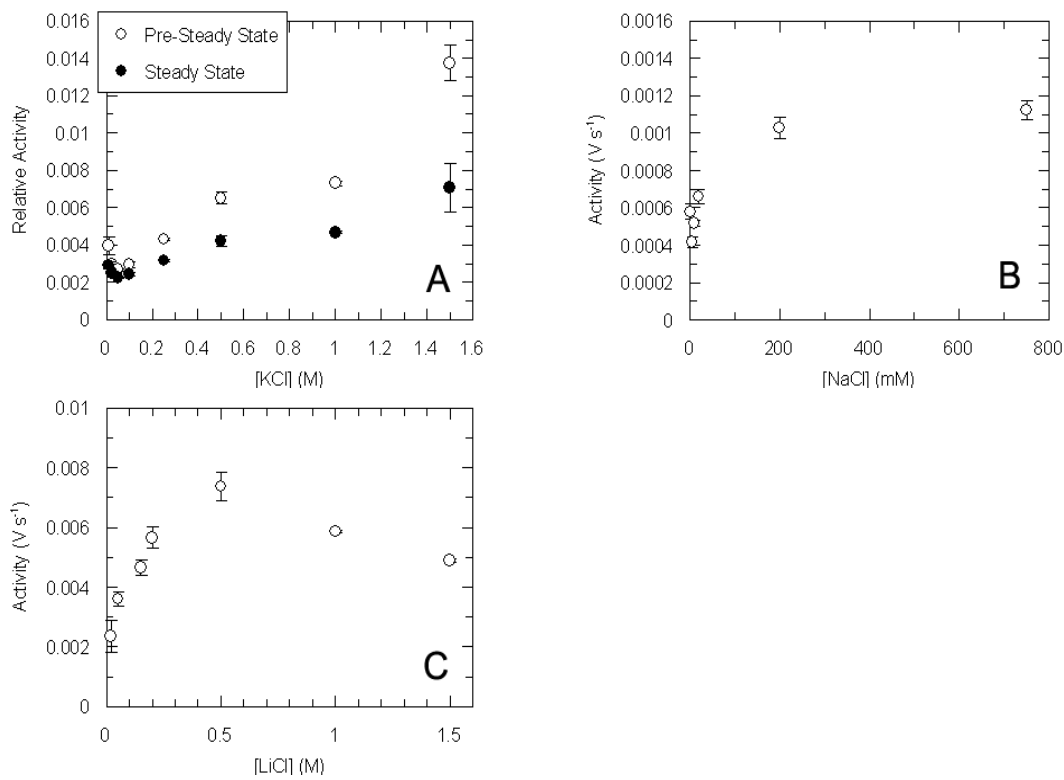
Figure 2.21: Effect of Ionic Strength on Proteasome Activity

The effect of various salts on proteasome activity was investigated, suggesting that it is largely an effect of ionic strength which leads to proteasome activation, not anything specific to any metal ions. In each case as potassium (panel A), sodium (panel B), or lithium (panel C) chloride salts are added, the rate of free AMC production increases. All reactions were done at pH 8.1 in TAPS buffer (25 mM) with 0.010% SDS and 250 μM EDTA present.
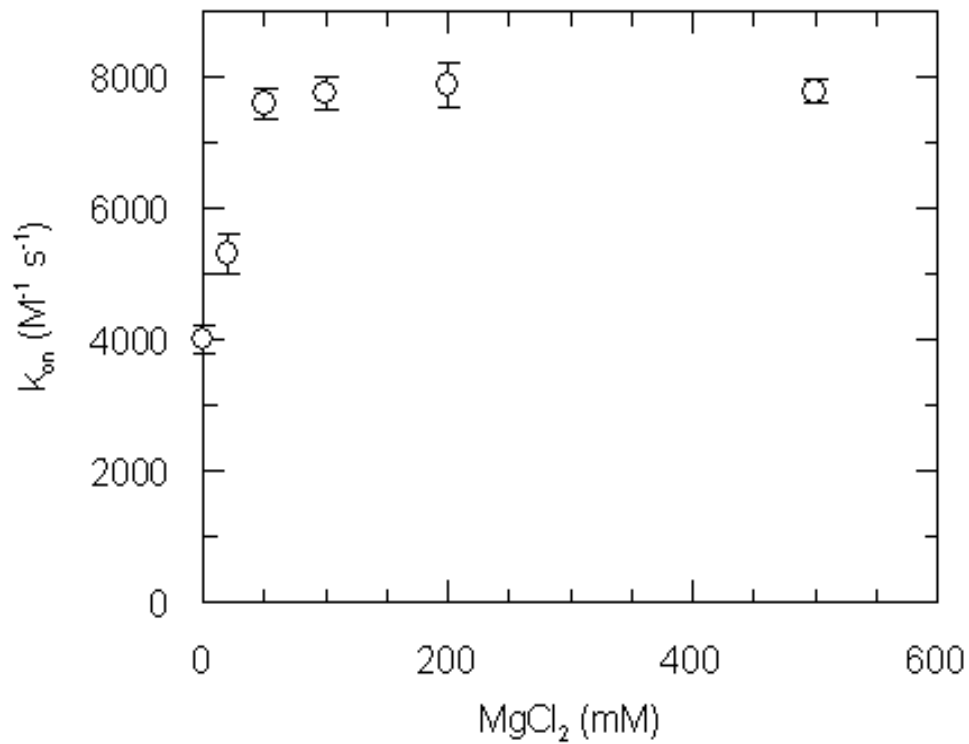
Figure 2.22: Effect of Magnesium at a Constant Ionic Strength

The effect of magnesium chloride on the inhibitor binding rate constant was measured at a constant ionic strength of 1.5 M. Potassium chloride was used to compensate the ionic strength. While no change occurs in the inactivation rate above 100 mM magnesium, there is an increase from 0 to 50 mM, suggesting a magnesium specific effect in this range. The enhanced proteolytic rate is largely due to the high ionic strength.

2.5 Discussion

The experiments described above address the mechanistic basis for activation of the 20S proteasome by SDS and magnesium chloride. Until now, these activators have not been rigorously examined within the context of the proposed proteolytic mechanism. The results presented here indicate that these activators, SDS and magnesium, act at separate points in the mechanism.

The results above demonstrate the use of the peptide aldehyde inhibitor Z-LLLal as a probe to monitor both early (leading up to the acyl-enzyme intermediate) and late events (after the formation of the acyl-enzyme intermediate) in proteolysis by the 20S proteasome from *Thermoplasma acidophilum*. Peptide aldehydes have been shown to be powerful inhibitors of both serine (Kuramochi et al., 1979) and cysteine (Dufour et al., 1995) proteases by forming a tetrahedral hemiacetal adduct with the enzyme that mimics the initial tetrahedral transition state during proteolysis by a serine protease enzyme (Kuramochi et al., 1979). If the mechanism of inhibition for the proteasome (Rock et al., 1994; Lee et al., 1998), a threonine nucleophile (Seemuller et al., 1995a), has analogous intermediates (Lowe et al., 1995), then the aldehyde inhibitor can be used to monitor early steps in the proteolysis mechanism. Furthermore, the inhibitor and peptide substrate are approximately the same size, three amino acids compared to four plus an *N*-terminal blocking group for each molecule, and are expected to have similar modes of binding so access to the proteolytic chamber can be monitored as well. The rate constants for

association of substrate and inhibitor can be determined by experimental determination of the rate of enzyme-inhibitor association, k_{on} (Morrison et al., 1988). As described below, progress curves such as those in Figure 2.3 can be used to directly monitor association and dissociation rates in response to various activators.

Several groups have noted a strong enhancement of activity in the presence of fatty acids, SDS and other detergent-like denaturants (Dahlmann, 1985; Shibatani et al., 1995; Arribas et al., 1990). Furthermore, it has been shown that this binding is stoichiometric in nature, suggesting a specific binding effect (Shibatani et al., 1995). However, the mechanism of activation has remained unclear. It has been proposed that SDS enhances proteolytic activity by increasing the size of the pore formed by the α-subunits, thus enhancing access to the proteolytic chamber for substrate (Baumeister et al., 1998). To test this hypothesis, the rate of inactivation by the peptide aldehyde Z-LLLal was monitored as a function of SDS concentration (Morrison et al., 1988). If the proposition were true, the rate constants of inactivation by inhibitor should follow the same trend observed for proteolytic activity. These results, however, show quite clearly that this is not occurring. Instead SDS is acting after the initial steps in the mechanism leading to an increase in the rate of decomposition of the inhibited enzyme. This increased decomposition rate would thus lead to an increased rate of free enzyme production, leading to an increase in detected activity against the substrate Suc-LLVY-AMC.

The same principles that were used to investigate the effect of SDS on proteolytic attack were used to dissect the nature of activation by magnesium chloride. Several groups have shown enhancement of proteolytic activity in response to added magnesium although the mechanism for activation has been unclear (Orlowski, 1993; Pereira et al., 1992; Akopian et al., 1997). The approach described in this chapter utilized the slow binding inhibitor Z-LLLal and additional salts to determine if it is a magnesium specific effect and at what stage activity is enhanced. By examining the binding rate for the inhibitor at various magnesium concentrations, the rate constant of substrate entry into the active site chamber and the initial nucleophilic attack can be measured.

Though the initial nucleophilic attack is greatly enhanced by magnesium, this effect is largely attributable to the increase in ionic strength. However, there is a specific Mg^{2+} effect at low concentrations. In the *T. acidophilum* 20S proteasome structure (PDB accession code 1PMA) (Lowe et al., 1995), there are no magnesium ions present in the coordinates although there are in the yeast 20S proteasome structure (PDB accession code 1RDB) (Groll et al., 1997). In the latter, magnesium ions are bound by several amino acids at the interface between subunits. A comparison of the sequences and structures reveals that the residues the magnesium ions are interacting with are conserved, such that a specific interaction between magnesium ions and the proteasome is plausible.

2.5.1 Thermodynamic Analysis of Magnesium Activation

The data for the effects of magnesium on the hydrolysis of the substrate peptide Suc-LLVY-AMC was analyzed to determine the K_i values at each magnesium concentration. From this analysis, the change in the free energy which occurs as Mg^{2+} is added can be calculated. This will hopefully reveal a thermodynamic basis for the observed kinetic rate enhancements observed under the increased ionic strength conditions.

As shown in Figure 2.18, there is an eight-fold increase in the k_{on} rate constant as magnesium is added to a final concentration of 500 mM. Furthermore, as shown in Figure 2.19, the rate constant k_{off} also increases as Mg^{2+} is added although not in a linear fashion as observed with k_{on}. Instead, the effect is nearly biphasic, increasing at low ionic strength, passing through a maximum and decreasing modestly at high ionic strength (greater than 100 mM), with a maximal effect of approximately six-fold. These values, k_{on} and k_{off}, can be combined to yield K_i values at specific magnesium concentrations. A hyperbolic rise in K_i as a function of Mg^{2+} concentration is observed, as shown in Figure 2.20. An approximately four-fold decrease in the affinity of the inhibitor Z-LLLal for the enzyme occurs as the ionic strength is increased by $MgCl_2$ to 1.5 M.

These data were then be analyzed as described in *Methods* to obtain the free energy change between the various states early in the proteolytic cycle.

When the K_i is analyzed, the changes in the free energy of the tetrahedral intermediate state, mimicked by the enzyme-inhibitor adduct hemiacetal, can be measured. When the rate constant k_{on} is analyzed, the changes in the free energy for the first transition state can be measured. This analysis is done relative to the figure obtained in the absence of added magnesium.

Values of $\Delta\Delta G$ were calculated according to Equation 2.5 at the various concentrations of magnesium tested. These values are shown in Figure 2.20, were an increase in the $\Delta\Delta G$ values in increasing magnesium concentrations is shown. Analysis of these data suggest an increased destabilization of the **HA** state as magnesium is added up to approximately 4.8 kJ mol^{-1}. This increased destablization would lead to a facilitated breakdown of this tetrahedral intermediate, increasing the back reaction as the enzyme regenerates free enzyme and substrate. Furthermore, this is consistent with the increase in the k_{off} values as shown in Figure 2.19, as well as with the decreasing steady state activity as magnesium is added.

The inhibition data in response to Mg^{2+} were further analyzed using Equation 2.6 to examine the thermodynamic effects on the first transition state of the proteolytic cycle (**TS1**). As shown in Figure 2.23, the change in the free energy for the first transition state, $\Delta\Delta G_{TS1}$, also decreases as Mg^{2+} is added to the reaction. An approximate increase of 4 kJ mol^{-1} is observed over the range of 0 mM Mg^{2+} to 500 mM Mg^{2+}. This indicates a destabilized ground state **ES**, which facilitates crossing the **TS1** barrier, leading to an increased

forward rate of peptide hydrolysis. No effect is observed on the back reaction, the decomposition of the **HA** intermediate to yield the **ES** form, when the **ES** form is affected.

When this information is assembled, the resultant thermodynamic diagram in Figure 2.23 emerges. In this scheme, both the ground state **ES** and the tetrahedral intermediate state **HA** are destabilized to lower the barrier to cross between them. This lowering would lead to both an increased binding rate constant for inhibitor binding as well as an increased value of k_{off} as magnesium is added. The inhibitor mimics the early steps in the proteolytic mechanism ending at the tetrahedral intermediate state (mimicked by the **HA** stage of the enzyme inhibitor adduct).

The conclusions from this analysis are that the added Mg^{2+} lowers the barrier between the **ES** and **HA** stages for the substrate hydrolysis reaction. This is manifested by both the increase in the rate of free AMC production and the increase in the difference between the steady state activity and the initial activity as more magnesium is added.
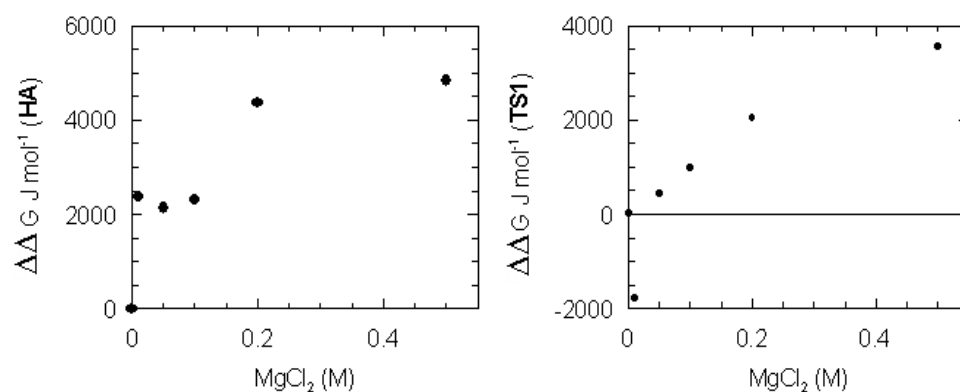
Figure 2.23: Relative Free Energy Effects of Mg^{2+}

Using the data for the binding of the inhibitor, including k_{on}, K_i and k_{off}, a thermodynamic analysis was performed in the absence and presence of Mg^{2+}. This data was analyzed as described in *Methods* using Equations 2.5 and 2.6. This measures the effects of magnesium on K_i and k_{on}, corresponding to the **HA** and **TS1** states, respectively. The increases in the relative free energies indicates that these states are becoming destabilized as magnesium ions are added.
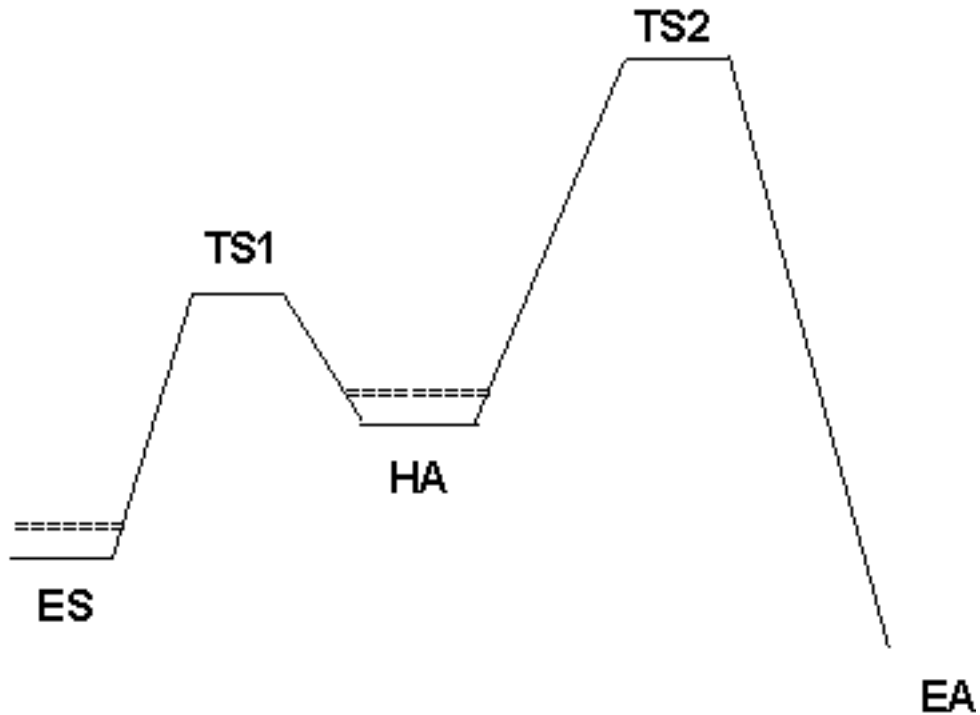
Figure 2.24: Effects of Mg^{2+} on Reaction Barriers

Analyzing the relative free energy changes as a result of magnesium binding, as described in *Methods* using Equations 2.5 and 2.6, the effects of magnesium ions on the relative heights of the energy barriers in the early events of the proteolytic cycle can be analyzed. The dashed lines in the figure represent the destabilization of the **ES** and **HA** states by the added magnesium. This leads to a lower energy requirement to cross these barriers, yielding the observed rate increases in the production of free AMC. However, the destabilized **HA** state also means that the back reaction can also occur more readily, observable in the increased difference between the pre-steady state and steady state reaction rates as shown in Figure 2.17.

2.5.2   Possible Role of Ionic Strength

A more general role for magnesium activation is in stabilization of the charged intermediates of the proteolytic cycle. As shown in Figure 1.7, the intermediates are anionic with a positively charged amino terminus. These charge separated complexes are high energy and would require stabilization. The increased ionic strength of the bulk medium around these complexes helps to screen the charges to increase their stability. This increased stability, in turn, can be manifested as both an increased forward reaction rate and an increased back reaction rate. This would be observable more readily in the steady state reactions where the increased enzyme-substrate intermediate concentrations would accumulate.

This role is more general than any specific magnesium effect, which would be consistent with the observed increase in activity for monovalent metal salts (such as NaCl or KCl) as well as non-metal salts, such as ammonium sulfate. This does not, however, explain the differences in the shapes of the curves as salts are added when magnesium is compared to KCl or other monovalent salt ions.

2.5.3   Activation Within the Proposed Mechanism

Putting all of this information together, these activators can be placed within the proposed mechanism (Wlodawer, 1995). As shown in Figure 2.25, the initial attack on the carbonyl carbon of the amide bond to be hydrolyzed is

sensitive to magnesium and ionic strength. During the course of proteolysis of Suc-LLVY-AMC, this leads directly to a faster rate of AMC production. Lastly, the decomposition of the enzyme-inhibitor adduct which leads to the restoration of the free enzyme is accelerated by the presence of SDS. The concentrations of SDS that lead to maximal activity are quite low, suggesting a binding effect rather than a participation in the mechanism akin to buffer activation. However, it is unclear as to how binding of SDS would lead to faster release of the second product.

In conclusion, this work demonstrates the use of the slow binding inhibitor Z-LLLal, which inhibits 20S proteasome function, as a tool to probe early or late events in the proteolytic mechanism. Using this technique, it has been shown that magnesium and SDS activation occur at different stages in the mechanism.
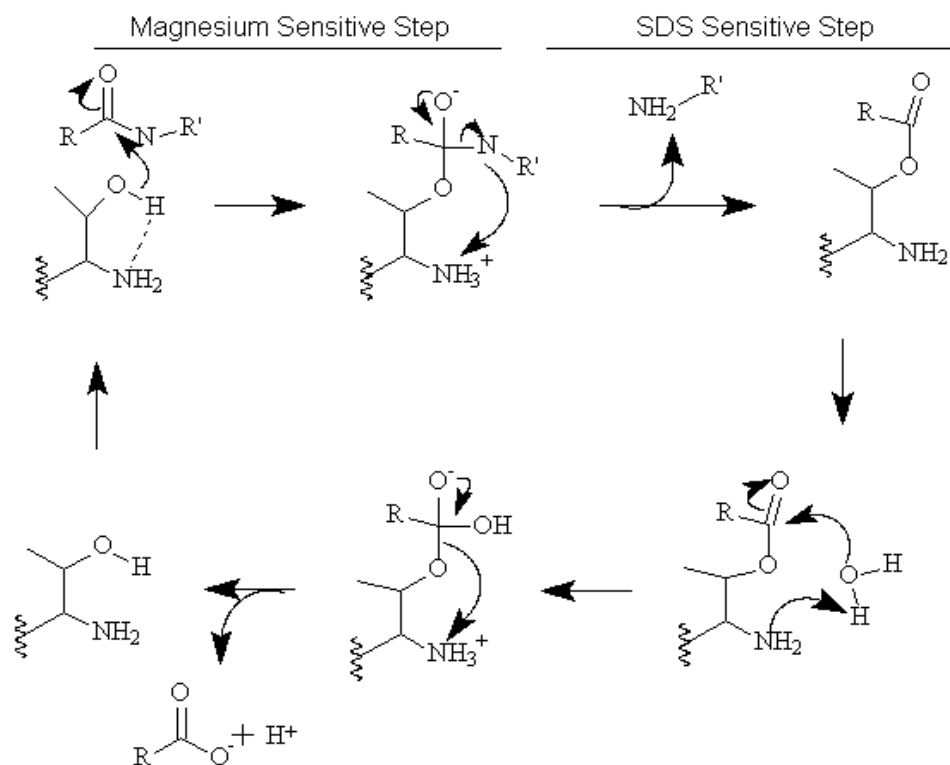
Figure 2.25: Role of SDS and Magnesium in the Proteolytic Mechanism
The steps affected by the activators SDS and magnesium are indicated in the proposed proteasome mechanism. Magnesium facilitates early events, while SDS facilitates the restoration of the free enzyme, each leading to an increased rate of free AMC production when the peptide substrate Suc-LLVY-AMC is reacted with the proteasome.

Chapter 3

Activation of Proteasome Catalyzed Peptide Hydrolysis by Buffer Ions

3.1 Abstract

The 20S proteasome from *Thermoplasma acidophilum* forms the core of the cytosolic protein turnover system and is able to cleave virtually any non-proline peptide bond. During the development of an *in vitro* continuous pH monitoring assay, it was found that proteolytic activity was nearly abolished by the absence of buffer ions. Investigations into the cause of this phenomenon indicate that the degree of activation is dependent upon the type of buffer used. Furthermore, it is the protonated form of the buffer that is involved in the activation as revealed by the pH dependence of activation for a single

buffer type. Because the initial rate of nucleophilic attack is not enhanced, the role of buffer catalyzed proton transfer to this activation has been assigned, which is consistent with the proposed proteolytic mechanism. These findings also have practical implications in the comparison of kinetic data from various laboratories.

3.2   Introduction

The proteasome is the central enzyme involved in intracellular protein turnover in all life forms (Dahlmann et al., 1989). This large, cylindrical particle is composed of 28 subunits in its core (Hegerl et al., 1991), with the possibility of additional subunits providing a cap structure for specific recognition of protein substrates (Lupas et al., 1995). The 20S proteasome from the archaebacterium *Thermoplasma acidophilum* is the simplest 20S proteasome, consisting of only two different types of subunits. The α- subunits form the outer heptameric rings and beta-subunits form the inner, catalytic heptameric rings. This seven-fold symmetry provides the potential for a simpler kinetic model than the eukaryotic proteasome (Dahlmann et al., 1992).

Based on the published crystal structure (Lowe et al., 1995) in conjuncture with mutagenesis and inhibition data (Seemuller et al., 1995a; Seemuller et al., 1995c), a mechanism for proteolysis has been proposed which involves the β-subunit *N*-terminal threonine acting as a nucleophile (Wlodawer, 1995). This

proposed mechanism is a variation on the catalytic triad mechanisms from serine proteases, and involves the amino terminus of the β-subunit (Wlodawer, 1995). To date, there have been no direct tests in solution of this mechanism. The results of the kinetic studies presented here support the proposed mechanism (Wlodawer, 1995) and implicate the involvement of additional functional groups in catalysis and inhibition.

Preliminary studies directed towards developing a continuous assay for proteolytic activity based on proton production following hydrolysis of the peptide bond revealed that activity was dependent upon the presence of buffer. Yu *et al.* reported a similar finding during examinations of the eukaryotic form of the enzyme (Yu et al., 1993), but these results were left unexplained. Upon closer examination, activation depends on both the structure and the protonation state of the buffer, with the protonated form of the buffer providing activation.

Monitoring the kinetics of inactivation by the peptide aldehyde Z-LLLal (Escherich et al., 1997), this thesis shows that activation by buffers in the solution occurs after the initial proteolytic attack. The conclusion drawn from these data is that buffer ions assist in proton transfer within the proteolytic mechanism (Wlodawer, 1995). These results have implications for both the proposed mechanism of proteolysis and the comparison of data between various research groups.

3.3 Materials and Methods

3.3.1 Materials

Materials and reagents were obtained as described in Section 2.3.1.

3.3.2 Proteasome Purification

The 20S proteasome was isolated and characterized as described in Section 2.3.2.

3.3.3 Proteolytic Assays

The proteasome catalyzed hydrolysis of the substrate peptide Suc-LLVY-AMC was performed as described in Section 2.3.5.

3.3.4 Inhibitor Studies

Inactivation of the 20S proteasome by the inhibitor peptide Z-LLLal was performed as described in Section 2.3.6.

3.3.5 pH Variations

Activity studies using the substrate Suc-LLVY-AMC or the inhibitor Z-LLLal at varying pH values were performed as described in Section 2.3.5 with the following buffers and pH ranges indicated: pH 5.6-6.2, MES; pH 6.5-7.5, MOPS; pH 7.5-8.8: TAPS; pH 9.1-10.0, CAPSO. Buffers were brought to the indicated pH value using HCl or NH_4OH.

3.3.6 Data Analysis

Analysis of the data for the hydrolysis of the peptide Suc-LLVY-AMC and the inactivation by the inhibitor peptide Z-LLLal was peformed as described in Section 2.3.7.

pH data analysis is based on mechanisms and equations published by Cornish-Bowden (Cornish-Bowden, 1995) and Tipton and Dixon (Tipton et al., 1979) to determine the effect of pH on enzyme activity and inactivation. Data for the hydrolysis of the substrate peptide Suc-LLVY-AMC as a function of pH was analyzed using the equation

$$a = \frac{a_{max}}{1 + 10^{pH - pK_a^2} + 10^{pK_a^1 - pH}} \tag{3.1}$$

where a is the observed activity and a_{max} is the maximum observed activity. The values of pK_a^1 and pK_a^2 are the two inflection points in the resulting bell shaped curve. Analysis of the binding constant, k_{on}, as a function of pH was analyzed using the equation

$$k_{on} = \frac{k_{on}^{low} + k_{on}^{max}(10^{pH - pK_a^1})}{10^{pH - pK_a^1}} - \frac{k_{on}^{max} + k_{on}^{high}(10^{pH - pK_a^2})}{10^{pH - pK_a^2}} \tag{3.2}$$

where k_{on}^{low} is the value of k_{on} at the lower pH limit, k_{on}^{max} is the value of k_{on} at the optimal pH, and k_{on}^{high} is the value of k_{on} at the higher pH limit.

Nonlinear least squares analyses were performed using Grafit 3.01 (Erithacus Software, Ltd.).

3.4 Results

3.4.1 Buffer Effect on Product Formation

During the development of a continuous assay for proteolytic activity, we found that there was a strong dependence of proteasome activity on the presence and concentration of buffer ions, as observed previously for the eukaryotic proteasome (Yu et al., 1993). Using the kinetics of inhibitor binding together with pH variations, the role of buffer in catalysis by the *T. acidophilum* 20S proteasome has been investigated.

The basic finding of activation is shown in Figure 3.1, showing several fluorogenic time traces in the presence of varying concentrations of buffer as the production of free AMC was measured. The rate of AMC production from the peptide substrate Suc-LLVY-AMC increases as TAPS buffer concentration is raised from 3 mM to 50 mM at pH 8.1. In the absence of added TAPS buffer, activity the low but detectable is attributed to residual phosphate and imidazole from the storage buffer (final phosphate concentration 50 μM, pH 8.0). No observable burst of AMC production is seen in the first 100 seconds of the reaction, even as more buffer ions are addded (Figure 3.2).
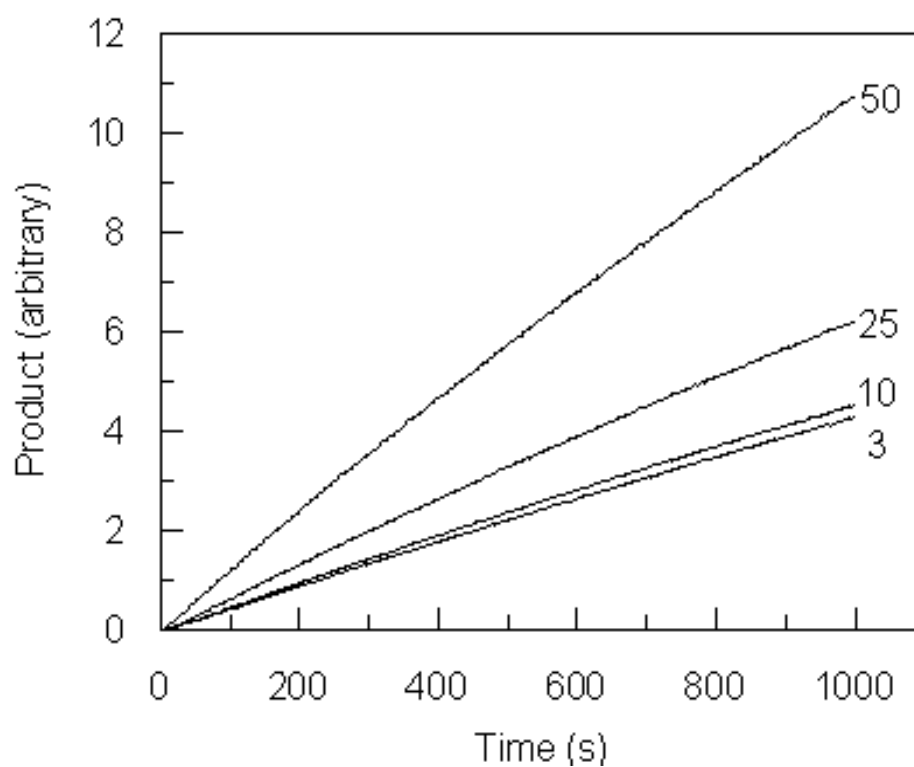
Figure 3.1: Effect of Buffer on Product Formation

The peptide substrate Suc-LLVY-AMC was reacted with purified recombinant proteasome at 45°C in TAPS buffer as described in Methods and free AMC production monitored. The concentration of TAPS buffer at pH 8.1 in mM is indicated in the figure. Product units are the recorded voltages of the fluorescence detector.
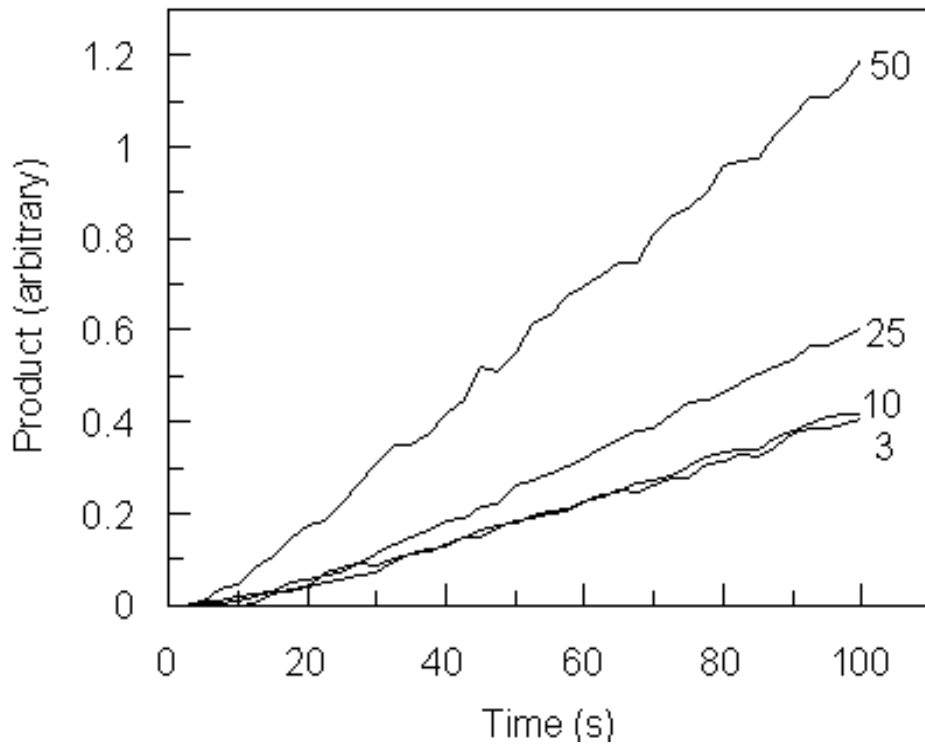
Figure 3.2: The Effect of Buffer Ions on Early Activity

This detailed expansion of the first 100 seconds of peptidase activity against the substrate peptide Suc-LLVY-AMC in increasing concentrations of buffer ions shows the lack of a burst of activity. This suggests that there is no accumulation of an intermediate leading to a slowdown of the enzyme's activity when buffer is added. The conditions are the same as those in Figure 3.1.

Buffer ions appear to be a requirement for enzyme stability and activity. When the residual phosphate is removed by dialysis, activity is lost entirely. Even with buffer replaced during the reaction, or after extensive equilibration with buffer ions, activity is not recovered (data not shown). This mirrors the findings from Yu *et. al* (Yu et al., 1993) where they also observed an irreversible loss of enzyme activity after removal of buffer ions.

The effects of several buffers are shown in Figure 3.3. The addition of TAPS, HEPES, Tris-HCl, and Tricine buffers also activate the proteasome over the same range of concentration, generating approximately a four-fold activation from 5 to 200 mM buffer. One common characteristic of these buffer ions is that the acid form is zwitterionic in this pH range. It is interesting to note the profile of activation by HEPES when compared to the other buffers in Figure 3.3. HEPES activation is hyperbolic, while the dependence of activity on buffer concentration for Tris-HCl, TAPS and Tricine are all more linear over this range. This may represent a specific interaction between HEPES and the enzyme which is not present in the other buffers examined, such as a non-covalent binding of the buffer ions to the enzyme.
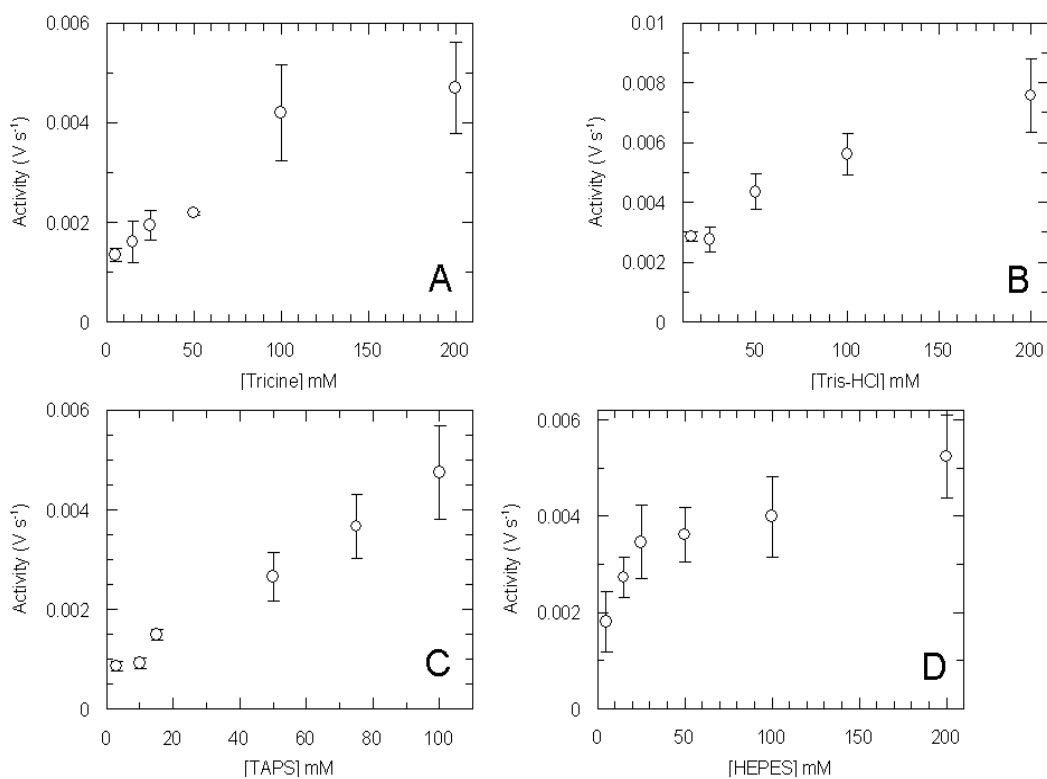
Figure 3.3: The Effect of Several Bifunctional Buffers

Several bi-functional buffers are able to enhance proteolytic activity to varying degrees. Tested were Tricine (panel A), Tris-HCl (panel B), TAPS (panel C), and HEPES (panel D), and all showed concentration dependent activation of proteasome catalyzed hydrolysis of the substrate peptide. Buffers in all experiments were supplemented with 100 mM NaCl, 0.010% SDS and 250 μM EDTA. The buffers were used at the following pH values and have the indicated pK_a values: Tricine: 8.0 (8.15); Tris-HCl: 7.8 (8.30); TAPS, 8.1 (8.4); HEPES, 7.5 (7.55).

3.4.2   pH Dependence of Activation and Inhibition

The effect of pH variations on both activity against the peptide substrate Suc-LLVY-AMC and the inhibitor Z-LLLal was next investigated. Such a study could help in identifying the number and protonation states of groups involved in catalysis. As shown in Figure 3.4, activity reaches a maximal value at about pH 9.0 before declining sharply. At lower pH values, there is no sharp inflection point. However, the proteolytic rate decreases steadily as the pH is decreased, to approach zero activity at pH 6.0. This data was fit to Equation 3.1 to determine the two pK_a values of 7.7 and 10.1. The pH profile for the binding of inhibitor with respect to pH is different. As shown in Figure 3.5, there is a narrow bell shaped profile centered at pH 8.5 with two inflection points at 8.3 and 8.9, respectively.
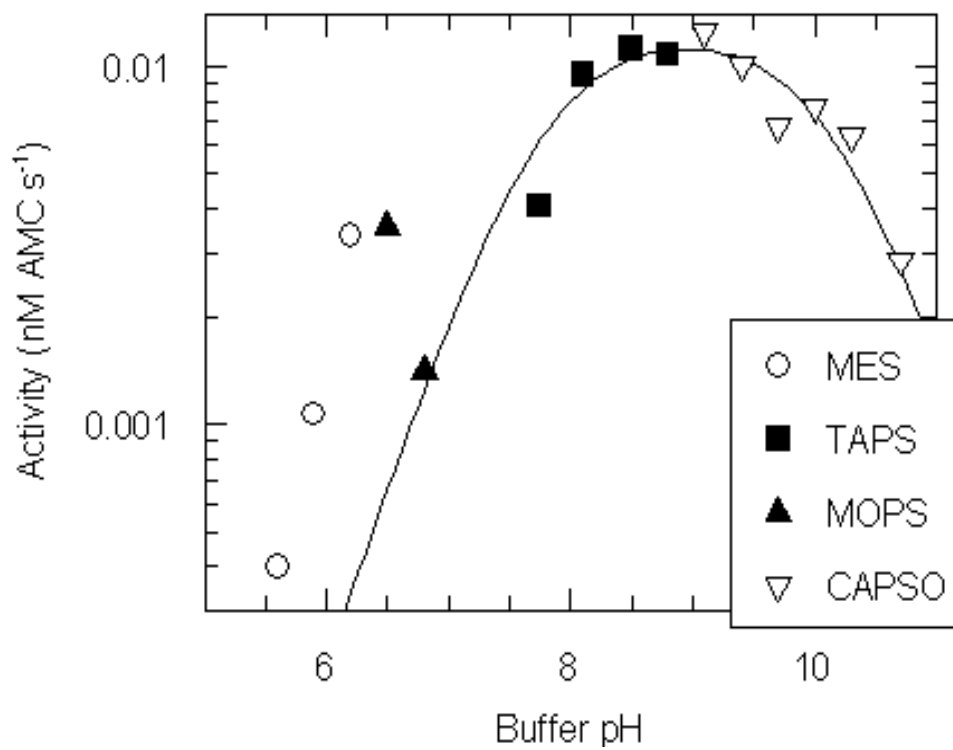
Figure 3.4: Effect of pH on Peptidase Activity

Purified recombinant proteasome was reacted in buffers of varying pH against the substrate Suc-LLVY-AMC and the resulting activity (reported in arbitrary fluorescence units per second) measured. Activity near pH 11 and below 5.5 are difficult to detect, as evidenced in the bell shaped activity profile above. The data were fit to Equation 3.1. The buffers used were as listed in *Materials* at a concentration of 25 mM.
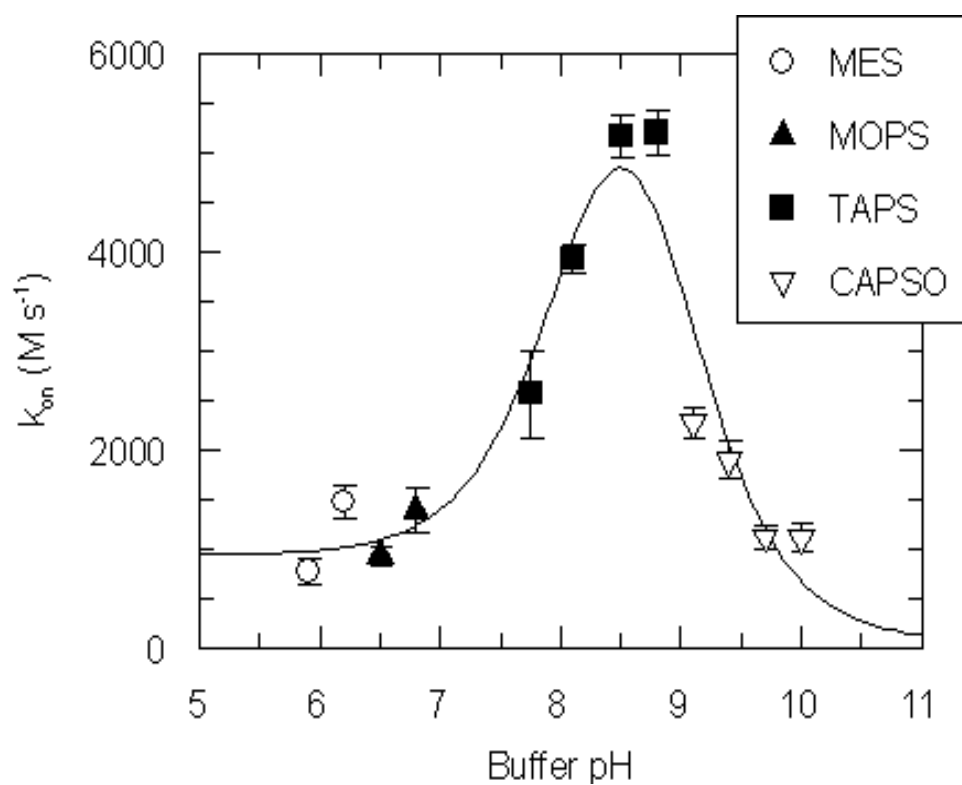
Figure 3.5: Effect of pH on Inhibitor Binding

The rate constant for inhibitor binding was measured as a function of pH and the data was analyzed using Equation 3.2. Two groups with similar pK_a values appear to be present, with an average pK_a value near 8.3. Conditions were the same as those in Figure 3.4.

This pH dependence was further investigated through the use of mono-functional aklylamine buffers. Activity assays using the substrate Suc-LLVY-AMC were performed using alkylated amines to replace the standard buffers. Buffers such as morpholine, diethylamine, and ethanolamine lead to inactivation of the enzyme as more buffer is added at high pH. However, when titrated below their pK_a, they activate the enzyme. As shown in Figure 3.6, increasing ethanolamine leads to a loss of activity at pH 10.8, but when protonated at pH 8.9 the enzyme is activated approximately two-fold. This is expanded upon in Figure 3.7, where the pH dependence of activation by ethanolamine is shown. At pH 9.9, where the graph of the natural log of the activation factor crosses the abscissa, there is no variation in activity with buffer concentration. The shape of the cuve suggests that deprotonation of a functional group results in the observed inhibition by buffer ions. However, it is difficult to conclude if this is the buffer or a functional group on the enzyme that is being titrated, since the pK_a of ethanolamine is approximately 10.0. Additional aklylamines were tested, as shown in Figure 3.8, but the nature of the effect is still unclear. Not tested was the reversibility of this effect on the enzyme, having been dialyzed against a higher pH and then returned to a more neutral pH.
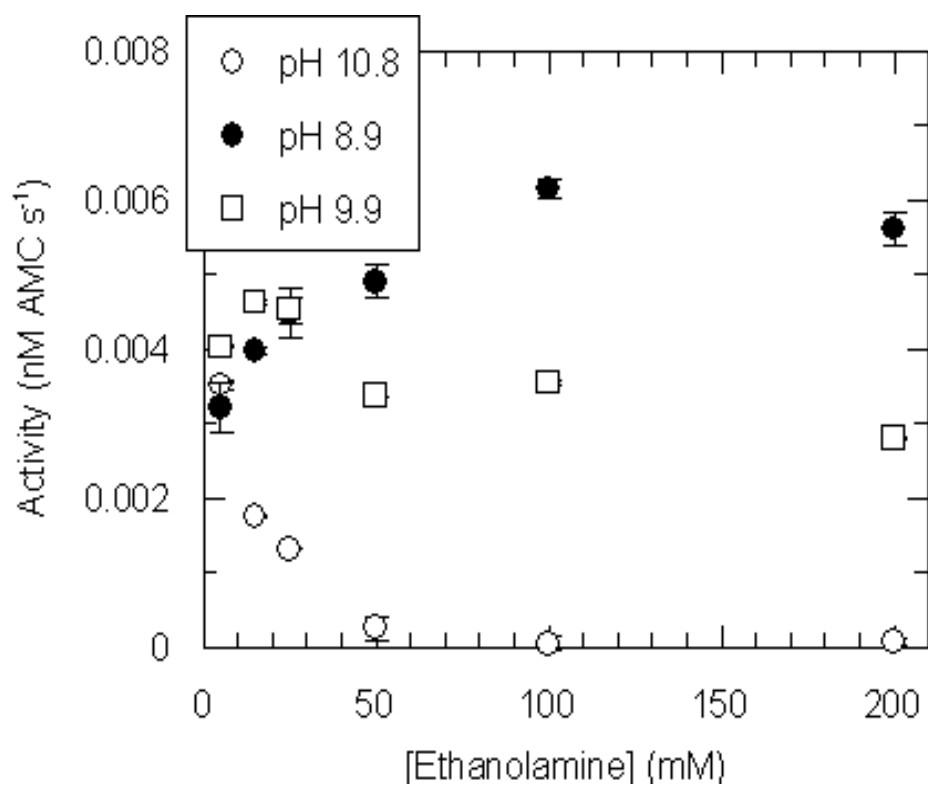
Figure 3.6: Activation and Inactivation by Ethanolamine is pH Dependent
The effect of ethanolamine at various concentrations was determined at three pH values, above, near, and below the pK_a of ethanolamine. Activity was measured in 100 mM NaCl, 0.010% SDS and 250 μM EDTA. pH was adjusted using HCl.
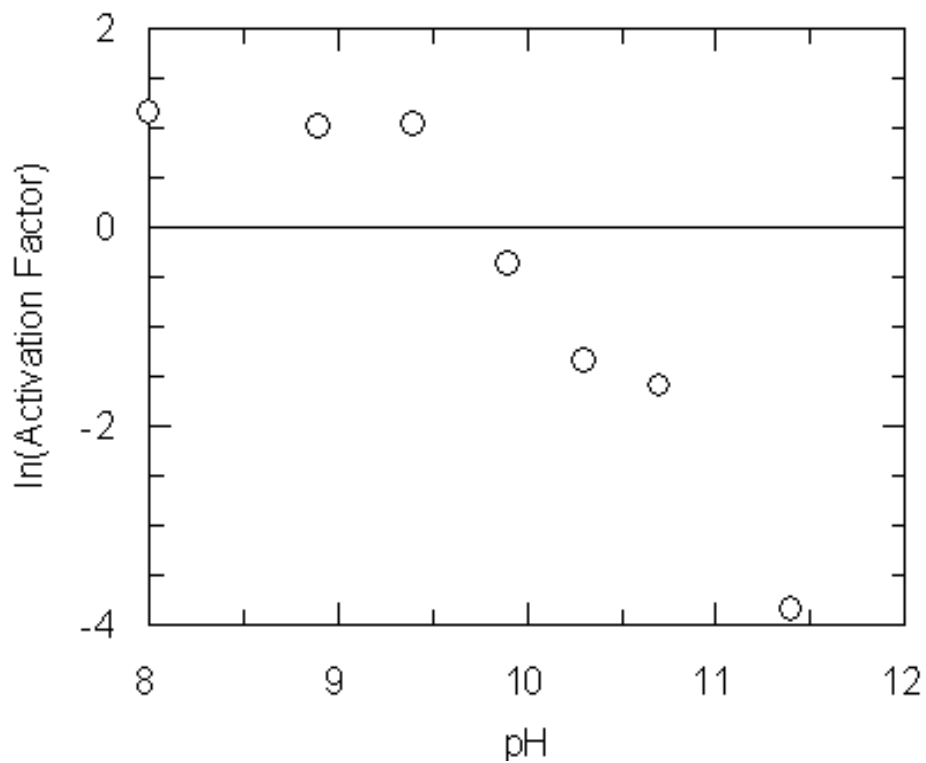
Figure 3.7: The Effect of pH on Ethanolamine Activation of the Proteasome
The pH of an ethanolamine based buffer solution was investigated on the prote-
olytic activity against the peptide substrate Suc-LLVY-AMC. The activation
factor is defined as the ratio of activity at 200 mM ethanolamine in buffer
compared to the activity at 5 mM ethanolamine. The activation below ap-
proximately pH 9.9 is suggestive of the enzyme interacting preferentially with
the protonated form of the buffer.
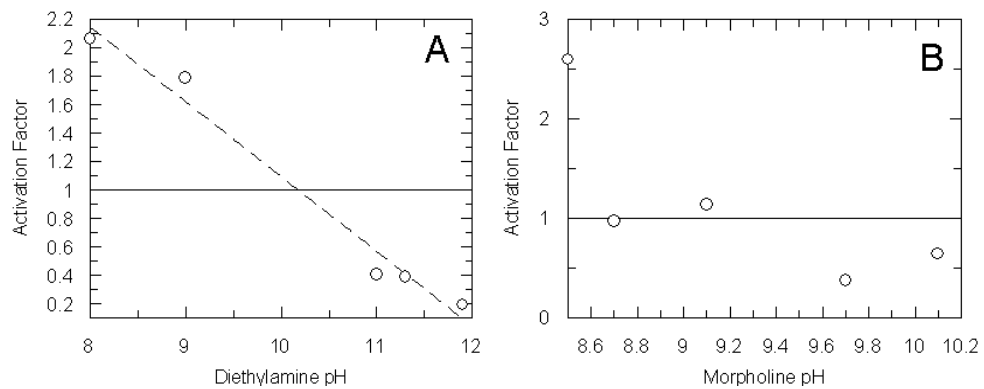
Figure 3.8: Activation of the 20S Proteasome by Diethylamine and Morpholine Using the same methods as shown in Figures 3.6 and 3.7, the effects of the alkylated amines diethylamine and morpholine on proteasome activity were examined. The pK_a of diethylamine is approximately 11.1, while the pK_a of morpholine is approximately 8.6. The data do not allow for any conclusions as to the which titration, the enzyme or the buffer, is causing activation of the enzyme. The activation factor is defined as the ratio of activity at 200 mM buffer compared to the activity at 5 mM buffer.

3.4.3 Buffer Does Not Enhance Initial Proteolytic Attack

Similar techniques were applied to examine at what stage buffer is enhancing activity as were done previously for SDS and magnesium by determining the dependence of the inhibitor binding rate constant, k_{on}, upon the concentration of buffer. As previously described, if buffer is enhancing the initial rate of proteolytic attack, leading to enhanced activity against the substrate Suc-LLVY-AMC, then that would be manifested as an increased rate constant for the development of inhibition. Shown in Figure 3.9, when TAPS is increased at a constant pH, the inhibitor binding rate constant, k_{on}, does not increase, but remains constant at about 1200 M^{-1} s^{-1}. In this concentration range of TAPS buffer, activity is increased approximately five-fold. This is elaborated on the possible role of buffer ions below in the Discussion section.
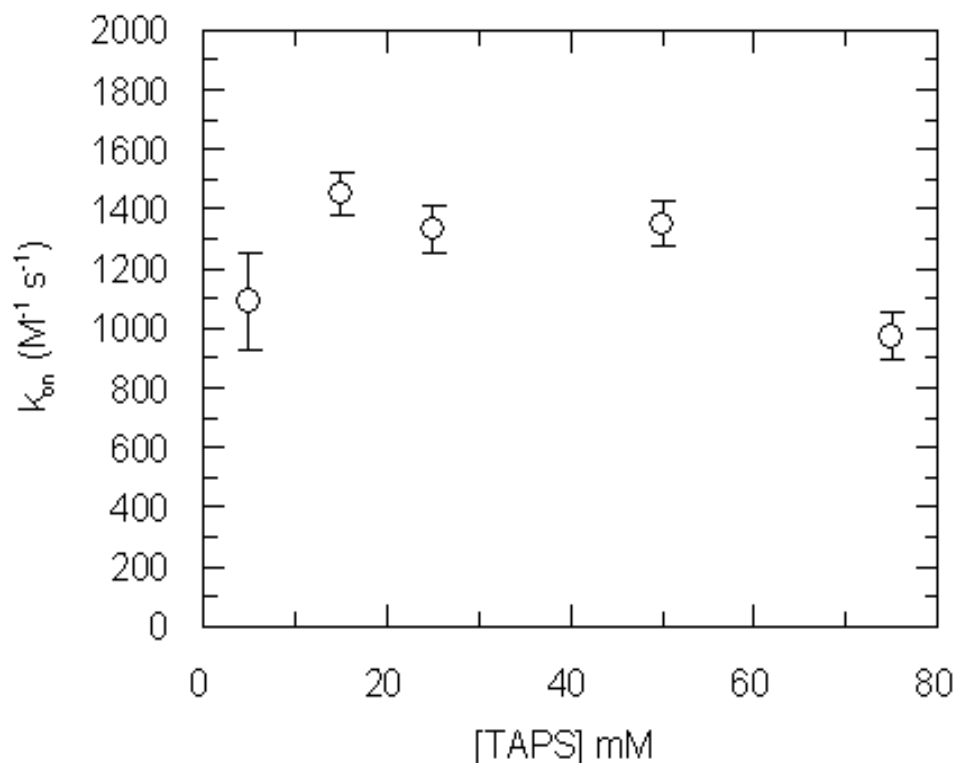
Figure 3.9: Effect of TAPS on Inhibitor Binding at a Constant pH

To examine if buffer enhances the rate of nucleophilic attack, the rate of inhibitor binding was measured at various concentrations of TAPS (with 100 mM NaCl, 0.010% SDS, 250 μM EDTA) at a constant pH. The lack of an increase in the rate constant of inactivation indicates that the enhancement of activity by buffer occurs after the initial states in the mechanism.

3.4.4 Buffer Enhanced Activity is Masked by Other Activators

As shown previously, Mg^{2+} is a potent activator of proteolytic activity. An additional activator, guanidine hydrochloride, has also been shown to have a strong effect at 0.5 M. To test if these activators work at the same point in the mechanism as buffer ions or at separate steps, buffer was titrated in the presence of 0.5 M magnesium or guanidinium. If they all affect activity at the same point in the mechanism, they may have additive effects when used in combination. As shown in Figure 3.10, activators such as guanidinium or magnesium mask the activation by buffer ions. The level of activation for both magnesium and guanidinium at a fixed, high concentration is maximal for that activator and independent of the concentration of buffer added.

3.4.5 Not All Zwitterionic Buffers Provide Activation

To test the generality of activation by zwitterionic buffers, the glycine derivatives glycylglycine and bicine were also tested. As shown in Figure 3.11, these fail to provide any increase in activity over the range tested. One facet that stands out in the Figure is that the initial activity of glycylglycine is almost two times higher than that of bicine.
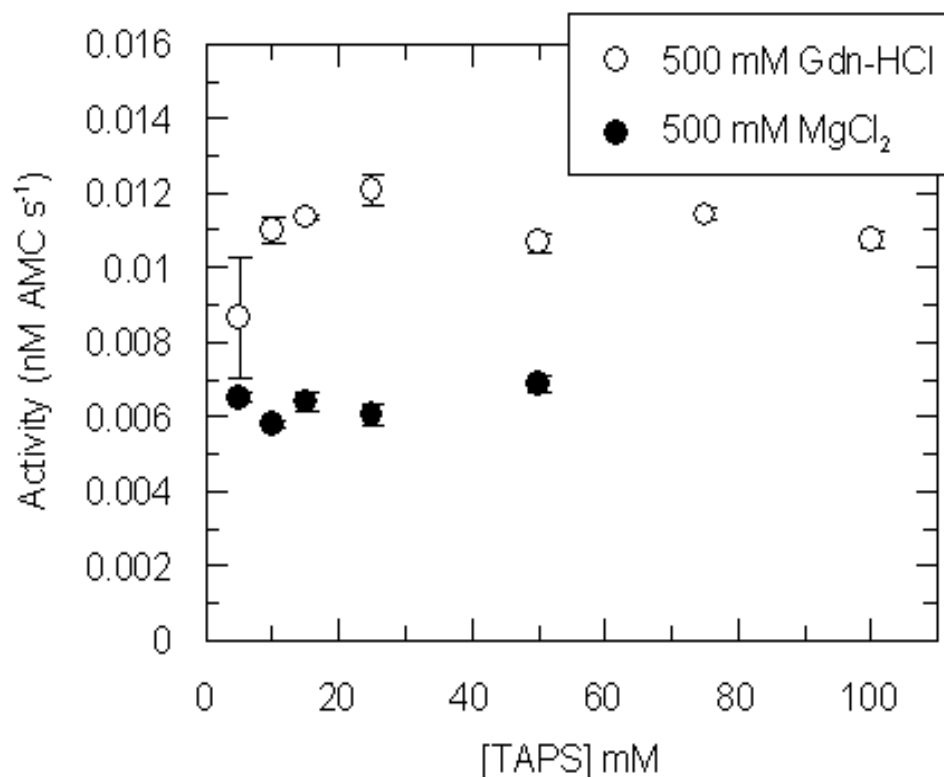
Figure 3.10: Other Activators Mask Buffer Activation

The effect of buffer activation was investigated in the presence of the known proteasome activators magnesium and guanidinium hydrochloride. As shown, buffer activation is masked by these other activators.
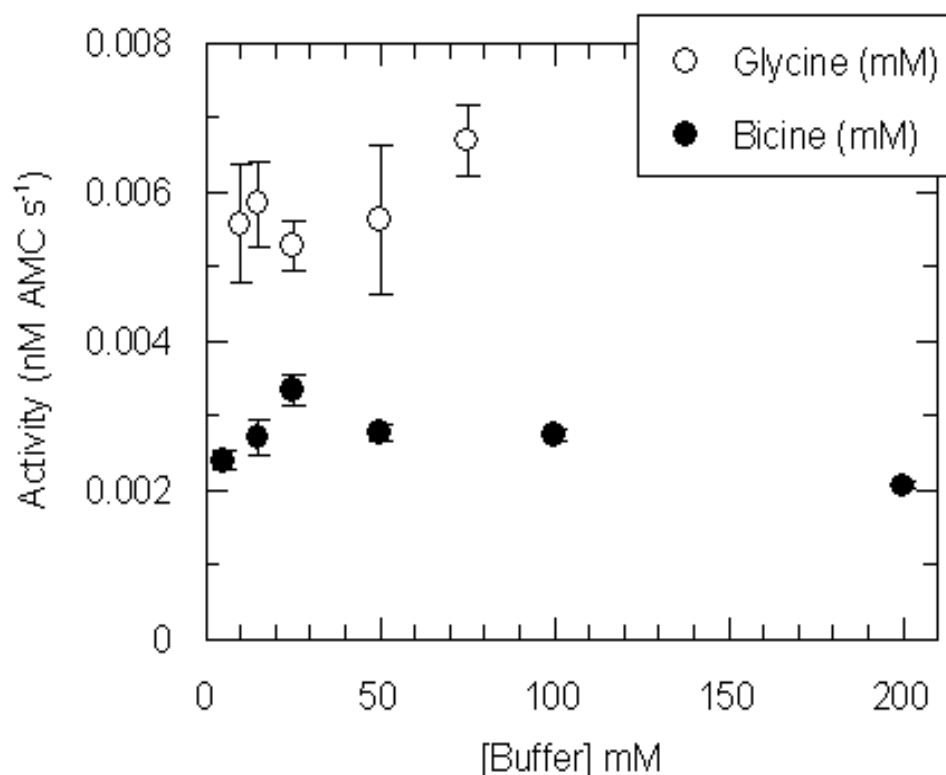
Figure 3.11: Lack of an Effect by Bicine and Glycylglycine Buffers

The effect on activity of the bi-functional buffers bicine and glycylglycine was investigated against the substrate Suc-LLVY-AMC. As is evident from the figure, no effect was seen over the ranges examined, in stark contrast to the effects of buffers such as TAPS and HEPES (Figure 3.3).

3.5 Discussion

The data presented here describe an unusual phenomenon in enzyme catalyzed reactions, the enhancement of activity by buffer ions. The data above, however, demonstrate a direct participation of the buffer ions in the catalytic cycle of the enzyme. The initial finding which led to this research was that the activity of the enzyme decreased dramatically when the concentration of buffer was reduced, as shown in Figure 3.1. The finding that when buffer is dialyzed away activity is lost, even when buffer is reintroduced, suggests some irreversible or nearly-irreversible change in the enzyme has occurred. The fact that several different buffer ions can enhance activity strengthens the proposition that there is participation by buffer ions in the mechanism. It is not entirely general, though, as glycine derivatives cannot enhance activity in a similar concentration dependent fashion.

Several approaches were used in an attempt to understand at what point in the mechanism the buffer ions are acting. In Chapter 2 it was shown that by using a small peptide aldehyde inhibitor, Z-LLLal, to monitor binding and dissociation rates, kinetic rate constants for the binding and release of substrate could be obtained. This permits the investigation of both early and late events in the proteolytic mechanism directly which would not be possible with the normal substrate peptide Suc-LLVY-AMC.

Since the value of k_{on} is unaffected by the buffer ion concentration, initial events of inhibitor binding are not altered by the concentration of buffer ions

present (Figure 3.9), suggesting that the initial events leading to proteolysis are also not affected. Analysis also shows that the late events, monitored by obtaining the dissociation rate constants of the inhibitor in increasing buffer ion concentrations, were not affected. This leaves only events in the middle of the proteolytic mechanism as possible points of action for buffer ions.

The data obtained with the alkylated amines, such as that in Figures 3.6 and 3.8, showed that the protonation state of the buffer ion was crucial for an enhancement of activity. However, it is still unclear if this effect is due to a titration of the enzyme's functional groups in the active site or the buffer ion. The data in Figure 3.8 do not clearly indicate where the inflection point is (the zero line in the figure). Extreme values of pH were tested, near pH 7 and pH 10, and the data from Figure 3.4 show a bell shaped activity profile. From this, it is clear that the protonation states of the reactants (substrate and enzyme) are important.

Coupled with the profile of activity as a function of pH, analysis of the data suggests a role of the buffer ion in proton transfer. Within the proposed mechanism of hydrolysis of peptides by the 20S proteasome are two proton transfer steps (Figure 3.12). The first is protonation of the leaving primary amine, and the second is deprotonatation of the water involved in the breakdown of the acyl-enzyme intermediate. In both cases, activity would be sensitive to a change in the pH which could either result in the protonation of a group that is to receive a proton, or the deprotonation of a group that donates a proton.
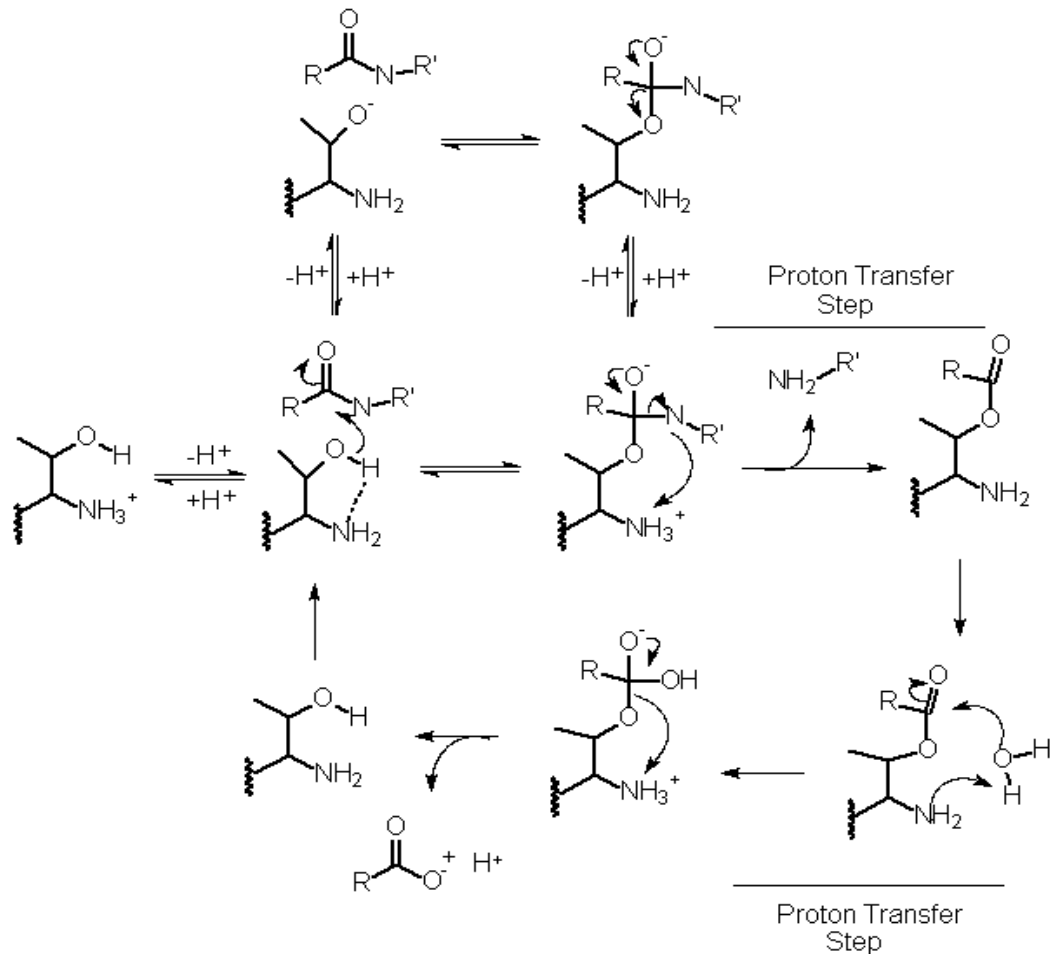
Figure 3.12: Proton Transfer Steps in the Proteasome Catalytic Cycle

In the putative mechanism of proteolysis, the amino-terminus of the catalytic α-subunit of the 20S proteasome is involved in proton transfer, accepting a proton from the catalytic threonine hydrozyl and donating it to the leaving amine group, then acting as a general base in the second half of the reaction to deprotonate the hydrolytic water molecule. These two intermolecular proton transfer steps, which would be sensitive to buffer assistance but would not be reflected in a reactivity of the nucleophile, are marked. For clarity, some hydrogens, which are not pH sensitive, are not shown.

Analyzing the data in Figure 3.1 suggests that it is the first proton transfer step, the transfer to the leaving primary amine, that is being affected by buffer ions. If it were later in the mechanism, a buildup of free AMC would be detected and the enzyme would be stalled in some intermediate form. This would be manifested as a burst of activity before a decrease in the rate of free AMC production. However, as is clearly shown in Figure 3.2, no such burst is detected under the conditions tested. Given the conditions of Figure 3.2, a several nanomolar burst of product would be expected, corresponding to 4-8 V of signal on the scale used in the Figure. The conclusion from this is that any proton transfer being facilitated by the enzyme occurs prior to the release of the first product. With a protein substrate this is the C-terminal peptide, and with the Suc-LLVY-AMC peptide substrate this first product is the AMC group.

The direct participation of buffer ions in the mechanism is possible due to the exposed nature of the active site to the bulk solvent. Examination of the crystal structures of the archaebacterial (Lowe et al., 1995) and yeast (Groll et al., 1997) forms of the enzyme reveals that the active site is not buried as is traditionally seen for other proteolytic enzymes. As such, buffer ions are free to diffuse into the active site with the substrate and participate in the reaction. It is possible that the enzyme evolved to depend on the presence of a general acid-base buffer, given the structure of the active site and the lack of activity in the absence of buffer ions.

This kind of participation by an external general catalyst has been seen previously for other enzymes. Proton relays assisted by external catalysts have been observed previously for fumarase (Rose et al., 1992) and for lactate dehydrogenase (Burgner et al., 1984b; Burgner et al., 1984a). In each case, the magnitude of the effect was sensitive to the buffer chemistry, concentration, and pH. These findings are similar to the types of effects observed for the *T. acidophilum* 20S proteasome, strengthening the conclusion that buffers are participating in the process of peptide bond hydrolysis.

Chapter 4

Effect of Proteasome Activators on Protein Hydrolysis

4.1 Abstract

Amide proteolysis of Suc-LLVY-AMC catalyzed by the 20S proteasome from *Thermoplasma acidophilum* has previously been shown to be activated by buffer ions, salts, ionic strength, denaturants and SDS. Whether this activation is exhibited with protein substrates destabilized by either carboxymethylation or acetylation has been explored. Tryptophan fluorescence of the derivatized substrate proteins was monitored as a function of time and used to measure the rates of degradation. The enhancement of protein degradation by the activators has been compared to the activation of the hydrolysis of the Suc-LLVY-AMC peptide. In all cases, activation of proteolysis of the derivatized protein was significantly less than the previously determined activation

of peptide hydrolysis. When examined in terms of the major events leading to proteolysis, it is proposed that the rate limiting events have shifted from the chemistry of proteolysis to events leading to the entry of the substrate protein into the active site chamber.

4.2   Introduction

The 20S proteasome forms the core of the protein turnover system in eukaryotic cells, yeast and some archaebacteria (Dahlmann et al., 1989). In eukaryotes, cap structures such as PA700 associate with the 20S proteasome core to form a larger, ATP-dependent protease capable of recognizing ubiquitin-tagged proteins (Coux et al., 1996). This allows for controlled cytoplasmic proteolysis through a centralized machine (Baumeister et al., 1998). Ubiquitin has been identified as a part of a larger protein in *T. acidophilum* (Wolf et al., 1993) when analyzed by *N*-terminal sequencing methods, but not in the genome of *T. acidophilum* (Ruepp et al., 2000). This leaves the mechanism of protein hydrolysis a mystery. However, proteasome cap structures from *Methanococus* were able to specifically increase the rate of protein hydrolysis catalyzed in an ATP-dependent fashion, in a manner that parallels eukaryotic 26S proteasome action (Benaroudj et al., 2000).

Because of this dramatic difference between the eukaryotic and prokaryotic forms of the proteasome, it has remained unclear as to the capacity for the 20S core particle to degrade protein molecules. Furthermore, several ideas have

been proposed regarding the role of small molecule activators of proteolysis in protein digestion by the proteasome (Akopian et al., 1997).

There are several events that occur during cellular injury or stress, incluing the rapid influx of metal ions into the cytosol from the external environment, and the release of free lipids into the cytosol. These events may help to regulate proteasome activity when it is needed, under cellular stress when proteins are damaged. Indeed, this may lead to activation of the proteasome against protein substrates as it does for peptide substrates (see Chapter 2 and references therein), allowing for the swift removal of damaged proteins. It has been reported that the proteasome can be responsible for up to 80% of total cellular protein turnover in the cytosol (McNaught et al., 2001).

Chapters 2 and 3 have examined the mechanism of activation of peptide hydrolysis by the 20S proteasome from *Thermoplasma acidophilum*, which enabled the dissection of the chemical mechanism of the proteolytic cycle. This chapter examines the effect of these activators on protein hydrolysis, a more physiologically relevant question. Fluorescence changes in the degraded proteins were used to measure the rates of degradation and the responses to the effects of various activators on proteolytic rates.

The known activators of the proteasome activity of peptide hydrolysis had no effect on protein degradation by the *T. acidophilum* 20S proteasome. Furthermore, only destabilized proteins can act as substrates. From this it was concluded that an equilibrium exists between two forms of the protein, only one

of which is accessible to the proteasome. The interconversion to the degradation prone form is the rate limiting step, leaving any rate enhancements within the chemical mechanism obscured. In the absence of any accessory proteins to destabilize the substrate, he proteasome can interact with the inaccessible form of the protein substrate, but it results in non-productive binding which cannot enter the proteolytic cycle. Overall, it appears that the susceptibility of proteins to be degraded by the 20S proteasome core particle depends chiefly on their stability.

4.3   Materials and Methods

4.3.1   Materials

Materials and reagents were obtained as described in Section 2.3.1.

4.3.2   Proteasome Purification

Recombinant proteasome was isolated and purified as described in Section 2.3.2.

4.3.3   Protein Substrate Preparation

Carboxymethylated substrates were generated by the reaction of protein substrates solubilized (25 mg ml^{-1}) in 25 mM phosphate buffer (pH 8.0) with iodoacetic acid. The reaction was performed at room temperature using an

excess amount of dry sodium iodoacetic acid and allowed to proceed for approximately 60 min. Reactants were separated by the method of Penefsky (Penefsky and S., 1977) using a Sephadex G-10 spin column equilibrated with ddH$_2$O. Acetylated protein substrates were generated by the reaction of the protein substrates solubilized (25 mg ml^{-1}) in 25 mM phosphate buffer (pH 8.0) with 5% (vol vol^{-1} acetic anhydride for approximately 60 min. Excess acetic acid was removed by passing a stream of dry nitrogen gas over the sample tube.

4.3.4 Proteolytic Assays

Hydrolysis of the peptide Suc-LLVY-AMC was performed and monitored as described in Section 2.3.5.

Protein substrates were hydrolyzed in the same buffer and under the same conditions, TAPS buffer (25 mM, pH 8.1 at 45°C, titrated using NaOH or NH$_4$OH), 100 mM NaCl, 250 μM EDTA, and 0.010% SDS (wt vol^{-1}). Data were acquired using an Applied Photophysics SX18 stopped flow fluorimeter, measuring the signal (reported in volts) from the intrinsic tryptophan fluorescence of the protein substrates using an excitation wavelength of 280 nm and monitoring the emission above 305 nm via a cut-on filter (Oriel, Stratford, CA, catalog number 51250) used with the emission detection photomultiplier. Protein substrate concentrations are as indicated.

4.3.5   Data Analysis

Analysis of the data for the hydrolysis of the peptide Suc-LLVY-AMC was performed as described in Section 2.3.7.

Analysis of the data for the hydrolysis of the protein substrates was performed in a fashion similar to that for Suc-LLVY-AMC. To calculate the pre-steady state activity, a linear fit to the first 30 seconds of the data was performed. To calculate the steady-state activity, a linear fit to the last 200 seconds of the data (of 1000 seconds of total data collection) was performed. Quantification of the signal (in volts) of the protein substrates to the concentration of the substrate protein (in mM) was not performed due to the contribution of the intermediate products to the signal in a non-linear fashion.

4.4   Results

4.4.1   The 20S Proteasome Core Partical Interacts with Protein Substrates

The association of the 20S proteasome, absent of any accesory proteins, and protein substrates was measured. Enzyme and substrates, the protein substrates and the peptide substrate (Suc-LLVY-AMC) were reacted under standard assay conditions. With a fixed concentration of Suc-LLVY-AMC and increasing amounts of protein substrates, the peptide Suc-LLVY-AMC acts as a reporter of accessibility to the proteasome active site. As shown in Figure 4.1,

as the concentration of the protein cytochrome c is increased in the reaction mixture, the activity of the proteasome against Suc-LLVY-AMC decreases. A similar result is shown in Figure 4.2, in which the proteasome was reacted with increasing amounts of the protein myoglobin, and again a decrease in the activity against the peptide Suc-LLVY-AMC is observed. These data demonstrate an interference of the protein substrates on peptide hydrolysis activity by the 20S proteasome caused by a direct interactions between the proteasome and the protein substrate.

The interaction between the substrate proteins and purified recombinant 20S proteasome is a specific interaction, as shown by the dependence of the signal amplitude on the concentration of enzyme in the reaction. As shown in Figure 4.3, this amplitude is from the fit of the data to a single exponential equation. In Figure 4.4, increasing concentrations of enzyme and a fixed concentration of substrate protein, carboxymethylated lysozyme, were reacted and the signal amplitude was measured. The increase in this amplitude as the enzyme concentration is increased is indicative of a specific interaction between the two.

4.4.2 The Proteasome Can Degrade Destabilized Proteins

To test the ability of the proteasome to degrade destabilized proteins, various protein substrates were reacted with the enzyme and their intrinsic tryptophan fluorescence was measured as a function of time. As protein substrates are denatured and hydrolyzed, their tryptophan residues will become solvent exposed, resulting in fluorescence quenching. There is essentially no background signal from the proteasome as it lacks tryptophan residues, permitting a specific observation to be made on the protein substrate.

Shown in Table 4.1 are the relative rates of proteolysis for various chemically modified proteins by the 20S proteasome under standard assay conditions. Both carboxymethylated and acetylated proteins are degraded by the proteasome under typical reaction conditions at rates that are measurable. To determine if the proteolysis rates are reasonable, these substrate proteins were reacted also with trypsin and chymotrypsin, much more efficient proteases. As shown in Table 4.2, the rate of loss of intrinsic tryptophan fluorescence for these substrate proteins is comparable when they are reacted with these other proteases. Using this information, there is a high confidence that the process measured was due to proteolysis and occurred with a reasonable and measurable rate.

This result was complemented by using SDS PAGE methods to monitor

the loss of protein substrates upon prolonged reaction with recombinant proteasome (data not shown). Chemically modified protein substrates were incubated overnight with either chymotrypsin or purified recombinant 20S proteasome and then resolved using an SDS PAGE gel. The loss of substrate band intensity for both sets of digestions provides supporting evidence that protein degradation is occurring.

4.4.3   SDS Has No Effect on Proteolytic Rates

To test the effect of the known peptide hydrolysis activator SDS on protein proteolysis rates, the intrinsic tryptophan fluorescence of substrate proteins was monitored over time as the substrate protein was reacted with purified recombinant proteasome. Enzyme and protein substrates were equilibrated under equivalent conditions with varying concentrations of SDS. Substrate and enzyme were then reacted and the rate of tryptophan fluorescence loss was measured. As shown in Table 4.3, the rate of tryptophan fluorescence change does not increase as SDS is added, unlike the activation observed for hydrolysis of the peptide Suc-LLVY-AMC.
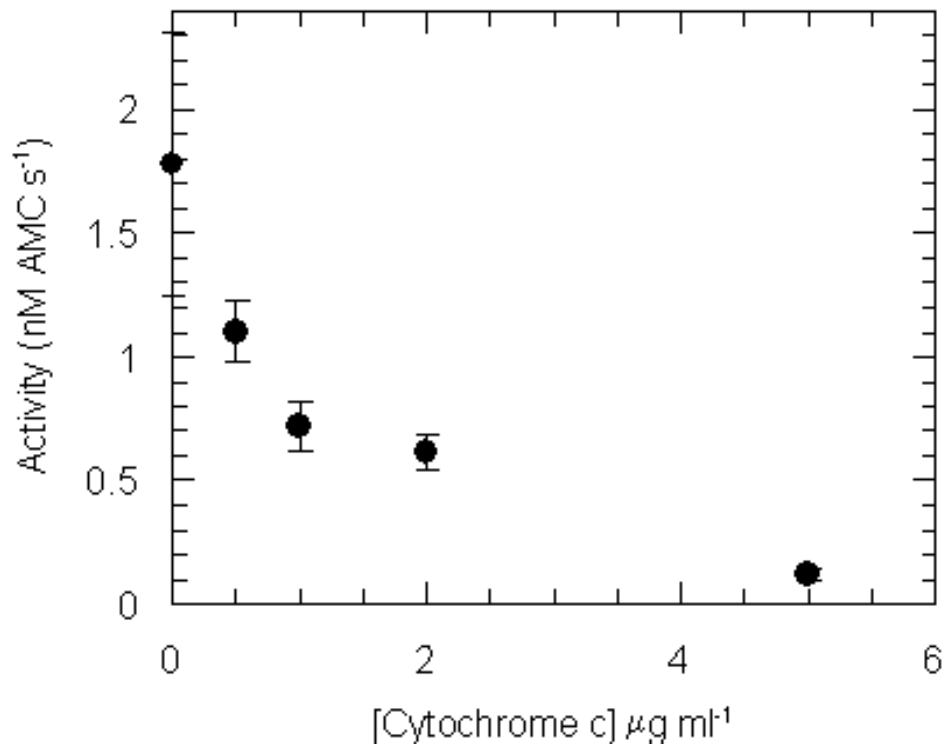
Figure 4.1: Cytochrome c Interacts with the 20S Proteasome Core Partical
The interaction of the protein substrate cytochrome c with the 20S proteasome
core particle was investigated using the peptide Suc-LLVY-AMC as a probe
for active site occupancy. Shown here is the activity of the production of
free AMC from the hydrolysis of the substrate peptide Suc-LLVY-AMC. The
decrease in activity suggests a specific interaction with the proteasome as the
protein substrate blocks access for other substrates to the active sites.
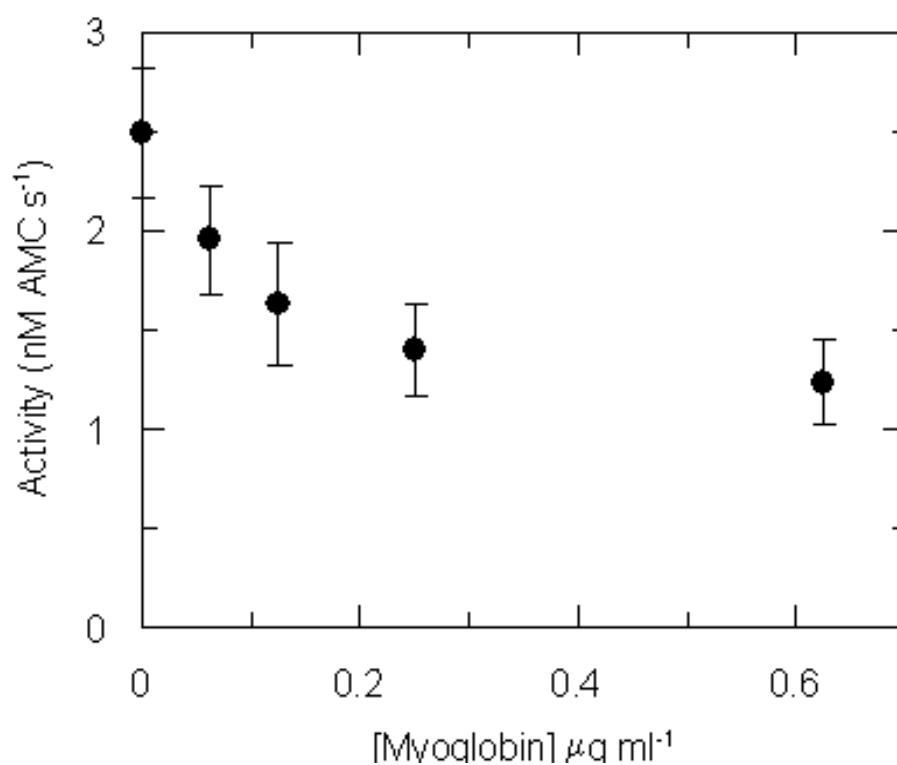
Figure 4.2: Myoglobin and the 20S Proteasome Core Partical Interact
The interaction of the proteasome with a protein substrate, myoglobin, was probed. The decrease in the rate of production of free AMC by 20S proteasome hydrolysis of the substrate peptide Suc-LLVY-AMC demonstrates an interaction between the proteasome and the protein substrate as it blocks access to the active site for the peptide.
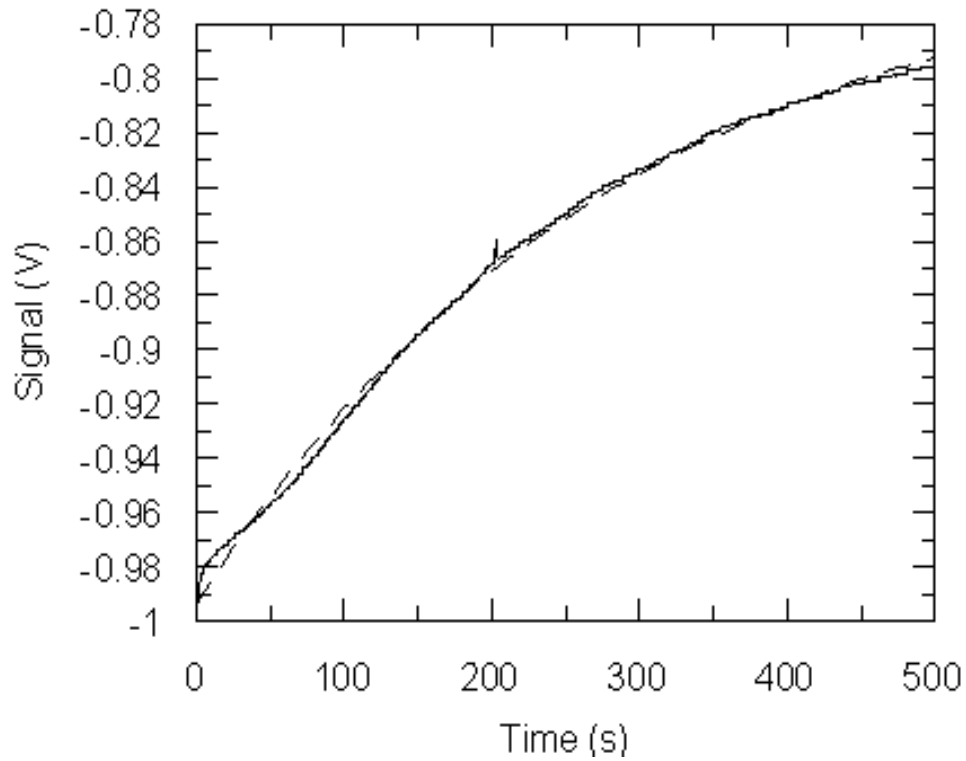
Figure 4.3: Exponential Signal of Protein Degradation

To investigate the nature of the enzyme-protein interaction, a series of measurements were taken in varying concentrations of enzyme. The protein substrate concentration remained constant in these experiments. In this panel, enzyme (150 μg ml^{-1}) and carboxy methylated (625 μg ml^{-1}) lysozyme were reacted and the signal due to the tryptophan fluorescence measured. The data was then fit (dashed line) to a single exponential equation and the amplitude of the change was recorded.
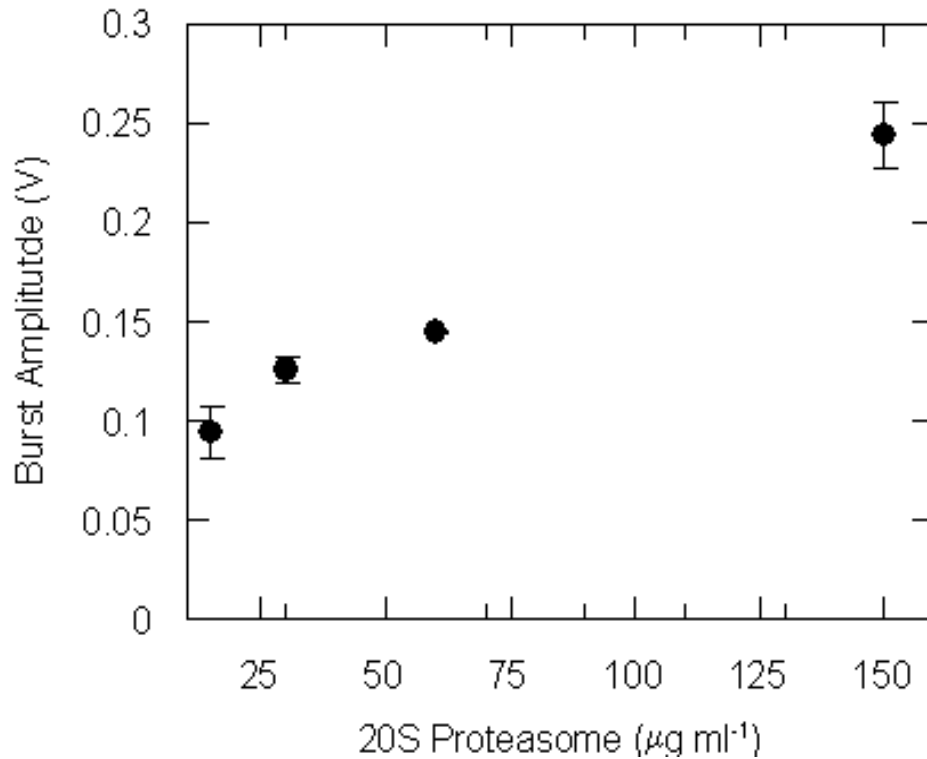
Figure 4.4: Specific Enzyme and Protein Substrate Interaction

To assay the nature of the enzyme and substrate protein interaction, the signal amplitude was measured as a function of enzyme concentration. The signal amplitude is defined as the amplitude of the fit of the data to a single exponential equation and is reported in volts. These amplitude values were then plotted against the enzyme concentration. The increase in the signal amplitude as a function of enzyme concentration is indicative of a specific interaction between the enzyme and the substrate protein. In this experiment, 625 μg ml^{-1} of carboxymethylated lysozyme was reacted with an increasing amount of purified recombinant 20S proteasome and the digestion of the protein substrate was monitored as described in *Methods*.

Substrate	Rate of Tryptophan Fluorescence Change (mV s^{-1})
CM-Lysozyme	0.560 ± 0.10
Ac-Lysozyme	-0.065 ± 0.04
CM-Casein	-0.178 ± 0.03

Table 4.1: Proteasome Degradation Rates Using Various Derivatized Proteins Activity was measured in TAPS buffer (25 mM TAPS, pH 8.1, 100 mM NaCl, 250 μM EDTA, 45°C) using tryptophan fluorescence (280 nm excitation, emission above 305 nm was collected). 0.07 μg ml^{-1} of purified recombinant proteasome was used with substrate concentrations of 0.2 μg ml^{-1}. Rates are expressed in mV s^{-1}, the unadjusted rate measured by the photomultiplier. Negative values indicate a loss of tryptophan fluorescence, and positive values an increase in the fluorescence over time. Similar values were seen for acetylated casein, and both carboxymethylated- and acetylated-ovalbumin.

	Rate of Tryptophan Fluorescence Loss (mV s^{-1})	
Enzyme	CM-Ovalbumin	Ac-Ovalbumin
20S Proteasome	0.15 ± 0.01	0.38 ± 0.08
Chymotrypsin	0.040 ± 0.08	0.28 ± 0.01
Trypsin	n.d.	0.24 ± 0.10

Table 4.2: Comparison of Proteolysis Rates for the 20S Proteasome and Other Proteases

Substrate proteins were reacted with purified trypsin, chymotrypsinogen, and recombinant 20S proteasome. Activity was measured by monitoring the rate of tryptophan fluorescence loss in the substrate protein as described in *Methods*. Rates are expressed as the loss in the fluorescence signal, expressed in mV per second which corresponds to the loss of the fluorescence from the tryptophan residues intrinsic to the protein substrates. The concentrations of chymotrypsin and trypsin were 0.1 μg ml^{-1} in buffer, and 20S proteasome was 0.07 μg ml^{-1} in buffer. Substrate concentrations were 0.2 μg ml^{-1} in buffer of each substrate protein.

	Rate of Tryptophan Fluorescence Loss (mV s^{-1})	
%SDS (wt vol^{-1})	CM-Ovalbumin	Ac-Ovalbumin
0	0.165 ± 0.012	0.214 ± 0.153
0.005	0.188 ± 0.006	0.040 ± 0.011
0.010	0.273 ± 0.085	0.045 ± 0.016
0.020	n.d.	0.137 ± 0.087
0.030	0.088 ± 0.006	0.094 ± 0.037

Table 4.3: Effect of SDS on Protein Digestion

Chemically modified proteins were reacted with purified 20S proteasome and the proteolytic activity measured in varying concentrations of SDS. Unlike what is observed with peptide hydrolysis, the proteasome does not seem to more rapidly hydrolyze protein substrates when SDS is added. The larger standard error values for the acetylated substrates are likely due to the lack of charge on the substrate, causing it to precipitate slowly during the course of the enzyme assay.

4.4.4   Magnesium Has No Effect on Proteolysis Rates

Magnesium and calcium salts are well known to stimulate fluorescent peptide hydrolysis. This has been shown to be due largely to the increase in ionic strength, although at low concentrations, a specific ion effect with magnesium is detectable (see Chapter 2). To test the effectiveness of metal ions and ionic strength on rates of protein proteolysis, the modified protein substrates were reacted with purified recombinant proteasome in the presence of increasing concentrations of magnesium, calcium, and potassium chloride salts. Shown in Table 4.4 is the rate of tryptophan fluorescence loss as a function of magnesium, calcium (Table 4.5), and potassium chloride salt (Table 4.6) concentrations. In all cases, the effects of the metals on proteolysis rates are minimal. Similar results were obtained for acetylated- and carboxymethylated lysozyme (data not shown). In each instance, the standard errors were larger at each data point for the acetylated protein substrates than for the carboxymethylated proteins due to a reduced charge on the substrate which resulted in a slow precipitation during the course of the reaction.

	Rate of Tryptophan Fluorescence Loss (mV s^{-1})	
MgCl$_2$ (mM)	CM-Ovalbumin	Ac-Ovalbumin
0	0.25 ± 0.01	0.206 ± 0.16
25	0.24 ± 0.01	0.105 ± 0.04
50	0.25 ± 0.01	n.d.
100	0.25 ± 0.01	0.162 ± 0.12
200	0.20 ± 0.02	0.127 ± 0.06
500	0.32 ± 0.16	0.193 ± 0.07

Table 4.4: Effect of Magnesium on Proteolysis Rates

To investigate the effects of added magnesium on the rates of proteolysis of modified protein substrates, recombinant 20S proteasome and substrate proteins were reacted in varying concentrations of magnesium chloride. Over this concentration range, from 0 to 500 mM, a ten-fold activation of peptide hydrolysis is commonly observed (see Figure 2.17).

	Rate of Tryptophan Fluorescence Loss (mV s^{-1})	
CaCl$_2$ (mM)	CM-Ovalbumin	Ac-Ovalbumin
0	0.214 ± 0.003	0.310 ± 0.255
25	0.280 ± 0.004	0.368 ± 0.137
50	0.237 ± 0.012	0.145 ± 0.048
100	0.217 ± 0.005	0.312 ± 0.120
500	0.231 ± 0.007	0.187 ± 0.095

Table 4.5: Effect of Calcium on Proteolysis Rates of Protein Substrates
To investigate the effects of added calcium on the rates of proteolysis of modified protein substrates, recombinant 20S proteasome and substrate proteins were reacted in varying concentrations of calcium chloride. Over this concentration range, from 0 to 500 mM, a five-fold activation of peptide hydrolysis is commonly observed (see Figure 2.16), similar to that of magnesium based activation.

	Rate of Tryptophan Fluorescence Loss (mV s^{-1})	
KCl (mM)	CM-Ovalbumin	Ac-Ovalbumin
0	0.249 ± 0.009	n.d.
25	0.271 ± 0.017	0.248 ± 0.193
50	0.227 ± 0.003	0.259 ± 0.204
100	0.264 ± 0.008	0.153 ± 0.103
200	0.143 ± 0.038	0.236 ± 0.081
500	0.179 ± 0.065	0.328 ± 0.186
1000	0.147 ± 0.027	0.328 ± 0.138
1500	0.117 ± 0.020	0.071 ± 0.049

Table 4.6: Effect of Potassium on Protein Substrate Hydrolysis

To investigate the effects of added potassium on the rates of proteolysis of modified protein substrates, recombinant 20S proteasome and substrate proteins were reacted in varying concentrations of potassium chloride. Over this concentration range, from 0 to 1500 mM, a seven-fold activation of peptide hydrolysis is commonly observed (see Figure 2.21).

4.4.5   Denaturants Do Not Affect Proteolysis

Previous research has shown that the denaturant guanidine hydrochloride can increase peptide hydrolysis up to six-fold, but that the denaturant urea is unable to increase activity against the peptide substrate Suc-LLVY-AMC (Akopian et al., 1997). Activity drops off above 0.5 M denaturant, presumably as the enzyme conformation changes. To test the effect of these additives on protein proteolysis, enzyme and modified protein substrates were equilibrated with increasing concentrations of denaturant, and then reacted while the tryptophan fluorescence of the substrate protein was measured. As shown in Tables 4.7 and 4.8, neither denaturant provides a dramatic increase in activity at concentrations up to 0.5 M.

4.5   Discussion

The above detailed experiments provide evidence that the proteasome can degrade destabilized proteins at an appreciable rate, but that known activators of peptide hydrolysis have little or no effect on protein degradation. This appears to be the first reported direct examination of the role of activators on protein digestion by the 20S proteasome.

	Rate of Tryptophan Fluorescence Loss (mV s^{-1})	
Urea (mM)	CM-Ovalbumin	Ac-Ovalbumin
0	0.154 ± 0.001	0.381 ± 0.009
25	0.198 ± 0.007	0.180 ± 0.014
50	0.199 ± 0.001	0.287 ± 0.018
100	0.207 ± 0.004	0.292 ± 0.016
200	0.202 ± 0.004	0.499 ± 0.010
500	0.200 ± 0.001	0.315 ± 0.009

Table 4.7: Effect of Urea on Proteolysis

To test the effect of the denaturant urea on the rates of protein hydrolysis, protein substrates and recombinant 20S proteasome were reacted in the presence of increasing amounts of urea. As seen with peptide substrates, there is no activation of proteolysis activity as urea concentrations are increased.

	Rate of Tryptophan Fluorescence Loss (mV s^{-1})	
Guanidine HCl (mM)	CM-Ovalbumin	Ac-Ovalbumin
0	0.210 ± 0.001	0.110 ± 0.07
25	0.160 ± 0.10	0.200 ± 0.10
50	0.160 ± 0.03	0.240 ± 0.15
100	0.190 ± 0.01	0.240 ± 0.10
200	0.150 ± 0.001	n.d.
500	0.190 ± 0.02	0.34 ± 0.08

Table 4.8: Effect of Guanidine on Proteolysis

To test the effects of the denaturant and proteasome activator guanidine hydrochloride on protein hydrolysis by the proteasome, proteolysis activity was monitored using the intrinsic fluorescence of the protein substrates. As guanidine hydrochloride concentrations were raised, the activity was measured. Over this range, peptide hydrolysis activities are raised several fold (see (Akopian et al., 1997)), but the above data shows that there is no effect on protein hydrolysis.

These findings are in strong contrast to the effects of activators on peptide hydrolysis that have been reported in the literature and in previous chapters of this thesis. It is unlikely that the chemistry of cleavage of the peptide bond in protein substrates differs from that in peptide substrates. The nature of the substrates differs significantly, though, in structure and size. The peptide substrate most often used with the *T. acidophilum* proteasome, Suc-LLCY-AMC, is too short in length to have any regular structure which would have to be unwound before entering the proteasome channel. Protein substrates, however, do not exist in extended conformations and must be denatured at the ends to permit entry through the narrow α-pore. The narrowness of the pore formed by the α-subunits prevents access of a hairpin loop of protein into the central chamber (Wenzel and Baumeister, 1995). This step would certainly involve the disruption of non-covalent bonds such as ionic pairings and hydrogen bonds, as well as the hydration of a significant amount of surface area. It is this difference in events before entry into the proteasome channel that underlies the discrepancies between peptide hydrolysis and protein degradation.

It has been proposed that SDS may widen the narrow pore formed by the α-subunits, permitting faster entry for substrates into the active site chamber (Baumeister et al., 1998). Previous chapters in this thesis have shown that this hypothesis was not found to be true, and the data using protein substrates was consistent with this finding. A wider entrance into the proteasome channel would manifest itself as an increased rate of proteolysis with increasing

SDS concentrations. If entry into the proteasome active site chamber is the rate determining step, the absence of SDS activation of proteolysis is consistent with a different role for SDS in proteasome mediated protein degradation. The concentrations of SDS used in these experiments are too low to significantly disrupt the structure of the substrate proteins. This was verified by CD spectral analysis (data not shown) of the protein substrates.

A lack of stimulation of proteasome activity was also obtained with magnesium, which is known to be a potent activator of peptide degradation by the proteasome. Despite high concentrations of magnesium, and hence a high ionic strength, no activation of proteolytic activity was observed. Prior investigations (Chapter 2) have shown that it is the ionic strength that is contributed by magnesium that leads to an enhancement of early events in peptide hydrolysis.

The activity of the proteasome against varying concentrations of a single protein substrate was measured. As shown in Figure 4.5, the lack of saturation in activity suggests a very high K_m value for this substrate. This is also consistent with the data in Table 4.9, in which the enzyme concentration was altered in the presence of a fixed substrate concentration and the activity was measured. This is in clear contrast to a typical Michaelis-Menten kinetic model, for which would a saturation point for the increasing protein substrate concentrations would be expected as well as a linear increase in activity of protein hydrolysis with increasing enzyme concentration in the reaction.

Enzyme (μg)	Rate of Tryptophan Fluorescence Loss (mV s^{-1})
0.03	1.27 ± 0.02
0.06	1.24 ± 0.05
0.12	1.28 ± 0.08
0.18	1.23 ± 0.04

Table 4.9: Enzyme Activity at a Fixed Substrate Concentration

To test the effect of varied 20S proteasome enzyme concentration at a fixed substrate protein concentration, varying concentrations of enzyme were reacted with a fixed concentration (125 μg ml^{-1}) of acetylated ovalbumin. The lack of an effect of the enzyme concentration on the measured activity (presented as mV s^{-1}, as described in *Methods*) suggests there is no role played by the enzyme in the rate determining step for the hydrolysis of the substrate protein.
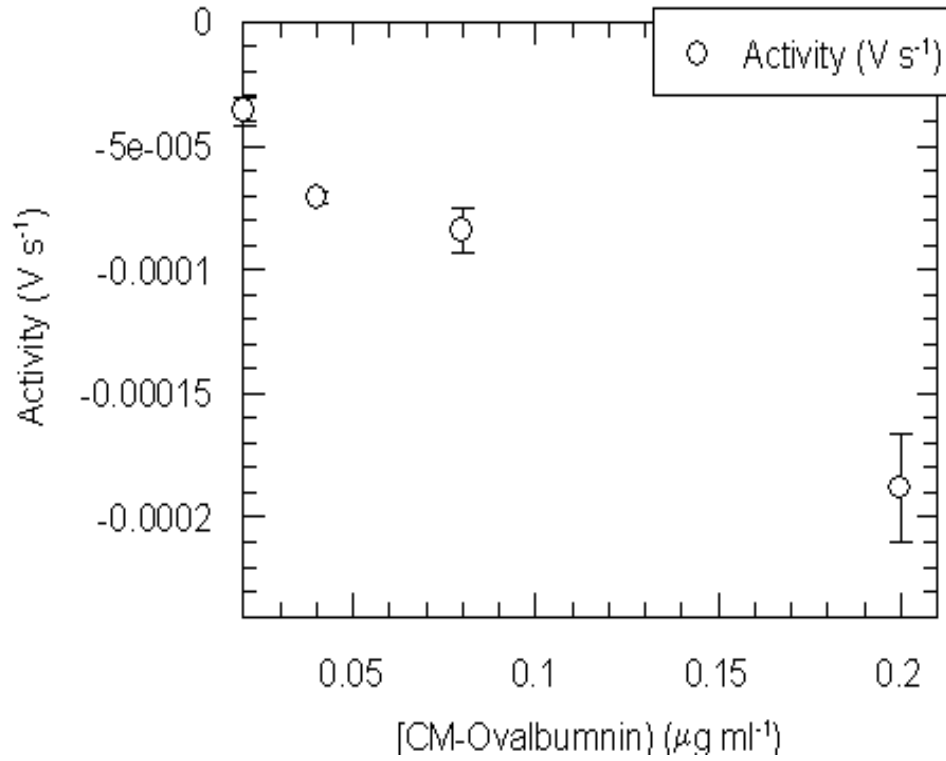
Figure 4.5: High Apparent K_m for Protein Substrates

To examine the general nature of a substrate affinity for the proteasome, modified protein substrate (in this experiment carboxymethylated ovalbumin) was added in increasing amounts and the activity of the proteasome (at a concentration of 0.07 μg ml^{-1}) was measured. As noted in the text, the lack of a saturation point observed in this figure suggests a more complicated process than a simple enzyme-substrate complex.

4.5.1   A Model for Protein Hydrolysis

The data collected here can be used to assemble a model of protein hydroly-
sis by the proteasom. This can be used to explain why activators of peptide
hydrolysis do not have any impact on proteolysis of large protein substrates.
Shown in Figure 4.6 is a model of how the proteasome reacts with destabi-
lized protein substrates. Substrate protein, depicted as **S** in Figure 4.6, must
undergo some form of an interconversion to a form accessible to the protea-
some. This is needed to allow entry into the proteasome active site chamber.
Furthermore, this interconversion is not facilitated by the proteasome. Only
when the protein is in an accessible form, designated $\mathbf{S}^*$ in the scheme, can
it enter into the proteolysis pathway. It is this interconversion step that is
rate limiting and obscures any mechanism enhancements brought about by
the peptide hydrolysis activators.

This technique is limited in that it can only detect large scale changes
which lead to solvent quenching of the protein fluorescence. Secondly, if any
events occur durig proteolysis which do not alter the quenching, no change in
the signal will be recorded and the event will remain undetected. However,
this technique represents an easy, direct way to monitor protein digestion by
the proteasome.

The activity of the proteasome against a single protein substrate at varying
concentrations was examined. As shown in Figure 4.5, the lack of a saturation
point suggests a very high K_m^{app} value for this substrate. This is consistent

with an interconversion step for the substrate to exist in two forms, only one of which can be broken down by the proteasome. This accessible form exists in a low concentration relative to the total amount of substrate protein present. Secondly, when the enzyme concentration is varied, the rates of protein digestion remain constant, indicating there is no direct participation of the proteasome in this step (Table 4.9). It is interesting to note that this steady state activity is constant in the presence of varying concentrations of enzyme despite increasing signal amplitudes, as shown in Figure 4.4.

One direct conclusion of these two scenarios, a high K_m^{app} value for substrate and conditions consistent with a low K_m value, is the presence of more than one form of the substrate. This simple model is the enzyme independent interconversion of the **S** and **S*** forms of the substrate, with a high equilibrium constant between the two (yielding a low concentration of the form that can react with the enzyme). The measured concentration of the substrate in these figures is therefore the sum of the two (or more) forms. To saturate the enzyme in a traditional Michaelis-Menten scheme would therefore take a high concentration of the **S*** form, the substrate form the enzyme can react with, requiring an even higher concentration of the **S** form. In the presence of accessory proteins, S* is generated at an increased rate, accelerating the rate of protein substrate breakdown. This interconversion between the **S** and **S*** forms occurs naturally in proteins.

$$\begin{array}{c} \mathbf{S} \\ \Big\downarrow \text{\textit{Rate Limiting}} \\ \mathbf{E+S^*} \rightleftharpoons \mathbf{ES^*} \longrightarrow \text{\textit{Regular Proteolysis}} \end{array}$$
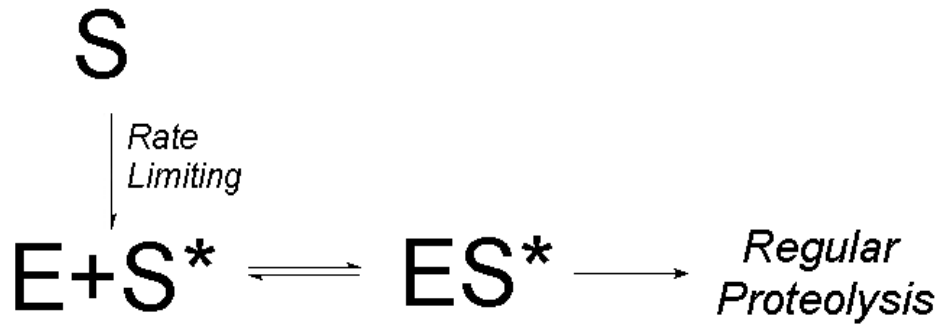
Figure 4.6: Degradation of Protein Substrates by the Proteasome

In this scheme, the protein substrate, designated by **S**, must first undergo an interconversion to an accessible form (**S***), which can enter the active site chamber. This becomes the rate limiting step in this new scheme, obscuring the effects of activators on the chemical mechanism of hydrolysis.

One consequence of this model is that the susceptibility of the protein to being a *T. acidophilum* proteasome substrate is directly related to its stability. Proteins that have an equilibrium concentration of the $\mathbf{S}^*$ form of the protein that is significant will be digested at a faster rate than more stable proteins, which have low concentrations of the $\mathbf{S}^*$ form at equilibrium. This is consistent with physiological findings that proteins that are marginally stable are more prone to degradation than stable proteins (Zhou et al., 2000; Andreatta et al., 2001; Miyake et al., 2000). As shown in Figure 4.6, this equilibrium in the presence of the enzyme is not reversible as the proteasome reacts with $\mathbf{S}^*$ before it can return to the $\mathbf{S}$ state.

These experiments are preliminary, and only tested on a few protein substrates. Secondly, proteins of varying stabilities were not tested. This could be tested with mutant proteins with varying stabilities, for example. This would help to investigate the relationship between stability and the efficiency of digestion by the proteasome in a more controlled fashion, utilizing neaarly identical sequences and structures.

One unanswered potential contradiction of the data in Tables 4.7 and 4.8 is that these denaturants should increase the concentration of $\mathbf{S}^*$ as they denature the protein, therefore increasing the rate of protein hydrolysis in this model. However, this is clearly not observed. One possible explanation is that the concentration of denaturants used, such as guanidine hydrochloride or urea, are too low to significantly alter the structure of the substrate proteins. The

data presented here is unable to provide an conclusive answer to this issue.

There are several chaperone and 'unfoldase' proteins that have been identified in *T. acidophilum* (Ruepp et al., 2000). These include VAT and GimC, as well as the thermosome chaperone (Waldmann et al., 1995). These proteins act on short lived or non-native proteins to either refold them, in the case of the thermosome and GimC, or to unfold them, in the case of VAT. If the chaperone action of the thermosome is unable to yield a correctly folded protein, it is thought that the 20S proteasome is then used to degrade these to smaller peptides, which are then acted on by other proteases to eventually yield free amino acids (Ruepp et al., 2000). How these protein substrates are selected to be acted on by these accessory proteins is not yet known. The 20S proteasome has been shown to act on misfolded and oxidatively damaged proteins by itself (McNaught et al., 2001), without the aid of the PA28 or PA700 cap structures in eukaryotes.

These conclusions are consistent with previous literature which found that the proteasome from *T. acidophilum* could break down proteins which are associated with the ubiquitin molecule (Wenzel and Baumeister, 1993). It is still not determined if the entry of protein substrates into the proteasome active site chamber is an active or passive process by the proteasome. A passive process has been proposed for another large multimeric protease, tricorn, which also works on large protein substrates (Brandstetter et al., 2001).

Protein products which exit the proteasome are then broken down by other

cellular proteases. There has been some evidence that the proteasome interacts with the tricorn protease *in vivo* in *T. acidophilum* (Tamura et al., 1998). Tricorn is a large hexameric protease which is thought to break down the peptides generated by the proteasome into amino acids in a processive manner (Brandstetter et al., 2001).

4.5.2 Conclusions

The above research has evaluated the effects of activators on protein hydrolysis, which have different impacts than are seen on peptide hydrolysis by the 20S proteasome. Because of the structural differences in the substrates and the resulting differences in the mechanisms of entry for the two types of substrates, these effects of activators are not observed on protein hydrolysis. Instead, the rate limiting step becomes the entry of substrate into the active site chamber, a step that is not facilitated by any of the tested activators. This has implications on the possible *in vivo* roles of activators, as well as means by which to enhance the breakdown of proteins by the 20S core particle.

Chapter 5

Cooperativity and Subunit Interactions

5.1 Abstract

The 20S proteasome is a large, multimeric enzyme composed of 28 subunits, with four rings of seven protein subunits each. This close proximity of protein subunits can readily lead to strong interactions and feedback mechanisms between adjacent subunits. Interactions can be manifested as positive or negative cooperativity with respect to substrate or other molecules, including non-Michaelis-Menten kinetics. Kinetic analysis of the behavior of the *T. acidophilum* 20S core particle reveals substrate induced inhibition and homotropic cooperativity by low levels of the peptide aldehyde inhibitor Z-LLLal, leading to a two-fold activation against the substrate peptide Suc-LLVY-AMC. Additionally, diffusion effects were analyzed and demonstrated increased solute

mobilities for the substrate, suggested facilitated diffusion in the presence of some solutes. Analysis of kinetic data together with structural data suggests possible mechanisms of subunit communication and provide an explanation for the observed cooperativity and activation or inhibition of the enzyme.

5.2 Introduction

The 20S proteasome core particle is a barrel shaped enzyme composed of four rings of seven subunits each (Grziwa et al., 1991). As noted in Chapter 1, the α-subunits will spontaneously form a ring structure, while the β-subunits will aggregate in the absence of some structural scaffold (Yao et al., 1999; Zwickl et al., 1994). The final quaternary structure of the enzyme arises out of a significant degree of contact between the β-subunits, and is held in place by the α-subunits.

Obviously the closeness of the subunits and their high degree of contact means that there is an increased likelihood for some form of positive or negative cooperativity between the subunits. The cooperativity would be manifested as non-Michaelis-Menten kinetics as well as being evidenced in ligand binding plots that deviate from simple saturation as represented by hyperbolic models. This cooperativity could arise from conformational changes within a subunit during the proteolytic cycle which are then propagated to a neighboring subunit to effect a similar change in that subunit.

These conformational shifts could arise from at least two factors. First,

the mere act of simply binding substrate or inactivator in the active site of the enyme could induce a structural change within a subunit. Secondly, stabilization of intermediates, or of an enzyme-inhibitor adduct, could cause similar changes as various residues move to stabilize this new structure.

Positive cooperativity would seem to be an advantageous strategy for *in vivo* circumstances. As more protein substrate is present, the enzyme would achieve a higher activity state which would potentially lead to the faster degradation of the target protein (Djaballah et al., 1992; Kuckelkorn et al., 1995; Piccinini et al., 2000). However, there is some evidence that negative cooperativity is observed (Gutsche et al., 2000; Dolenc et al., 1998).

Conflicting evidence has been found for the presence and types of cooperativity in the 20S proteasome core particle from *T. acidophilum* when analyzed in terms of metal ion effects, inhibitor binding, and substrate reactivity. However, when analyzed in light of other groups' data, cooperativity effects are most likely present and can occur in both positive or negative directions.

To test these findings and to attempt to clarify conflicting evidence, a series of experiments were undertaken to analyze the cooperative behavior of the *T. acidophilum* 20S proteasome core particle. The number of active sites per proteasome particle can be directly assayed by stoichiometric binding of a small inhibitor. Substrate binding curves can be used to assess non-Michaelis-Menten behavior for enzyme activity. The use of a small inhibitor, which mimics the intermediates of the normal substrate hydrolysis cycle, can be used

to assay for homotropic cooperativity. A variety of small molecules which can form non-covalent interactions with protein subunits were used to investigate bridging between subunits. Lastly, additional solutes in the reaction mixture which affect the viscosity of the solution but not the active sites of the enzyme can be used to investigate diffusion effects on substrate entry.

5.3   Materials and Methods

5.3.1   Materials

Materials and reagents were obtained as described in Section 2.3.1. The PDB (Berman et al., 2000) structure files 1PMA (*T. acidophilum* 20S proteasome) and 1RYP (*S. cerevicea* 20S proteasome) were used for structural analyses.

5.3.2   Inhibitor Binding

Inhibition of the proteasome by the peptide aldehyde inhibitor Z-LLLal solubilized in DMF (final concentration not more that 0.1% DMF) was followed by monitoring its activity as a function of time using the substrate Suc-LLVY-AMC. To measure the binding constant, k_{on}, enzyme in buffer was reacted against a solution containing both substrate and inhibitor and the activity against the substrate peptide Suc-LLVY-AMC was measured as described in Section 2.3.6.

5.3.3 Tryptic Peptide Substrate Generation

Purified lysozyme was dissolved to a final concentration of 100 μg ml^{-1} in water and digested overnight with purified trypsin (5 μg ml^{-1}) at 37°C. The reaction was stopped by the addition of PMSF, which inhibits trypsin but does not affect the proteasome (Seemuller et al., 1995c). These peptides were then used without further purification in proteasome assays.

5.3.4 Peptide Hydrolysis Assays

Hydrolysis of the peptide Suc-LLVY-AMC was monitored and the data analyzed as described in Section 2.3.5.

5.3.5 Structural Analysis

Proteasome core particle structure files were downloaded from the PDB website (Berman et al., 2000) and analyzed using molecular viewing programs to examine structural details. Structures 1PMA (*T. acidophilum* (Lowe et al., 1995)) and 1RYP (yeast (Groll et al., 1997)) were used for the studies. The applications Weblab Viewer (Molecular Simulations, Inc.), RasMol (Roger Sayle and GlaxoWellcome), SwissPDB View (Guex et al., 1997), and VMD (UIUC Theoretical Biophysics Group) were used to visualize and analyze the structures.

5.3.6   Data Analysis

Data for the inhibition of the proteasome by Z-LLLal was analyzed to yield the inhibition constants, K_i, k_{on} and k_{off}, as described in Section 2.3.7.

5.4   Results

5.4.1   Substrate Inhibition

To test the effect of substrate on activity, a constant amount of 20S proteasome was reacted with a variable amount of peptide substrate. As shown in Figure 5.1, with this peptide, non-Michaelis-Menten kinetics are observed. The enzyme displays substrate inhibition at levels above 40 μM Suc-LLVY-AMC, with approximately a 50% decrease in activity observed. As shown in Figure 5.1, after an initial increase in activity which appears to be hyperbolic, an exponential decrease to a final level of activity occurs.
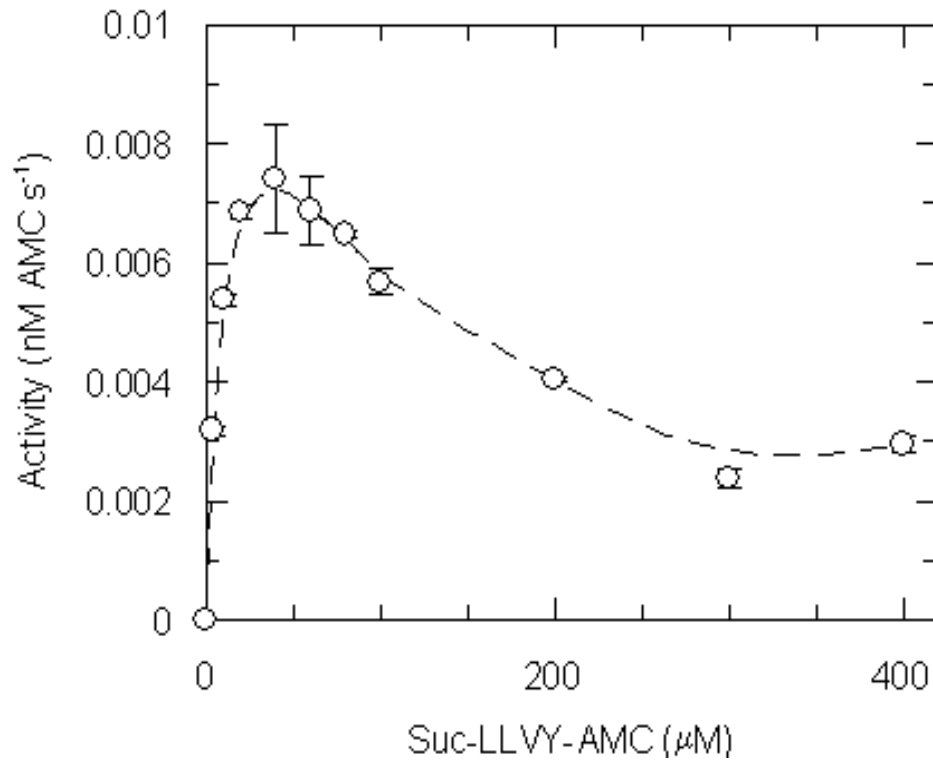
Figure 5.1: Substrate vs. Activity Shows Substrate Inhibition

In this experiment, substrate was added in increasing amounts to a fixed concentration of purified recombinant 20S proteasome and the activity measured. The result shows a deviation from Michaelis-Menten kinetics with substrate inhibition, suggestive of negative cooperativity in the enzyme.

5.4.2   Number of Active Sites per Molecule of Enzyme

In order to begin to assess the nature and type of cooperativity which may
be present in the 20S proteasome core particle, it is vital to assess the number
of functional active sites per enzyme molecule in solution. This provides
a baseline measurement to understand the standard assay conditions of the
enzyme. The most direct method to measure this is to titrate the enzyme
with an inhibitor and assay the remaining activity. As shown in Figure 5.2, a
linear extrapolation of the data from the middle portion of the plot suggests
that at least 12 and possibly 14 active sites per particle are active in solution.
With this data, any increase or decrease in the activity of the enzyme in terms
of increased chemical reactivity can be measured. Because the number of ob-
served active sites is the maximum expected, any increase in activity is not an
increase in the number of functioning active sites.
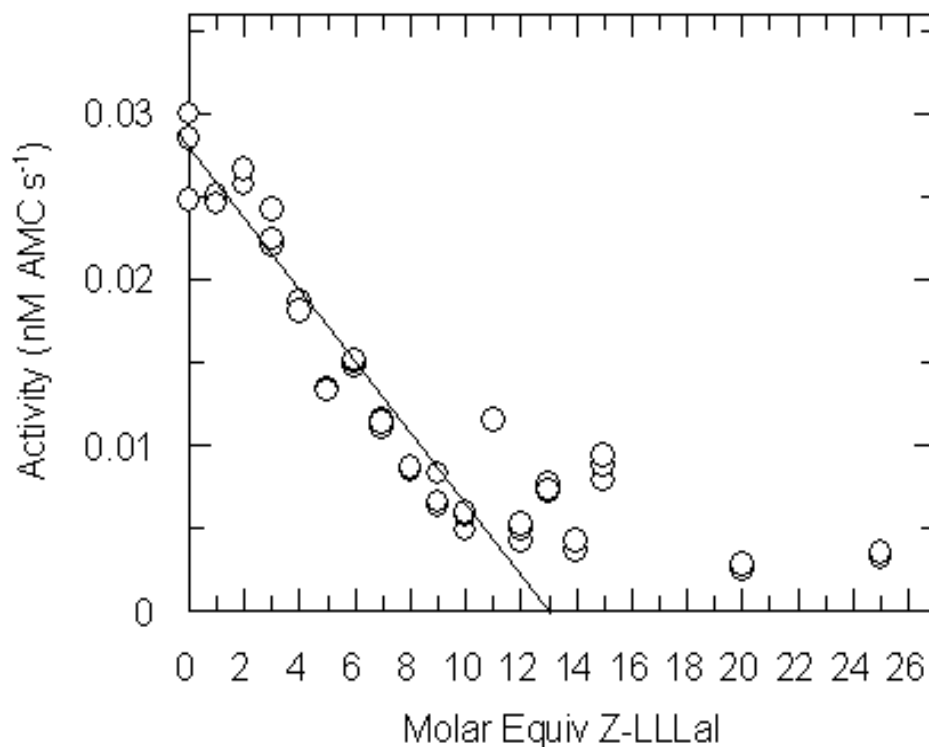
Figure 5.2: Titration of Z-LLLal Binding

As described in *Methods*, the inhibitor peptide Z-LLLal was reacted overnight in varying ratios of concentrations with purified recombinant 20S proteasome. The resulting activity was measured using the substrate peptide Suc-LLVY-AMC. As is evident from the data above, if the center data is extended, there is approximately a 12:1 ratio of inhibitor molecules to proteasome molecules, suggesting nearly all active sites are accessible in solution.

5.4.3 Positive Cooperativity

As discussed in previous chapters, the peptide aldehyde inhibitor Z-LLLal can be used to probe early events in the proteolytic mechanism. The enzyme-inhibitor adduct mimics the tetrahedral intermediate. Binding of the aldehyde inhibitor has revealed positive cooperativity between subunits. As shown in Figure 5.3, at subsaturating levels of inhibitor, an increase of activity against the peptide substrate occurs. This effect only occurs under certain assay conditions and is metal ion and pH-dependent. This observation is contrary to an independent active site model, in which the increase in inhibitor concentration would result in an approach to zero activity, as shown in Figure 5.3 in the filled symbols and fit to Equation 2.3.

5.4.4 Exogenous Peptide Effects

To test the effects of other peptides on the specific activity against the peptide Suc-LLVY-AMC, tryptic peptides of lysozyme were added to a reaction of purified 20S proteasome and a constant amount of substrate peptide (Suc-LLVY-AMC), and the production of free AMC was measured. As more tryptic peptides are added, a decrease in activity against the substrate Suc-LLVY-AMC occurs. This is clearly illustrated in Figure 5.4.
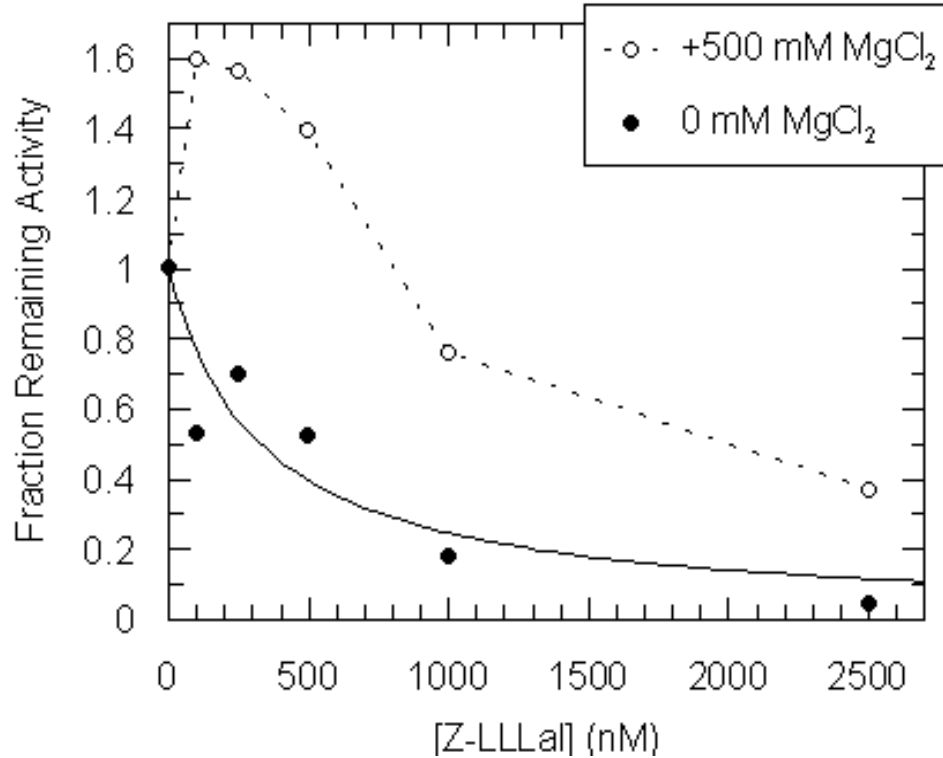
Figure 5.3: Homotropic Cooperativity in the Presence of Peptide Aldehyde
Enzyme and peptide aldehyde inhibitor were reacted and the activity mon-
itored using the peptide substrate Suc-LLVY-AMC (20 μM) in the absence
(closed symbols) and presence (open symbols) of 500 mM magnesium chlo-
ride. The solid line is a fit of the data to Equation 2.3, the dashed line is a
smooth fit to the data. The increase in activity at low inhibitor concentra-
tions in the presence of MgCl$_2$, above the activity in the absence of inhibitor,
is suggestive of some form of homotropic activation (see text).
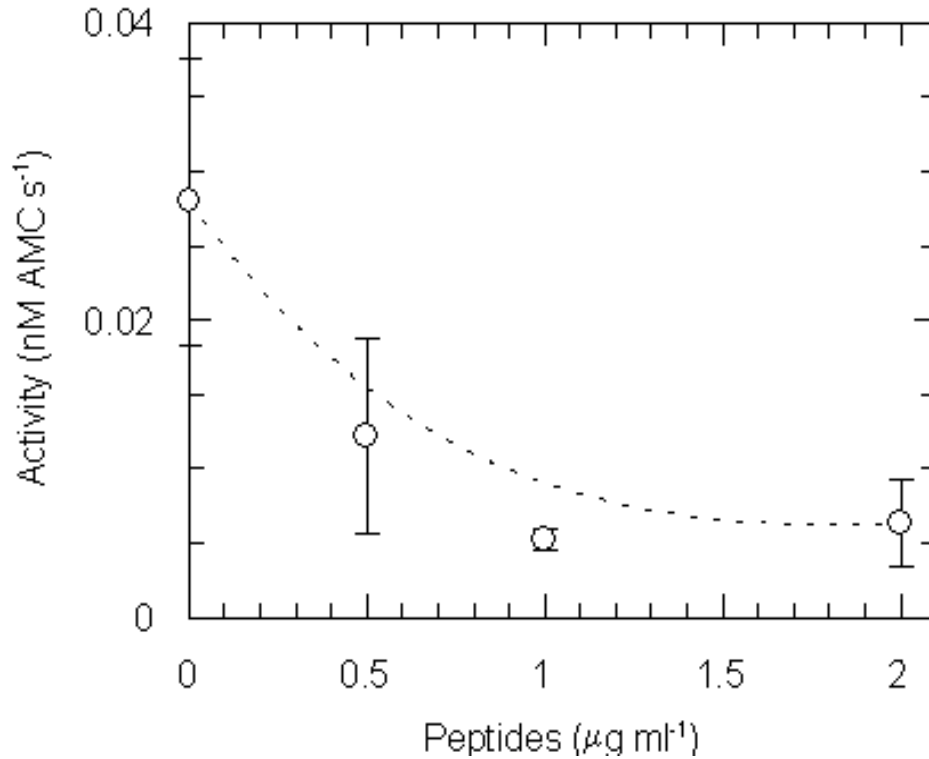
Figure 5.4: Competition by Peptides Suggests a Lack of Cooperativity

To test the generality of the effect of an active neighboring active site on activity, tryptic peptides of lysozyme were added to the reaction of purified 20S proteasome and the substrate Suc-LLVY-AMC (20 μM) and the rate of free AMC production was measured. If an active subunit were activating a neighboring subunit, an increase in the rate of AMC production should be observed (see text). However, the data shown here fits a simple first order model for the interaction of peptide substrate and the enzyme. This first order fit indicates a lack of any cooperative effects and instead displays simple competition for the active sites by the two types of substrates.

5.4.5   The Effect of Added Solutes on Substrate Entry

One source of rate enhancements could be an increased diffusion constant into the active site chamber. This could come from various chemical solutes outside of the enzyme core, affecting the diffusion coefficient for small molecules to enter the active site chamber, such as the substrate peptide. This increased diffusion constant would be manifested as a higher rate of substrate and enzyme interaction, visible as an increased rate of the enzyme.

Interestingly, when the intact or acetylated protein lysozyme is substituted, there is a dramatic increase in the activity of the proteasome against the substrate peptide Suc-LLVY-AMC (Figure 5.5). To determine at which step in the reaction this effect was being generated, inactivation kinetics were measured as a function of lysozyme concentration. As shown in Figure 5.6, this effect is on the association rate, as measured by the increase in k_{on} rate constants as a function of lysozyme concentrations. This effect is specific for lysozyme only, and does not work for other proteins such as ovalbumin, apoferritin, or casein.

To examine the role of viscosity on the enhancement of the activation of the enzyme, various solutes were included to lower the diffusion constant in the reaction. The addition of sucrose or PVP-10 to the reaction mixture increases the viscosity, lowering the mobility of the reactants (and products). If any enhancement of activity were through diffusion, the increased inert solute concentration would cause the same effect.
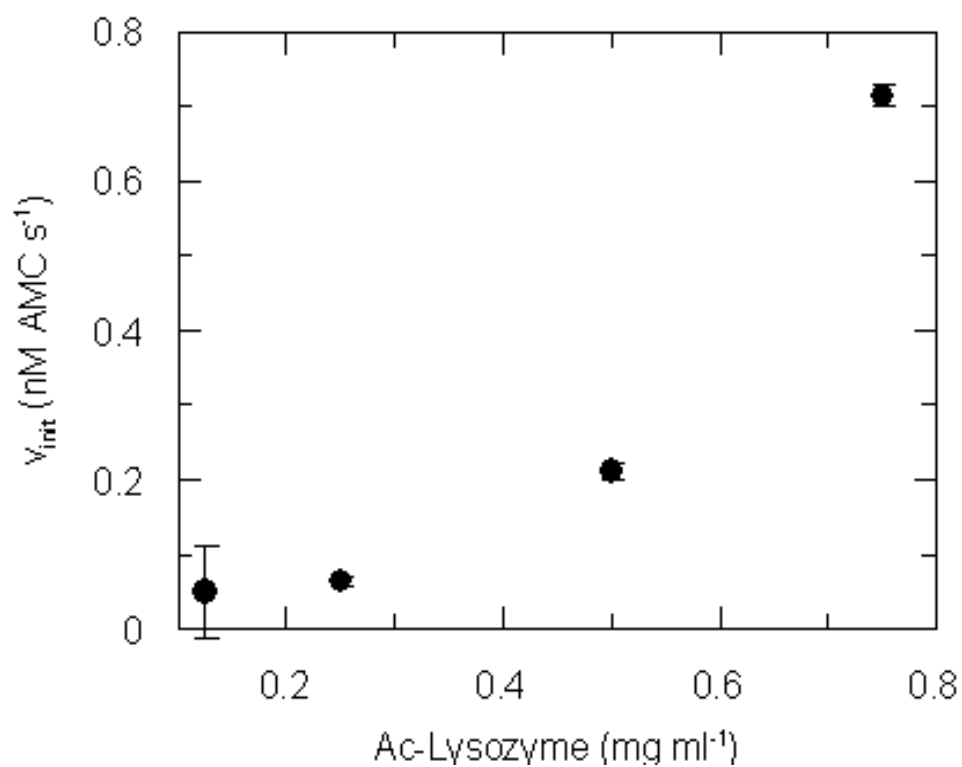
Figure 5.5: Effect of Acetylated Lysozyme on Peptide Hydrolysis
The addition of acetylated lysozyme to the reaction mixture between the substrate peptide Suc-LLVY-AMC and purified recombinant proteasome causes a marked increase in the pre-steady-state hydrolysis rate of the substrate peptide. Over the concentration range tested here an approximately 20-fold effect was observed on the rate of AMC production.
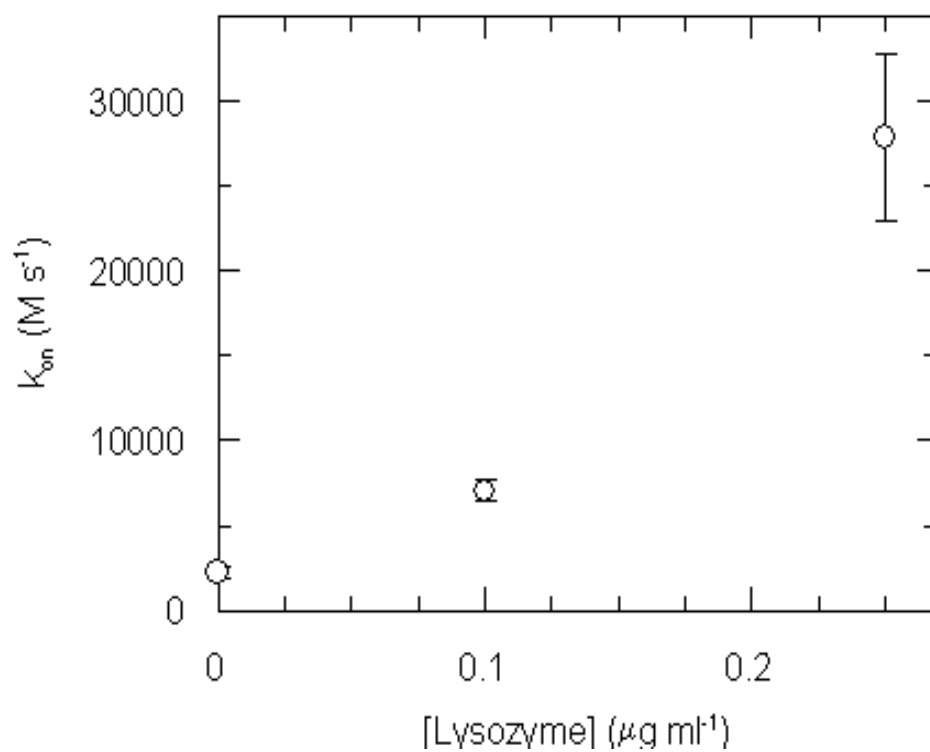
Figure 5.6: Effect of Lysozyme on k_{on}

To test what role added intact purified lysozyme was having on peptidase activity (see text), the inhibitor binding rate constant k_{on} was measured in the presence of increasing amounts of lysozyme. The increase in this parameter mirrors the increase in activity seen against the substrate Suc-LLVY-AMC when lysozyme is added to the reaction mixture (data not shown).

To test the effect of solutes on substrate diffusion, various molecules covering a large range of sizes, from under 100 Da to over 8000 Da, were chosen for use. There were expected to be chemically inert with respect to the chemistry performed by the enzyme. These solutes were mixed with the enzyme-substrate reaction and the resulting activity monitored. As shown in Figure 5.7, there was an increase in the activity due to the presence of PEG molecules in the reaction between substrate and enzyme. The increase in the rate of hydrolysis of the peptide Suc-LLVY-AMC increases for other PEG molecules in this concentration range, including PEG-5000, PEG-2000 and PEG-1450 (data not shown). This observation was further investigated using the approach outlined in Chapter 2, using the kinetics of enzyme inactivation by the small peptide inhibitor, Z-LLLal, to monitor active site reactivity. The findings of these experiments revealed that this effect was on the breakdown of the **HA** state, observed in the value of the rate constant k_{off} (Figure 5.8). Furthermore, if the role of these added solutes was to alter the diffusion coefficients of the reactants, then the effect would be more general, and be observed for molecules such as sucrose and PVP-10, which also affect solvent viscosity. However, as shown in Table 5.1, the small inert solute sucrose has no effect on the activity of the enzyme against the substrate peptide.
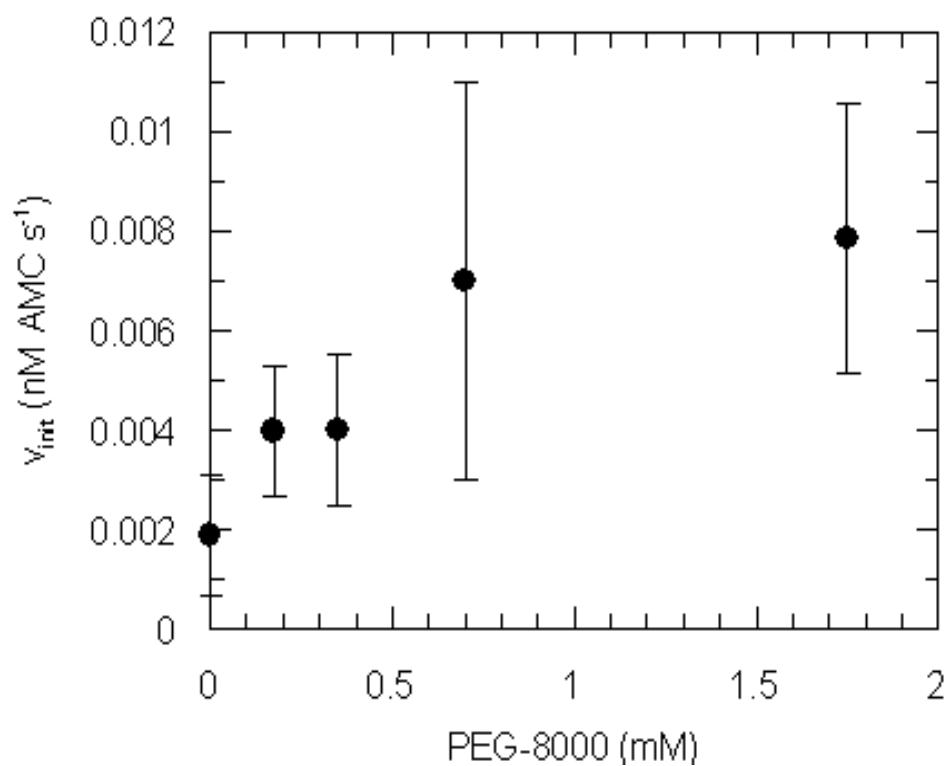
Figure 5.7: Effect of Added PEG Molecules on Peptide Hydrolysis Activity
The effect of added PEG-8000 on the hydrolysis of the peptide Suc-LLVY-AMC was monitored as a function of PEG concentration. The increase in the initial activity mirrors the increases seen for other PEG molecules, such as PEG-5000, PEG-2000 and PEG-1450.
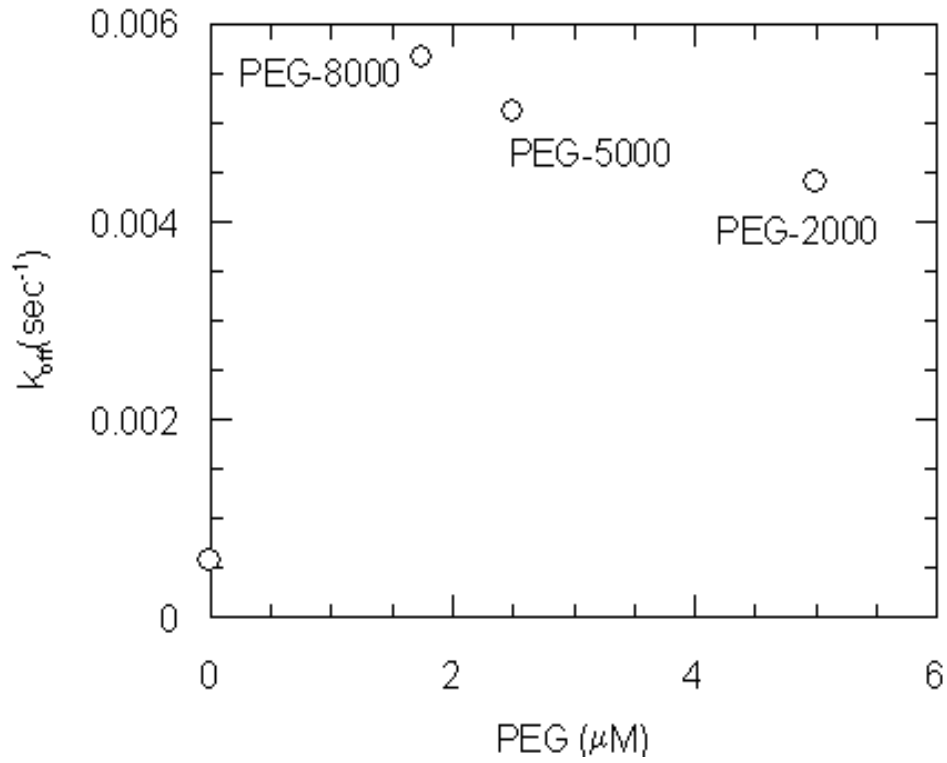
Figure 5.8: Effect of PEG Molecules on k_{off}

To test the general nature of the effect of the chemical potential, and hence the diffusion constant (see text) on substrate hydrolysis, the inhibition constant, k_{off}, was measured in the presence of various concentrations of PEG molecules of various lengths. The rate enhancements seen in Figure 5.7 comes from the same effect as does SDS, namely the increased rate of the regeneration of free enzyme.

% Sucrose (wt vol^{-1})	Rate of Free AMC Production (mV s^{-1})	
	Pre Steady State	Steady State
0	3.74 ± 0.22	3.49 ± 0.16
2	3.77 ± 0.10	3.36 ± 0.01
10	3.63 ± 0.30	3.26 ± 0.30
15	3.60 ± 0.05	3.26 ± 0.15
25	3.36 ± 0.43	3.16 ± 0.26
40	2.87 ± 0.52	2.90 ± 0.15

Table 5.1: Effect of Sucrose on Proteasome Activity

To test the effect of a small solute on proteasome activity, sucrose was added in increasing amounts to the proteasome-substrate reaction mixture and the resulting activity recorded. Sucrose is not expected to react with the proteasome active site or with the enzyme structure in an appreciable way. Despite a slight decrease in activity across this range of sucrose concentrations, activity remains nearly constant as the viscosity of the solution increases due to the increasing sucrose concentration. This is in marked contrast to the larger effects of macromolecules, such as PEG, on the viscosity of the solution, suggesting a different source of the effect (see text).

5.4.6 Magnesium Interactions and Effects

As shown in Figure 2.17, added magnesium activates the peptide hydrolysis by the enzyme in a hyperbolic fashion. This suggests a specific interaction between the enzyme and the metal ion. Comparison of the crystal structure of the 20S proteasome from *T. acidophilum* (Lowe et al., 1995) and the structure from yeast (Groll et al., 1997) reveals a possible magnesium binding site. In the yeast structure, several magnesium ions are visible, which are not visible in the archaebacterial structure at its lower resolution (3.4 Å vs 2.7 Å). In each case, however, magnesium ions were part of the crystallization conditions (Lowe et al., 1995; Groll et al., 1997). Several residues are involved in binding magnesium ions in the yeast structure, which lie between subunits of the enzyme (Groll et al., 1997). These residues are also present, in similar positions, in the *T. acidophilum* structure, which is expected given the high sequence homology shown in Figure 1.5. The structural similarity between the two types of subunits, α and β, between the two sources of proteasome particles also suggests a high degree of sequence similarity. These magnesium ions are shown in Figure 5.9 in their placement in the yeast 20S proteasome structure.
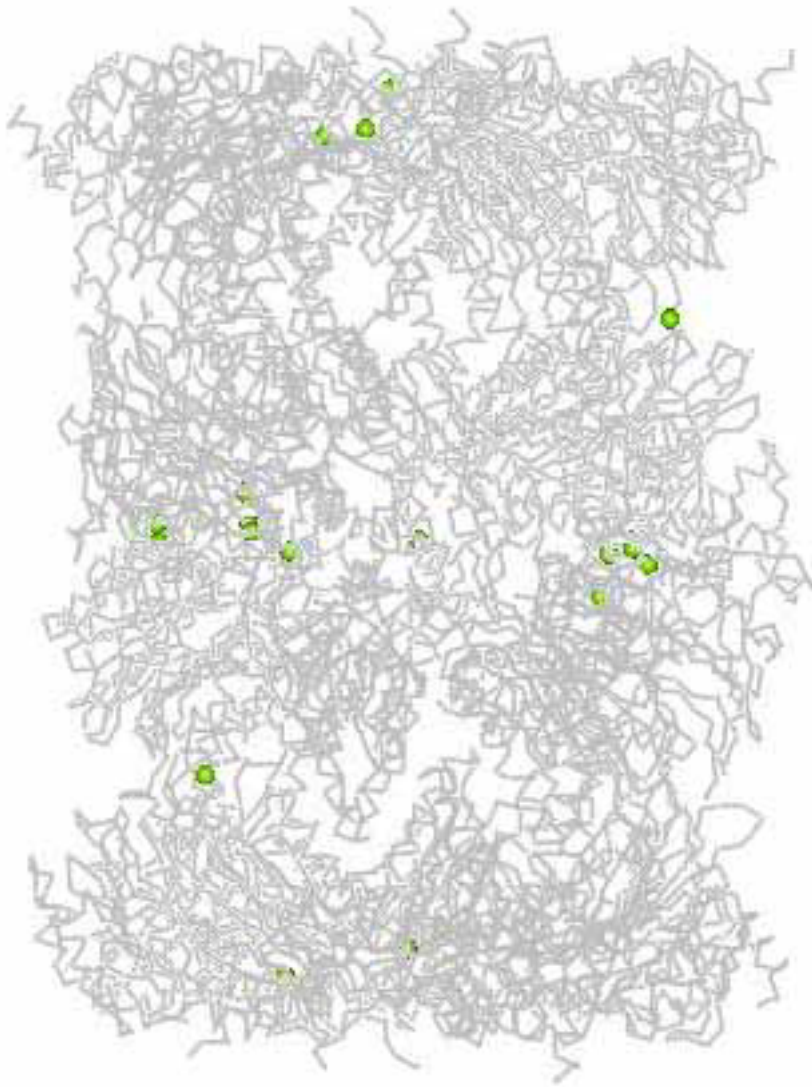
Figure 5.9: Magnesium Ions in Yeast 20S Proteasome Structure

The structure file for the yeast 20S proteasome core particle (Groll et al., 1997), PDB accession code 1RYP, was analyzed to view the included magnesium ions in the structure. The protein backbone is shown in light grey while the magnesium ions are shown as green spheres. They are mainly centered between the various β-subunits although some are located between various α-subunits. The visualization was done using Weblab Viewer.

5.4.7   Lack of Urea Activation

As shown by Akopian *et al.* (Akopian et al., 1997) the denaturant guanidine hydrochloride was shown to be capable of enhancing the peptidase activity of the 20S proteasome core particle, while the denaturant urea cannot. These two compounds are commonly substituted for one another when denaturing proteins, having nearly identical effects.

However, the failure of urea to cause even an observable enhancement of activity against the peptide substrate Suc-LLVY-AMC suggests that it is not merely the effect of guanidine hydrochloride as a denaturant that is causing the observed activation. If this were true, we would expect to see a similar activation profile with increasing urea concentrations. As shown in Figure 5.10, this is not the case. These results for urea and guanidinium closely resemble those from Akopian *et al.* (Akopian et al., 1997).

To isolate the chemical effects of the denaturants from the ionic strength effects, these experiments were repeated with urea by supplementing an equimolar amount of sodium chloride and the activity against the substrate Suc-LLVY-AMC was measured. As shown in Figure 5.10, the activity profile of urea-sodium chloride mimics that of urea, not of guanidine hydrochloride.
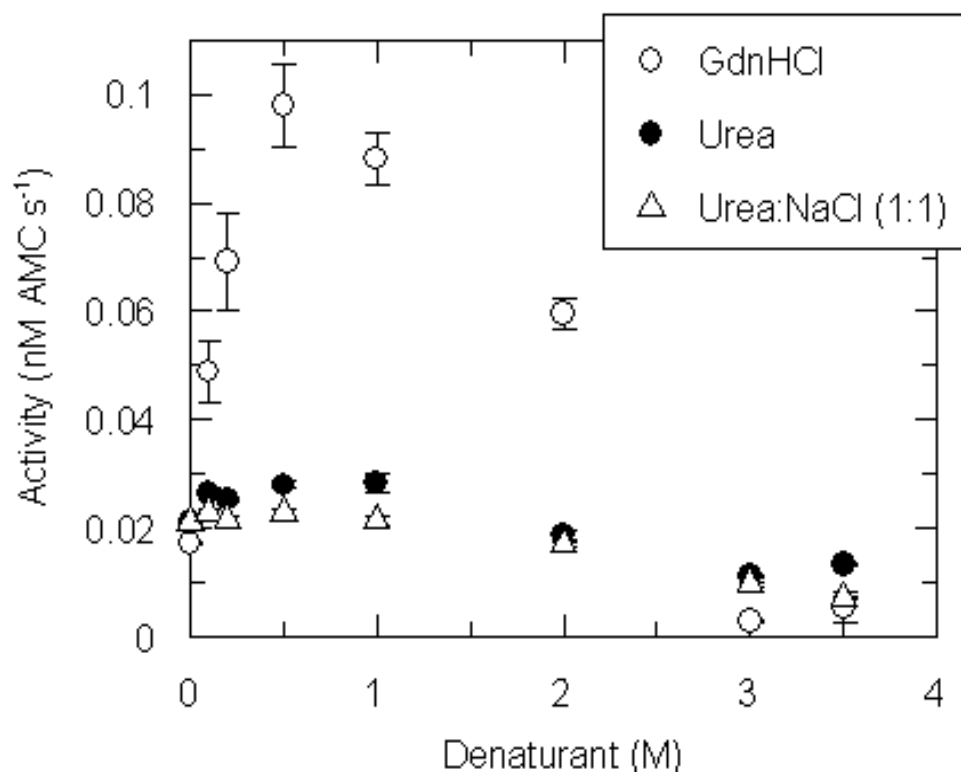
Figure 5.10: Effect of Denaturants and Salt on Activity

To differentiate between chemical effects specific to either urea or guanidine and the effect of the increase in ionic strength as guanidine hydrochloride is added, urea was supplemented with NaCl in equimolar amounts and the activity was measured using the substrate Suc-LLVY-AMC. Clearly observable are the overlapping curves for both urea and urea with NaCl, indicating the observed activation of the enzyme by guanidine hydrochloride is not due to the ionic strength.

To test additional chemical properties of guanidine hydrochloride, the derivative molecules *N, N*-dimethyl-guanidine hydrochloride and 1,1,3,3-tetramethyl-guanidine hydrochloride were added to the reaction of the substrate Suc-LLVY-AMC and purified proteasome. These molecules were chosen to block the hydrogen bond donors at the end of the molecule and to interfere selectively with the bridging capacity of the molecule. While there was modest activation in the presence of the *N, N*-dimethyl-guanidinium hydrochloride, the data with 1,1,3,3-tetramethyl-guanidine hydrochloride was inconclusive, since total inactivation of the enzyme at 50 mM after an initial increase in activity at 25 mM was observed.

5.5 Discussion

The above experiments provide some evidence that there exist various forms of cooperativity within the 20S proteasome from *T. acidophilum.* However, it is unclear as to what is the nature of this cooperativity, either positive or negative.

The quaternary structure of the 20S proteasome core particle makes cooperativity both possible and likely. Each subunit is in direct contact with several of its neighbors, both within the same ring of protein and in the adjacent rings. This high degree of contact would facilitate the propagation of conformational changes from one subunit to another. Furthermore, the tightly packed nature of the subunits within the core particle would almost ensure that even modest

conformational changes within a subunit would affect the neighboring subunit.

5.5.1   Negative Cooperativity

The most striking and convincing evidence for cooperativity is from the saturation data with the substrate peptide Suc-LLVY-AMC, as shown in Figure 5.1. After a rapid initial increase in the rate of free AMC production, which reaches a plateau value at about 40 μM, a decrease in the rate of substrate hydrolysis occurs and a final activity is reached. Several other substrates were reacted with the proteasome in order to test the generalizability of this phenomenon, but they each failed to react significantly.

This substrate activity profile for Suc-LLVY-AMC is similar to the one published by Stein *et al.* (Stein et al., 1996) for the eukaryotic 20S proteasome. This could be due to an artifact with this substrate and the methods of quantification, however. If there is a non-linear response of fluorescence and AMC production, this could account for the observed decrease in the rate of AMC production at higher substrate concentrations. Alternatively, if the substrate were quenching or scattering the fluorescence of the product, this would also account for the observed decrease in activity.

Other groups have found evidence that the proteasome undergoes some changes to decelerate its activity in the presence of large substrates (Dolenc et al., 1998). This reduced catalytic activity could be due to the large size of the substrate or consequences of this. These effects include slow rates of

diffusion or physical blockage of substrate entry to the active site or blocked product release.

5.5.2 Positive Cooperativity

Various treatments seem to promote positive cooperativity in the 20S proteasome. Under certain conditions, subsaturating concentrations of the peptide aldehyde inhibitor Z-LLLal lead to an increase in peptidase activity against the substrate Suc-LLVY (Figure 5.3). This effect can be due to the increase in the number of active sites available within the proteasome or an increased activity at each active site. As shown in Figure 5.2, at least 12 and possibly 14 active sites are available in solution. If the increased activity were coming as a result of an increased number of available active sites, the maximal increase in activity would be 1/7th the initial activity. However, as shown in Figure 5.3 this is clearly not the case, since the observed increase is greater than 1/7th the initial activity. Hence, the most likely explanation is an increased reactivity of the active sites and not more active sites being available for reactions with substrate or inhibitor.

Other groups have investigated the eukaryotic proteasome with various substrates and found evidence for positive cooperativity (Arribas et al., 1990; Djaballah et al., 1992). Certain substrates, but not all, show a sigmoidal pattern for activity when substrate is added (Djaballah et al., 1992). This is a distinctive pattern for positive cooperativity with substrate (Cornish-Bowden,

1995). No discernible trend as to the nature of the substrates, based on their amino acid composition nor their substituent, has been reported.

5.5.3 Effect of Diffusion

One possible means by which the enzyme could increase its activity in the presence of an increased amount of substrate is through effects on diffusion. Substrates enter the active site chamber of the proteasome only by diffusion, unaided by the enzyme. Some activators affect the chemistry of the hydrolysis of the substrates, as shown for magnesium ions, SDS, and buffer ions (Chapters 2 and 3). Increases in the rate at which substrate accesses the active site can also increase the rate of the reaction between the enzyme and substrate. It was suggested that SDS increased this reaction rate by widening the pore of the α- subunits, allowing an increased rate of substrate entry (Baumeister et al., 1998). As was shown in Chapter 2, this is not the case, but this is still a sound principle for increasing the rate of the proteasome's reaction with peptide substrates.

Diffusion is related to several factors, including temperature, solute mobility, the friction between the solute and solvent, and the viscosity of the medium (Katchalsky and Curran, 1946). The Planck-Einstein equation relates the diffusion constant, D, to the gas constant, R, the temperature, T, and the solute mobility, represented by ω_s:

$$D = RT\omega_s \tag{5.1}$$

The solute mobility, ω_s, is inversely proportional to the frictional coefficient of the solute, f_s:

$$\omega_s = \frac{1}{f_s} \tag{5.2}$$

Furthermore, the Stokes equation is used to relate this frictional coefficient, f_s, to the particle's radius, a, and the solvent viscosity, η:

$$f = 6\pi a \eta \tag{5.3}$$

These equations can be combined to give an expanded form of the Stokes-Einstein relationship:

$$D = \frac{kT}{6\pi a \eta} \tag{5.4}$$

Armed with these relationships, the effects of various additivies to the enzyme-substrate reaction mixture can be assayed. These simple relationships assume ideal behavior such as non-ionic species and non-interacting solutes. In the absence of more complete data about enzyme and substrate interactions, these are the only models that can be analyzed.

An interesting observation can be made when the data for the solutes PEG and PVP-10 are analyzed in terms of Equation 5.4. The radius of the substrate solute, a, remains constant in the experiments as does the temperature, T. However, the viscosity of the solution, η, *increases*, which should have the effect of *lowering* the diffusion constant D. If the reaction rates between the substrate and the enzyme are directly related to the diffusion constant D, the activity of the enzyme should decrease. Instead, an *increase* in the activity of

the enzyme against substrate is observed, attributable to a decreased solute frictional coefficient, f_s, an increased solute mobility, ω_s. One conclusion is that there is facilitation of the diffusion of substrate into the active site chamber by the added solutes PEG, PVP-10, and even lysozyme. An interaction between the solutes and the substrate would account for this. In effect, the macromolecule (e.g. PEG, PVP-10) would carry the substrate peptide, Suc-LLVY-AMC, into the active site chamber. This seems unlikely, though, given the bulk which would be added to the substrate with the added solutes.

One additional explanation is through the import of the added macromolecule solute into the active site chamber, to decrease the available space for the substrate peptide to reside. Large macromolecule substrates are threaded through the pore into the active site just as protein substrates would be. However, because they do not react with the enzyme's threonine nucleophile, they simply take up space inside the active site chamber. This reduces the available space for the substrate to reside in solution, increasing the encounter probability between the active site nucleophile and the substrate peptide. However, this is inconsistent with the observed effects in Figure 5.8, where the longer PEG molecule, PEG-8000, causes a larger effect on k_{off} than the smallest tested PEG molecule, PEG-2000. This is consistent with the lack of a similar effect when sucrose is added to increase the viscosity, η, affecting the diffusion constant, D. Sucrose is too small to have a noticeable effect on the available volume of the active site chamber of the 20S proteasome.

174

However, this second hypothesis fails to explain why lysozyme can cause such an effect while other proteins tested, such as ovalbumin and casein do not. Presumably, either these proteins are not able to enter the active site chamber or intact lysozyme is unable to react with the active site nucleophile. As such, this hypothesis is more tenuous than the proposed effects on the diffusion constant, that was described above.

5.5.4 Bridging Between Subunits

One central idea in this model of cooperativity, the modulation of the activity of the active sites by their neighboring subunits, is the propagation of conformational changes between subunits through their contact (Yu and Koshland, 2001). This contact may be facilitated by exogenous, multivalent bridges between the subunits. These bridges could be formed by multivalent metal ions such as Mg^{2+} or Ca^{2+} or small organic molecules such as guanidinium. This bridging and increased subunit contact could then amplify the conformational changes and any rate effects.

In the yeast 20S proteasome structure, several magnesium ions are bound between the subunits. This coordination comes from several negatively charged residues which are in homologous positions in the *T. acidophilum* 20S structure. However, in the simpler structure no metal ions are visible in the coordinates.

As shown in Figure 5.10, there is a marked difference between the effects

of urea, even with added NaCl, and guanidinium hydrochloride. One possible explanation for this difference is the increased ionic strength due to the salt guanidinium hydrochloride, while urea is a neutral molecule. As reported by Smith and Sholtz (Smith and Scholtz, 1996), when the ionic strength of urea denaturation is increased using sodium chloride, similar denaturant effects for both molecules appear and any differences minimized. However, the data in Figure 5.10 indicate that this is clearly not the source of this difference.

One possible explanation which would be consistent with this above evidence is a conformation change upon formation of the enzyme-inhibitor adduct. Upon formation of the anionic hemiacetal, the enzyme changes conformation slightly to stabilize this structure. This conformational change is enough to alter the conformation of an adjacent subunit, leading to an increased reactivity. Proteins are known to undergo structural and energetic changes upon ligand binding events (Miller et al., 1997). When magnesium ions are present, they are able to bind in the intersubunit space to increase the contacts between the two subunits. This increased contact area increases the magnitude of the propagation between subunits.

An additional, though less likely, explanation is that the effects are through chemical effects between the subunits. As active sites accumulate intermediates, the charge density within the active site chamber increases. Additional active sites generating charged intermediates becomes increasingly unfavored,

leading to a negative feedback cycle. This would be manifested overall as negative cooperativity. However, this seems quite unlikely as the distance between active sites is approximately 28Å. In this instance, screening of the charges by the bulk solvent will prevent this from becoming an appreciable effect.

The main advantage of this type of activation is that the enzyme becomes more active, the more substrate it has to process. When one subunit becomes acylated, as it would be during a transition state of the proteolytic mechanism, other subunits become more reactive. This would lead to increased activity as the enzyme processes protein substrates, leading to more efficient processing. Larger substrates, such as proteins, could easily span adjacent subunits and would therefore be affected by this type of activation. Smaller substrates would not see this activation, since they would be free to react with non-neighboring active sites.

While the above describes the use of conformational changes as a mechanism for activation of the enzyme, the same mechanism could lead to a depression of enzyme activity. If the conformational shifts induced by one subunit in another lead to a lowering of activity, then this negative effect would be propagated along the subunits.

5.5.5   Data from Other Groups

Several other investigations into the nature and type of cooperativity in the 20S proteasome have yielded a similarly inconclusive set of findings. Subsaturating amounts of the inhibitors lactacystin and epoxomicin have been found to display positive and negative cooperativity (Schwarz et al., 2000). Divalent metal ions have also been shown to affect the cooperative nature of the kinetics of the 20S proteasome (Djaballah et al., 1992). Others have found negative cooperativity in the presence of increased substrate concentrations (Dolenc et al., 1998). Some reports show a mixture of effects on various kinetic facets due to activator binding (Arribas et al., 1990).

Other groups have been unable to find any evidence for either positive or negative cooperativity (Myung et al., 2001b). Yet another group has detected changes in the structure of the enyme in the proteolytic cycle, suggesting some conformational shifts between active forms of the enzyme (Djaballah et al., 1993). In light of this conflict in the literature as to the cooperativity of the proteasome, these findings are not surprising and reveal that the proteasome is a significantly more complex enzyme than it may at first appear.

5.5.6   Conclusions

The above data, unfortunately, do not support any conclusions as to the nature or magnitude of cooperativity in the proteasome. We have found evidence for both positive and negative cooperativity and been able to support both

types through conformational changes. The conformational changes rely on the extensive surface contact between the subunits. However, the reproducibility of these observations, coupled to the multimeric nature of the proteasome structure, would seem to indicate that there are cooperativity effects present in the 20S proteasome.

Chapter 6

General Summary and Future Directions

6.1   General Discussion

In this thesis, several facets of the mechanism of proteolysis by the *Thermoplasma acidophilum* 20S proteasome have been examined. Through examinations of the mechanism of activation by metal ions, detergents, and buffer ions, as well as examinations of the cooperativity of the enzyme, several details of the proteasome mechanism have emerged. Several groups have demonstrated the effects of various activators on the proteasome although the mechanisms have remained unresolved. In the preceding chapters, the mechanisms of activation by metal ions and SDS have been provided, the activation by buffer ions presented, and the effects of these activators on protein hydrolysis described as well.

The proteasome, one of the defining members of a class of enzymes known as the *N*-terminal nucleophiles (Brannigan et al., 1995), utilizes a novel nucleophilic residue, a threonine (Seemuller et al., 1995b), to hydrolyze the substrate peptide. Other participating functional groups are glutamate 17, lysine 33 and the alpha amino terminus (Wlodawer, 1995). This work has strengthened the proposed mechanism (Figure 1.7), as well as illuminated various rate limiting steps present within it.

6.1.1 Analysis Using Inhibition Kinetics

This thesis has demonstrated the utility of following the kinetics of a slow binding inhibitor to monitor early stages of proteolysis (Morrison et al., 1988). The binding and release rate constants, together with inhibitor affinities, can be monitored in response to various factors (Williams et al., 1979) such as metal ions, temperature, and pH to infer the effects of these factors on the early events of substrate hydrolysis.

One of the underlying assumptions of the use of the peptide aldehyde inhibitor Z-LLLal is that the chemistry of inhibition closely mirrors the corresponding events within the proteolytic cycle. Numerous studies have shown that aldehyde inhibitors inactivate serine proteases through the formation of a hemiacetal on the nucleophilic side chain (Muszkat et al., 1983). This mimics the tetrahedral intermediate found in the proteolytic cycle (Lowe et al., 1995; Dufour et al., 1995).

The implicit assumptions in this are that the chemistry and physics lead-ing to this stage are the same, that the chemistry of the nucleophilic attack on the peptide and aldehyde carbonyls are the same, and consequently that activators or other inactivators will similarly affect both the mechanisms of peptide hydrolysis and of inactivation of the enzyme.

The physics and chemistry of entry of the substrate and inhibitor molecules to the proteolytic chamber should be similar. In both cases, each molecule is of approximately the same solubility and similar sizes. Neither molecule thus far has an identified carrier accessory protein or subdomain on the proteasome. As such, diffusion rate constants for each into the active site should be similar.

For both, the reactivity with the enzyme should be similar. In each case desolvation of the carbonyl and of the nucleophile prior to the attack must occur. Both carbonyls are presumably hydrogen bonded to the active site residues. Any effects on this step should be manifested for both reactants. The binding of either, the substrate peptide and the inhibitor molecule, are likely to be slightly different, depending on the steric conditions in the P1' position. The aldehyde inhibitor peptide has no P1' residue, while the substrate peptide has the large aromatic AMC structure in this position.

6.1.2 Using Peptide Hydrolysis as an Active Site Probe

As a complement to the use of the inhibitor Z-LLLal, using the substrate peptide Suc-LLVY-AMC as a probe of active site occupancy has demonstrated

additional facets of the proteasome mechanism. Using this approach, the rates of free AMC production can be monitored. The active site can be occupied by either a protein substrate or by an inhibitor molecule.

The specific interaction of the proteasome with protein substrates has been demonstrated using this approach. By reacting the 20S proteasome core particle with cytochrome c (as shown in Figure 4.1) or myoglobin (Figure 4.2) and the peptide Suc-LLVY-AMC, the decrease in the rate of AMC production can be attributed to the association of the proteasome with the protein substrate. This is clear evidence of the ability of the 20S proteasome core particle, which does not hydrolyze ATP or utilize any subunits to unfold the protein substrates, to begin to digest protein substrates. It has been argued that to achieve this association, a proteasome cap structure similar to the 19S of PA28 subunits in eukaryotes would be required (Benaroudj et al., 2000).

6.1.3 Cooperativity Effects

Several important features of the 20S proteasome's quaternary structure were analyzed in terms of how they affect any cooperativity effects within the mechanism. The enzyme's structure of 28 protein subunits is tightly arranged as a barrel structure, with each β-subunit having six direct neighbors and each α-subunit having four direct neighbors. This means that any structural changes

within any subunit could be propagated through contacts with adjacent subunits. Through this mechanism, positive or negative effects could be communicated through the enzyme.

At this time, the evidence for either the presence or nature of cooperativity within the 20S proteasome from *T. acidophilum* is inconclusive. Positive cooperativity can be observed under subsaturating conditions with the inactivator peptide Z-LLLal at slightly acidic pH values or increased magnesium concentrations. However, substrate inhibition is observed, presumably through some negative cooperativity effects. Lastly, no cooperativity is seen when a proteolytically generated set of peptides is added, only a modest decrease in activity due to the competition for active sites by the substrates, peptides and the detectable peptide Suc-LLVY-AMC.

As discussed in Chapter 5, facilitated diffusion into the active site chamber does not appear to play a major role in the proteolytic mechanism. While PEG molecules increase the enzyme's activity, the effect appears to be on the rate of the **HA** intermediate decomposition (Figure 5.8). Furthermore, this effect should have been general for both PEG and PVP-10, but clearly is not. This suggests that the effect is due to the chemistry of PEG, which is not shared by PVP-10.

6.1.4 Points of Activation

One of the biggest questions answered in this thesis is to the specific kinetic steps of the proposed mechanism in which the known activators cause an effect. Previously, it had been argued that both SDS and magnesium operate at the same point in the proteasome mechanism (Akopian et al., 1997), which would explain their interference with each other during activation. However, the data in this thesis have shown clearly this is not the case.

There is observed a lack of effect by SDS on the rate constant for association of the inhibitor or substrate (Figure 2.7). This indicates that SDS acts primarily on the release rate constants of the products of the reaction. This can be confirmed with the data in Figure 2.14, which clearly shows an increase in the rate constant of inhibitor release, corresponding to the release of the first product, the AMC portion of the peptide Suc-LLVY-AMC. In contrast, magnesium acts on both the rate constant of binding in the active site (Figure 2.18) and on the rate constant for release of product, although to a less significant degree (Figure 2.19). This effect is largely due to the ionic strength of the medium (compare Figure 2.18 and Figure 2.22), which increases dramatically with added magnesium.

The data presented in this thesis demonstrates that the activation of the 20S proteasome by SDS is similar to that seen by other research groups, namely an increase of proteolytic activity followed by a decrease of activity to below basal (0% SDS) levels. This activation also occurs through other detergents

such as Triton X-100 (Figure 2.13), but has not been observed for similar molecules such as fatty acids of various lengths (data not shown). These combined results clearly indicate that a more complex molecule than a long hydrocarbon chain and a negatively charged head group is needed for enzyme activation.

The most likely explanation for activation by SDS and similar molecules is a direct binding action. Shibatani *et al.* has shown a dose-dependent activation profile for the 20S proteasome in response to SDS, a response which mirrors the concentration of the enzyme in the reaction mixture (Shibatani et al., 1995). This binding, in turn, most likely alters the conformation of the 20S proteasome increasing the rate constant of release of the product and enhancing the activity of the enzyme overall. This is consistent with the findings of Stein *et al.*, who proposed an SDS induced conformational shift in the proteasome (Stein et al., 1996). This conclusion was based on activity profiles and a kinetic model which includes different forms of the enzyme. This would also provide an explanation for the inactivation of the enzyme at higher SDS concentrations.

Additionally, a novel activator for the catalytic mechanism has been identified and its step in the activation process isolated. Buffer ions assist in the proton transfer steps to the released product. This step is crucial to continuing the proteolytic cycle in a productive fashion. Although there are two proton transfer steps in the hydrolysis mechanism as shown in Figure 3.12, it

is the first step that is promoted by the presence of a buffer ion acting as a proton relay. If it were the second step, such as during the hydrolysis of the acyl-enzyme intermediate, a burst of AMC product formation would be seen at low buffer concentrations. This is clearly not the case when the data in Figures 3.1 and 3.2 are analyzed. The practical implication of this data is that the comparison of data between groups can be made more difficult if the assay conditions differ in the buffer composition or pH values.

In contrast, magnesium and other ionic salts act to provide thermodynamic stability to the transition state, facilitating both the forward (observed in the values of k_{on} for the inhibitor as well as increasing activity against the substrate Suc-LLVY-AMC) and the reverse reaction. This corresponds to the decomposition of the tetrahedral intermediate to yield the reactants (observed in the values of k_{off} for the inhibitor binding). As shown in Figure 2.23, this stabilization is several kJ mol^{-1}. While magnesium is likely to bind directly to the *T. acidophilum* 20S core particle as well (Figure 5.9), these binding sites appear to be distal from the active site and are not expected to directly lead to the observed activation of the enzyme through chemical participation.

The above activation mechanisms are centered on the chemical steps in the hydrolysis reaction. As shown in Chapter 4, these steps are not rate limiting for protein hydrolysis, and instead the entry of the substrate into the active site chamber becomes rate limiting.
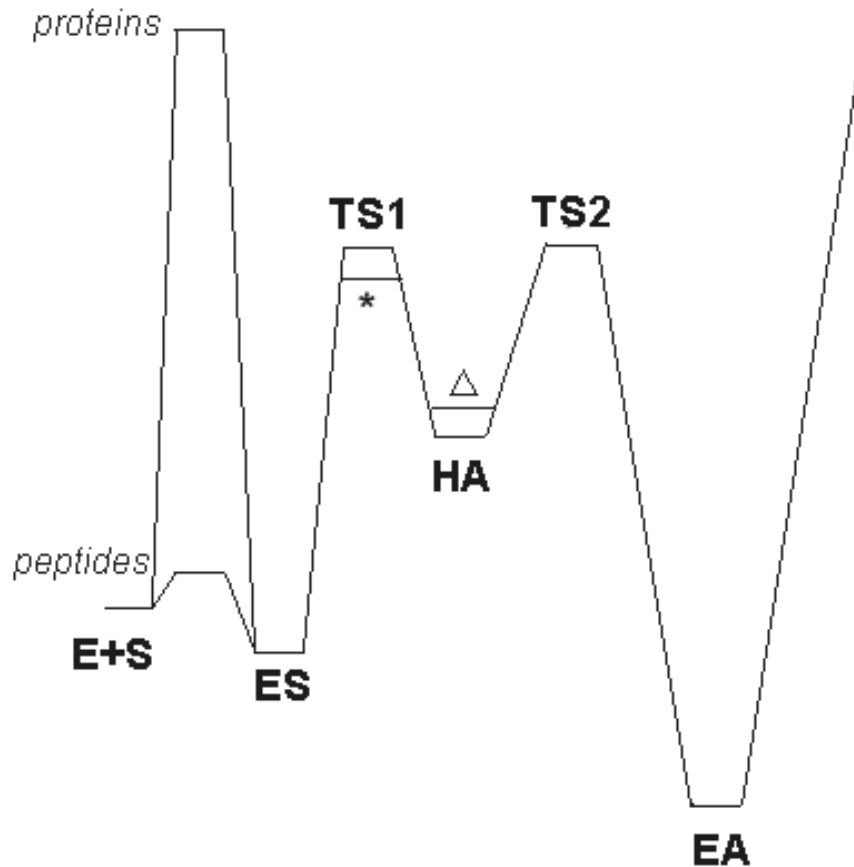
Figure 6.1: The Effect of Activators in the Energy Barrier Diagram

This Figure illustrates the effects of the activators on proteasome activity in terms of the relative energy barriers in the initial stages of the reaction. The initial entry from the E+S stage to the ES stage (with the entry of the substrate into the active site chamber) is a large, rate limiting barrier for proteins, but not so large for peptides. Upon formation of the ES complex, the first transition state TS1, which can be lowered by added magnesium or ionic strength (indicated by *), is crossed to yield the hemiacetal stage. The energy of this intermediate can be raised by the addition of SDS or buffer ions (indicated by Δ). After the second transition state TS2, the acyl enzyme (EA) forms. The relative energies for the later stages are unknown and not addressed by this thesis. While TS1 and TS2 appear to be independent but of similar height, they may be interconnected (see text).

When this information is assembled, an energy profile of the reaction can be created. While not entirely to scale, the relative heights and positions can be described. Furthermore, only the preliminary steps have been assayed by these methods. This is shown graphically in Figure 6.1.

There exists a significant energy barrier for proteins to enter the active site, leading to the **ES** complex. This barrier exceeds all others in the chemical steps of the proteolysis and is rate determining. Peptides, in contrast, have a small energy barrier reflective of their free diffusion into the active site chamber. Formation of the acyl-enzyme intermediate (**EA**) proceeds through a tetrahedral hemiacetal (**HA**) stage with two transitions states, **TS1** and **TS2**. Magnesium and other ions which affect the ionic strength of the medium can lower the energy barrier of the first transitions state to form the **HA** state from the **ES** complex. SDS and buffer ions act at the same stage, destabilizing the **HA** state, leading to increases in the rate of the formation of the **EA** species or, alternatively, increased rates of release of the substrate to return to the **ES** stage. The energy barriers **TS1** and **TS2** are of similar height, indicated by their paired rate limiting effects (both magnesium and SDS enhance activity). They are not entirely independent of one another, as suggested by Figure 6.1, however any strong relationships between the two is undefined by the data in this thesis.

6.1.5   Role of the Quaternary Structure

The data from the experiments conducted in this thesis research in conjunction with the data from other groups can be assembled to assess the role of structure in the function of the proteasome. The quaternary structure of the 20S proteasome may contribute to its function in a variety of ways. The structure of the proteasome affords it four advantages over a monomeric proteolytic enzyme. These are advantages similar to other multimeric, barrel shaped enzymes like GroEL and the Tricorn protease.

First, the quaternary structure of the proteasome allows for a functional mimicry of organelles (Baumeister et al., 1997; Baumeister and Lupas, 1997). In crowded cells, organelles provide a crucial factor: compartmentalization. Organelles such as the Golgi and the endosome perform special tasks on a limited substrate base. Access to these organelles is restricted by complex mechanisms to ensure that only the correct molecules become substrates. By being isolated from the rest of the cell, the enzymes that perform the specialized tasks are restricted from acting on the wrong substrates (Baumeister et al., 1998).

In lower life forms such as archaeons which lack discrete organelles, the potential exists for specialized enzymes to act on the wrong substrates. All cells, from prokaryotes to eukaryotes, need to perform protein turnover at all times, but the proteins that need to be degraded are a limited set of those within the cell. In such organisms, the shape of the proteasome keeps the

active sites away from the cytosol, where the general population of cellular proteins are found. Access to the proteasome active sites is guarded, so that only selected proteins become substrates (Groll et al., 2000). This is evidenced in the necessity of a protein to be destabilized by some means, such as chemical modification, for it to become a substrate. While no gating mechanisms, such as accessory proteins like PA28 or PA700, were used or have been found in the *T. acidophilum* genome, only proteins which can enter the active site chamber by threading through the α-subunit pore can become substrates. This action must occur in an ATP-independent process through actions by the 20S core particle and the protein substrate.

The interior of the chaperone GroEL allows it to unfold proteins by presenting a surface rich in hydrophobic residues (Chan et al., 1996). As shown in Figure 6.2, inspection of the 20S proteasome structure from *T. acidophilum* show no such extensive hydrophobic surface, negating the idea that this chamber is used to keep proteins unfolded as substrates. Instead, it appears that proteins have to unfold prior to entering this active site chamber, based on data from Chapter 4 along with previous work by Baumeister and colleagues (Wenzel and Baumeister, 1995). As such, the structure of the proteasome seems to enforce the requirement of accessibility to the backbone, through unfolding, on its substrate proteins.
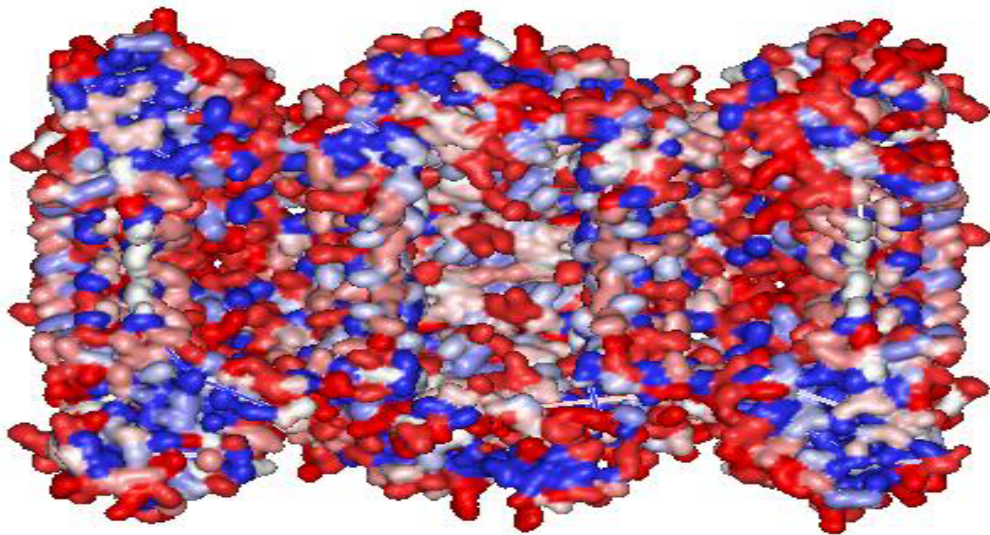
Figure 6.2: Characteristics of the Proteasome Interior

In this view (the proteasome cut at the barrel axis) the hydrophobicity of the proteasome interior is examined. Blue indicates a hydrophobic area, red indicates a hydrophilic area. No extensive patches of hydrophobic surface area exist which may be used to hold a protein unfolded as it is acted upon by the proteasome. The structure file 1PMA (Lowe et al., 1995) was used with the visualization tool WebLab Viewer (MSI Software).

Secondly, the structural arrangement of the proteasome allows for an optimized efficiency of protein digestion. Albery and Knowles (Albery and Knowles, 1976) described two strategies used by nature to improve enzyme catalysis, namely, the perfection of activity by a single enzyme or the association of multiple enzymes within a pathway. The advantage gained in the second strategy is that the diffusion of the product of one enzyme within a metabolic pathway to the next enzyme, where the metabolite now becomes a substrate, is diminished or can almost vanish. Considering that the degradation of proteins to polypeptides is a multiple protease pathway, the association of multiple proteases within the proteasome may increase the catalytic efficiency of the process (protein degradation). This facet of the proteasome structure was recently utilized to develop a high affinity inhibitor using a PEG spacer with aldehyde groups on both ends (Loidl et al., 1999).

The collective data from experimental evidence suggests that the proteolytic efficiency of the proteasome β-subunit is not as well developed as specialized proteases such as trypsin or chymotrypsin (Stein et al., 1996). This could be explained by its broad substrate preferences. Perhaps an evolutionary sacrifice accounts for its high substrate promiscuity but low catalytic efficiency. By including a large diffusion coefficient as the substrate protein moves from one protease to the next during its degradation, the proteasome is forming a spatial complex to diminish the loss of overall catalytic efficiency.

When the data from Chapter 4 are analyzed both in terms of the protea-some acting as a single catalytic site as well as a collection of catalytic sites, an improved understanding emerges. Since the small peptide Suc-LLVY-AMC is too small to interact with more than one active site at a time, it provides a measure of the catalytic efficiency of a single subunit. The data from Figures 2.17 and 2.10 suggest a "slow acting" proteasome when compared to reactions between the same substrate and chymotrypsin. However, as shown in Table 4.2, the 20S proteasome core particle is able to digest protein substrates with an activity comparable to these single active site proteases.

The most direct explanation is the enhancement of activity due to the presence of 14 active sites within the confines of the central catalytic cavity. The eukaryotic proteasome, such as that from yeast, is probably the best enzyme to demonstrate this principle as it contains a heterogeneous population of catalytic subunits (Groll et al., 1997), yielding a heterogeneous population of proteases (Orlowski, 1993), which is perhaps the best adaptation of this concept. In this manner, the active sites with differing specificities can cleave the diverse peptide bonds present in proteins more efficiently than a single type of protease.

Thirdly, the structure of the proteasome assures the completion of the protein digestion cycle. The pores at the entryways to the proteasome's interior, formed by the α-subunits between the cytosol and the antechamber and the antechambers and the catalytic chamber, are small. It has been shown that

only a single polypeptide chain can fit through this opening into the proteasome chamber (Wenzel and Baumeister, 1995). The cross sectional area to diffuse substrate into the proteasome catalytic chamber is small (Lowe et al., 1995; Groll et al., 1997). This barrier is overcome by helper complexes (such as PA28 in eukaryotes) which may help feed the protein substrates into the enzyme barrel. This provides specific recognition of substrates as well as facilitated diffusion into the proteasome interior.

Similar problems with respect to peptide length exist for products leaving the catalytic chamber. Because of its small cross sectional area, the diffusion of degraded polypeptides will be slow. Exit rate constants for products will therefore increase (assuming the absence of assistance) only if the polypeptides decrease in size. Thus, the shape of the proteasome, a barrel with small openings at either end, would seemingly promote proteolysis until the substrate protein is reduced to small polypeptides.

Lastly, the cytosolic location of the proteasome allows for a readiness of the products (peptides and amino acids) for the next step in the metabolic process of protein breakdown (Ruepp et al., 2000). In considering the first point above, it might appear wasteful not to use an existing mechanism for compartmentalization in eukaryotes for protein turnover, such as organelles like the endosomes. There is a significant advantage, however, for keeping such a mechanism in the cytosol. For example, polypeptides that are produced by the proteasome are immediately available for further degradation into single

amino acids by additional enzymes. These final products immediately enter a pool of amino acids within the cell to be broken down in metabolism or reused in the synthesis of new proteins (Ruepp et al., 2000). In doing this, the cell does not have to develop a means of exporting the different amino acids from the endosome back into the cytosol, a process that would require multiple proteins to ensure that only amino acids get exported to the cytosol from the endosome.

6.1.6   An Open Active Site

Inspection of the 20S proteasome crystal structure (Lowe et al., 1995) reveals an active site that is exposed to the bulk solution. This structural facet is shown in Figure 6.3, with the threonine nucleophile residue highlighted in red. This is in contrast to an enzyme such as chymotrypsin which has a buried active site, isolated from solvent (Freer et al., 1970). One possible explanation for this is to accommodate a variety of substrate proteins and their varied sizes. An active site specialized to act on one type of peptide bond would have a shape suited for a limited substrate base to optimize interactions. To work on many different types of substrates, the proteasome active site is as open as possible to accept many different types of peptides.
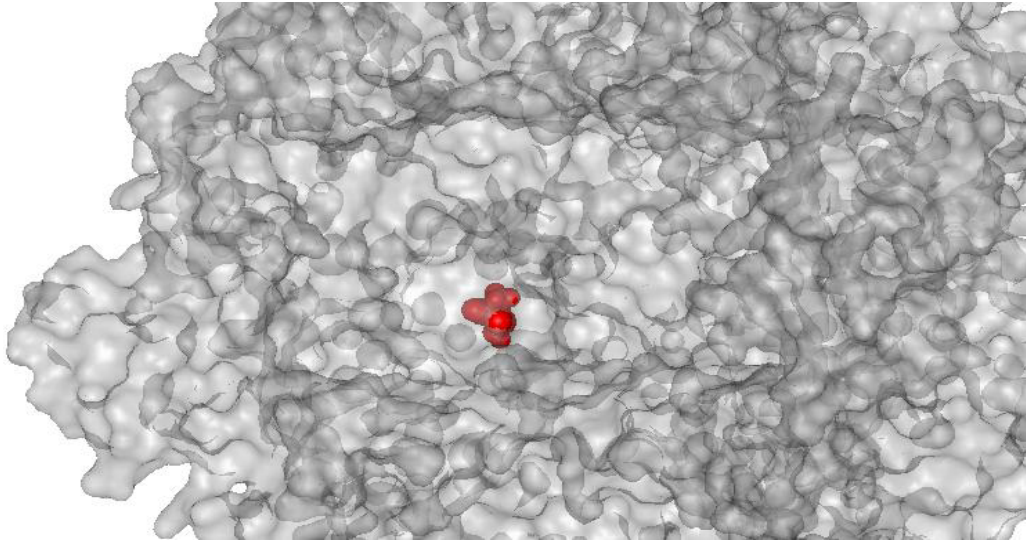
Figure 6.3: The Proteasome Active Site is Open to Solvent

In this illustration, the proteasome structure from *T. acidophilum* was analyzed to demonstrate the accessibility of the active site nucleophile to the bulk solvent. Using the PDB structure 1PMA (Lowe et al., 1995), a surface was generated with a probe radius of 1.5 Å, slightly larger than the size of a water molecule's probe radius, typically 1.4 Å, with the nucleophilic threonine residue shown in red. In this close up of the active site, part of the chamber is cut away, exposing the active site nucleophile.

The consequences of this are numerous and visible in the experiments in this thesis. Most strikingly, the proteasome is activated by buffer ions (Chapter 3), which are able to interact with the active site chemistry and shuttle protons between the enzyme and products as shown in Figure 3.12. They are able to interact with the reactants because the active site is accessible to solvent ions.

One consequence of this is a reduced catalytic efficiency, as the proteasome is unable to optimize interactions with one type of substrate. Optimization would entail a high number of specific tight interactions between the enzyme and the substrate to position it for rapid catalytic action. This is often manifested as a low K_m value and a high k_{cat}/K_m. The lack of such optimized interactions is evidenced by the multiple types of activators of the proteasome, such as ionic strength, denaturants like guanidine hydrochloride, and SDS treatment. This is further evidenced by the thermodynamic stabilization of the transition state by magnesium ions as discussed in Figure 2.23. All of these observations point towards mechanisms which can improve the efficiency of the active site, sometimes through direct action, adding functionality missing due to the openness of the active site. This includes improving the binding of the substrate to the enzyme, such as by lowering the value of K_m by increasing the binding rate k_{on} or lowering the dissociation rate k_{off}. Alternatively, by improving the rate constant for bond hydrolysis, k_{cat}, improved enzymatic efficiency can also be achieved. This can result in transition state stabilization as is proposed for the activation by magnesium (Chapter 2).

The activation of the enzyme's catalysis by buffer ions as we have proposed in Figure 3.12 is consistent with the involvement of the amino terminus. At the pH values of the experiments, the amino terminus of a protein can act as a general acid-base catalyst. The pH profile of inactivation shown in Figure 3.5 suggests at least two groups with an average pK_a of 8.5, which could reflect the amino terminus (pK_a of about 8.0 in solution) and lysine 33 (pK_a of about 10.5), which could be modulated in the folded protein. These assignments are consistent with the data of activity vs pH shown in Figure 3.4 with at least two groups with pK_a values of greater than 10 and approximately 7. Together, all of this is consistent with the proposed proteasome mechanism (Wlodawer, 1995) involving the amino terminus and lysine 33 as active site residues with the threonine nucleophile.

6.2   Remaining Questions

While the above data have provided some illumination of the chemical mechanism of the proteasome, there remain some unanswered facets. The major unanswered question is the presence and nature of any cooperativity within the 20S proteasome core particle. The quaternary structure lends itself to communication between the subunits, due to the tightly packed nature of the core particle. However, as discussed above, the data here are unable to interpret without ambiguity what deviations from normal enzyme kinetics are present.

Understanding this cooperativity would be vital to understanding the response of the proteasome to events which yield significant amounts of substrate proteins. These include cellular stress, cell cycle events, and problems in the protein synthesis mechanism. Such data would help illuminate the effectiveness of the proteasome as a response enzyme.

Secondly, while the data presented in this thesis have helped to strengthen the proposed chemical mechanism of substrate hydrolysis, the kinetic mechanism remains vague. The effects of metal ions and ionic strength needs more rigorous data for analysis such as polyelectrolyte theory. This will be required to more accurately describe the effects of activators within the proteasome mechanism. Additionally, this information could be vital to developing inhibitors to work selectively at particular mechanistic or kinetic points, trapping the enzyme in an inactive state or providing an increase in activity.

6.3 Future Directions

Three great questions remain for the proteasome structure in general, for both the eukaryotic and the archaebacterial form, which can be addressed using the *T. acidophilum* proteasome. Each of these would be useful in determining the contribution of the quaternary structure and the diversity of active sites to the overall function of the enzyme.

6.3.1　The Structure of the Bound Peptide

The structure of the bound peptide would be a useful question to answer. The structure of the 20S proteasome is unique for a protease, and raises some intriguing questions about this structure for the activity of the enzyme.

To test this, NMR experiments would be the preferred method, since this technique is able to reveal detailed structural information about select positions. A large peptide with a C-terminal aldehyde group can be anchored at the active site. Using ^{15}N labeled residues, one per peptide and in various positions, the position dependent flexibility of the bound peptide can be assessed. By using the T2 relaxation time as a function of position, the flexibility of the peptide could be measured.

This question is important because it can help determine several facets of proteasome efficiency. If proteins are interacting with the chamber walls and stretched between neighboring active sites, that would suggest a molecular basis for the "molecular ruler" hypothesis (Kisselev et al., 1998a; Wenzel et al., 1994) where product peptides have a size distribution that is centered around 8-10 amino acids, the distance between neighboring active sites. Secondly, it would suggest a possible mechanism by which the proteasome can keep proteins accessible to the active sites and available for digestion.

6.3.2 The Role of Dual Pores

The contribution of *two* pores to the enzyme's function, with one on either end, remains an interesting question. While at first it may appear that one could have simultaneous substrate entry and product release through these two pores, the fact is that there is nothing that prevents the simultaneous entry of substrates on both ends at once.

One set of experiments to test this would be to affix the proteasome particle to a solid surface as a support. This would effectively block the use of one end of the proteasome for passage of substrate or product. This could be accomplished by attaching cysteine residues to a gold plated surface. The single cysteine residue per α-subunit may have to be moved, via mutagenesis, to a more surface accessible location to accomplish this design.

What is anticipated is a general slowdown of the proteasome activity as there is introduced an asymmetry to substrate entry and exit. With two pores, the exit of products through one pore does not block entry of substrate into another pore. With one pore, as substrate enters, product is unable to leave through the blocked pore. At an extreme, the proteasome could eventually "fill up" with product and become clogged, at which point it ceases to operate on new substrate. Eventually these peptides, internalized to the active site chamber, are further broken down and can exit through diffusion.

6.3.3 The Contribution of Varied Active Sites

The reason the archaebacterial source of the enzyme was chosen for the studies in this thesis was for its homogeneous composition of active sites. The eukaryotic enzyme has diverse β-subunits, which would have made the kinetic interpretation of the data significantly more difficult.

However, it would be useful to build 20S core particle complexes using a single type of α- and β-subunits from the eukaryotic sources. This could be accomplished using a similar recombinant expression system to that of the *T. acidophilum* system used in these studies. In this manner, the kinetics and activities of any one type of eukaryotic 20S proteasome subunit could be assayed. Furthermore, using inactive β-subunits, any activities specific to the α-subunits could be directly measured. This would reveal otherwise hidden activities.

Combinations of the active sites, then, could be tested using this method. One difficulty is arriving at a homogenous population of combinations, including the arrangement of the subunit types within each particle. Within any population of enzyme particles there will be a heterogenous distribution of arrangements, possibly leading to a low resolution of results. This could be achieved using selective expression in *E. coli* systems, analogous to that used to express the recombinant *T. acidophilum* proteasome, or by selective affinity tagging of the eukaryotic proteasome subunits and then selective purification using affinity reagents and columns. Data obtained using this approach would

be patterns of protein cleavage (different subunits cleave preferentially after different substrate residues), kinetic rates, and the average length of products. This would help illuminate the effects of the subunit changes in response to various immune system signals which have been shown to occur.

Bibliography

Adams, J., Palombella, J., V., Elliott, and J., P. (2000). Proteasome inhibition: a new strategy in cancer treatment. *Invest New Drugs*, 18(2):109–21.

Akiyama, K., Kagawa, S., Tamura, T., Shimbara, N., Takashina, M., Kristensen, P., Hendil, B., K., Tanaka, K., and Ichihara, A. (1994). Replacement of proteasome subunits X and Y by LMP7 and LMP2 induced by interferon-gamma for acquirement of the functional diversity responsible for antigen processing. *FEBS Lett*, 343(1):85–8.

Akopian, N., T., Kisselev, F., A., Goldberg, and L., A. (1997). Processive degradation of proteins and other catalytic properties of the proteasome from *Thermoplasma acidophilum*. *J Biol Chem*, 272(3):1791–8.

Albery, W. J. and Knowles, J. R. (1976). Evolution of enzyme function and the development of catalytic efficiency. *Biochemistry*, 15(25):5631–40.

Altschul, S. F., Madden, T. L., Schaffer, A. A., Zhang, J., Zhang, Z., Miller, W., and J., D. (1997). Gapped BLAST and PSI-BLAST: a new generation of protein database search programs. *Nucleic Acids Research*, 25:3389–402.

Andreatta, C., Nahreini, P., Hovland, R., A., Kumar, B., Edwards-Prasad, J., Prasad, and N., K. (2001). Use of short-lived green fluorescent protein for the detection of proteasome inhibition. *Biotechniques*, 30(3):656–60.

Arribas, J., Castano, and G., J. (1990). Kinetic studies of the differential effect of detergents on the peptidase activities of the multicatalytic proteinase from rat liver. *J Biol Chem*, 265(23):13969–73.

Baba, T., Minamikawa, H., Hato, M., and Handa, T. (2001). Hydration and molecular motions in synthetic phytanyl-chained glycolipid vesicle membranes. *Biophys J*, 81(6):3377–86.

Baumeister, W., Cejka, Z., Kania, M., and Seemuller, E. (1997). The proteasome: a macromolecular assembly designed to confine proteolysis to a nanocompartment. *Biol Chem*, 378(3-4):121–30.

Baumeister, W. and Lupas, A. (1997). The proteasome. *Curr Opin Struct Biol*, 7(2):273–8.

Baumeister, W., Walz, J., Zuhl, F., and Seemuller, E. (1998). The proteasome: paradigm of a self-compartmentalizing protease. *Cell*, 92(3):367–80.

Beitz, E. (2000). TeXshade: shading and labeling of multiple sequence alignments using LaTeX 2ϵ. *Bioinformatics*, 16:135–9.

Benaroudj, N., Goldberg, and L., A. (2000). PAN, the proteasome-activating nucleotidase from archaebacteria, is a protein-unfolding molecular chaperone. *Nat Cell Biol*, 2(11):833–839.

Bennett, C., M., Bishop, F., J., Leng, Y., Chock, B., P., Chase, N., T., Mouradian, and M., M. (1999). Degradation of alpha-synuclein by proteasome. *J Biol Chem*, 274(48):33855–8.

Berman, H. M., Wesbrook, J., Feng, Z., Gilliland, G., Bhat, T. N., Weissig, H., Shindyalov, I. N., and Bourne, P. E. (2000). The Protein Data Bank. *Nucleic Acids Res*, 28:235–42.

Bogyo, M., McMaster, S., J., Gaczynska, M., Tortorella, D., Goldberg, L., A., and Ploegh, H. (1997). Covalent modification of the active site threonine of proteasomal beta subunits and the *Escherichia coli* homolog HslV by a new class of inhibitors. *Proc Natl Acad Sci U S A*, 94(13):6629–34.

Bradford and M., M. (1976). A rapid and sensitive method for the quantitation of microgram quantities of protein utilizing the principle of protein-dye binding. *Anal Biochem*, 72:248–54.

Brandstetter, H., Kim, S., J., Groll, M., Huber, and R. (2001). Crystal structure of the tricorn protease reveals a protein disassembly line. *Nature*, 414(6862):466–70.

Brannigan, A., J., Dodson, G., Duggleby, J., H., Moody, C., P., Smith, L., J., Tomchick, R., D., Murzin, and G., A. (1995). A protein catalytic framework with an N-terminal nucleophile is capable of self-activation. *Nature*, 378(6555):416–9.

Burgner, W., J., Ray, and J., W. (1984a). The lactate dehydrogenase catalyzed pyruvate adduct reaction: simultaneous general acid-base catalysis involving an enzyme and an external catalyst. *Biochemistry*, 23(16):3626–35.

Burgner, W., J., Ray, and J., W. (1984b). On the origin of the lactate dehydrogenase induced rate effect. *Biochemistry*, 23(16):3636–48.

Cardozo, C., Vinitsky, A., Michaud, C., and Orlowski, M. (1994). Evidence that the nature of amino acid residues in the P3 position directs substrates to distinct catalytic sites of the pituitary multicatalytic proteinase complex (proteasome). *Biochemistry*, 33(21):6483–9.

Chan, S., H., Dill, and A., K. (1996). A simple model of chaperonin-mediated protein folding. *Proteins*, 24(3):345–51.

Chatterjee, S., Dunn, D., Mallya, S., Ator, and A., M. (1999). P'-extended alpha-ketoamide inhibitors of proteasome. *Bioorg Med Chem Lett*, 9(17):2603–6.

Chu-Ping, M., Vu, H., J., Proske, J., R., Slaughter, A., C., DeMartino, and N., G. (1994). Identification, purification, and characterization of a high molecular weight, ATP-dependent activator (PA700) of the 20S proteasome. *J Biol Chem*, 269(5):3539–47.

Cormack, T., M., Baumeister, W., Grenier, L., Moomaw, C., Plamondon, L., Pramanik, B., Slaughter, C., Soucy, F., Stein, R., Zuhl, F., and Dick, L. (1997). Active site-directed inhibitors of *Rhodococcus* 20 S proteasome. Kinetics and mechanism. *J Biol Chem*, 272(42):26103–9.

Cornish-Bowden, A. (1995). *Fundamentals of Enzyme Kinetics*. Portland Press, London, U.K.

Coux, O., Tanaka, K., Goldberg, and L., A. (1996). Structure and functions of the 20S and 26S proteasomes. *Annu Rev Biochem*, 65:801–47.

Dahlmann, B. (1985). High-M_r cysteine proteinases from rat skeletal-muscle. *Biochem Soc Trans*, 13(6):1021–3.

Dahlmann, B., Becher, B., Sobek, A., Ehlers, C., Kopp, F., and Kuehn, L. (1993). In vitro activation of the 20S proteasome. *Enzyme Protein*, 47(4-6):274–84.

Dahlmann, B., Kopp, F., Kuehn, L., Hegerl, R., Pfeifer, G., and Baumeister, W. (1991a). The multicatalytic proteinase (prosome, proteasome): comparison of the eukaryotic and archaebacterial enzyme. *Biomed Biochim Acta*, 50(4-6):465–9.

Dahlmann, B., Kopp, F., Kuehn, L., Hegerl, R., Pfeifer, G., and Baumeister, W. (1991b). The multicatalytic proteinase (prosome, proteasome): comparison of the eukaryotic and archaebacterial enzyme. *Biomed Biochim Acta*, 50(4-6):465–9.

Dahlmann, B., Kopp, F., Kuehn, L., Niedel, B., Pfeifer, G., Hegerl, R., and Baumeister, W. (1989). The multicatalytic proteinase (prosome) is ubiquitous from eukaryotes to archaebacteria. *FEBS Lett*, 251(1-2):125–31.

Dahlmann, B., Kuehn, L., Grziwa, A., Zwickl, P., and Baumeister, W. (1992). Biochemical properties of the proteasome from thermoplasma acidophilum. *Eur J Biochem*, 208(3):789–97.

Darland, G., Brock, T. D., Samsonoff, W., and Conti, S. F. (1970). A thermophilic acidophilic mycoplasm isolated from a coal refuse pile. *Science*, 170:1416–18.

Dick, R., L., Aldrich, C., Jameson, C., S., Moomaw, R., C., Pramanik, C., B., Doyle, K., C., DeMartino, N., G., Bevan, J., M., Forman, M., J., Slaughter, and A., C. (1994). Proteolytic processing of ovalbumin and beta-galactosidase by the proteasome to a yield antigenic peptides. *J Immunol*, 152(8):3884–94.

Dick, R., L., Cruikshank, A., A., Destree, T., A., Grenier, L., McCormack, A., T., Melandri, D., F., Nunes, L., S., Palombella, J., V., Parent, A., L., Plamondon, L., Stein, and L., R. (1997). Mechanistic studies on the inactivation of the proteasome by lactacystin in cultured cells. *J Biol Chem*, 272(1):182–8.

Dick, R., L., Cruikshank, A., A., Grenier, L., Melandri, D., F., Nunes, L., S., Stein, and L., R. (1996). Mechanistic studies on the inactivation of the proteasome by lactacystin: a central role for clasto-lactacystin beta-lactone. *J Biol Chem*, 271(13):7273–6.

Ditzel, L., Huber, R., Mann, K., Heinemeyer, W., Wolf, H., D., and Groll, M. (1998). Conformational constraints for protein self-cleavage in the proteasome. *J Mol Biol*, 279(5):1187–91.

Djaballah, H., Rivett, and J., A. (1992). Peptidylglutamyl-peptide hydrolase activity of the multicatalytic proteinase complex: evidence for a new high-affinity site, analysis of cooperative kinetics, and the effect of manganese ions. *Biochemistry*, 31(16):4133–41.

Djaballah, H., Rowe, J., A., Harding, E., S., Rivett, and J., A. (1993). The multicatalytic proteinase complex (proteasome): structure and conformational changes associated with changes in proteolytic activity. *Biochem J*, 292(Pt 3):857–62.

Dolenc, I., Seemuller, E., and Baumeister, W. (1998). Decelerated degradation of short peptides by the 20s proteasome. *FEBS Lett*, 434(3):357–61.

Dufour, E., Storer, C., A., and Menard, R. (1995). Peptide aldehydes and nitriles as transition state analog inhibitors of cysteine proteases. *Biochemistry*, 34(28):9136–43.

Elofsson, M., Splittgerber, U., Myung, J., Mohan, R., Crews, and M., C. (1999). Towards subunit-specific proteasome inhibitors: synthesis and evaluation of peptide α',β'-epoxyketones. *Chem Biol*, 6(11):811–22.

Escherich, A., Ditzel, L., Musiol, J., H., Groll, M., Huber, R., and Moroder, L. (1997). Synthesis, kinetic characterization and X-ray analysis of peptide aldehydes as inhibitors of the 20S proteasomes from *Thermoplasma acidophilum* and *Saccharomyces cerevisiae*. *Biol Chem*, 378(8):893–8.

Felsenstein, J. (1989). PHYLIP – Phylogeny Inference Package (Version 3.2). *Cladistics*, 5:164–6.

Freer, T., S., J., K., Robertus, J.D., Wright, H.T., Xuong, and H., N. (1970). Chymotrypsinogen: 2.5-angstrom crystal structure, comparison with alpha-chymotrypsin, and implications for zymogen activation. *Biochemistry*, 9:1997–2009.

Gaczynska, M., Goldberg, L., A., Tanaka, K., Hendil, B., K., Rock, and L., K. (1996). Proteasome subunits X and Y alter peptidase activities in opposite ways to the interferon-gamma-induced subunits LMP2 and LMP7. *J Biol Chem*, 271(29):17275–80.

Gaczynska, M., Rock, L., K., Goldberg, and L., A. (1993). Role of proteasomes in antigen presentation. *Enzyme Protein*, 47(4-6):354–69.

Gao, Y., Lecker, S., Post, J., M., Hietaranta, J., A., Li, J., Volk, R., Li, M., Sato, K., Saluja, K., A., Steer, L., M., Goldberg, L., A., and Simons, M. (2000). Inhibition of ubiquitin-proteasome pathway-mediated IκBα degradation by a naturally occurring antibacterial peptide. *J Clin Invest*, 106(3):439–48.

Glickman and H., M. (2000). Getting in and out of the proteasome. *Semin Cell Dev Biol*, 11(3):149–58.

Groettrup, M. and Schmidtke, G. (1999). Intracellular processing of viral and tumor antigens by proteasomes. *Schweiz Med Wochenschr*, 129(44):1660–5.

Groll, M., Bajorek, M., Kohler, A., Moroder, L., Rubin, M., D., Huber, R., Glickman, H., M., and Finley, D. (2000). A gated channel into the proteasome core particle. *Nat Struct Biol*, 7(11):1062–7.

Groll, M., Ditzel, L., Lowe, J., Stock, D., Bochtler, M., Bartunik, D., H., and Huber, R. (1997). Structure of 20S proteasome from yeast at 2.4Å resolution. *Nature*, 386(6624):463–71.

Groll, M., Heinemeyer, W., Jager, S., Ullrich, T., Bochtler, M., Wolf, H., D., and Huber, R. (1999). The catalytic sites of 20S proteasomes and their role in subunit maturation: a mutational and crystallographic study. *Proc Natl Acad Sci U S A*, 96(20):10976–83.

Groll, M., Koguchi, Y., Huber, R., and Kohno, J. (2001). Crystal structure of the 20 s proteasome:tmc-95a complex: a non-covalent proteasome inhibitor. *J Mol Biol*, 311(3):543–8.

Grziwa, A., Baumeister, W., Dahlmann, B., and Kopp, F. (1991). Localization of subunits in proteasomes from *Thermoplasma acidophilum* by immunoelectron microscopy. *FEBS Lett*, 290(1-2):186–90.

Grziwa, A., Maack, S., Puhler, G., Wiegand, G., Baumeister, W., and Jaenicke, R. (1994). Dissociation and reconstitution of the *Thermoplasma* proteasome. *Eur J Biochem*, 223(3):1061–7.

Guex, N., Peitsch, and C., M. (1997). SWISS-MODEL and the Swiss-PdbViewer: An environment for comparative protein modeling. *Electrophoresis*, 18:2714–23.

Gutsche, I., Mihalache, O., and Baumeister, W. (2000). ATPase cycle of an archaeal chaperonin. *J Mol Biol*, 300(1):187–96.

Hegerl, R., Pfeifer, G., Puhler, G., Dahlmann, B., and Baumeister, W. (1991). The three-dimensional structure of proteasomes from *Thermoplasma acidophilum* as determined by electron microscopy using random conical tilting. *FEBS Lett*, 283(1):117–21.

Higgins, D. G., Bleasby, A. J., and Fuchs, R. (1992). CLUSTAL V: improved software for multiple sequence alignment. *Computer Applications in the Biosciences*, 8(2):189–91.

Hochstrasser, M., Johnson, R., P., Arendt, S., C., Amerik, A., Swaminathan, S., Swanson, R., Li, J., S., Laney, J., Pals-Rylaarsdam, R., Nowak, J., Connerly, and L., P. (1999). The *Saccharomyces cerevisiae* ubiquitin-proteasome system. *Philos Trans R Soc Lond B Biol Sci*, 354(1389):1513–22.

Ii, K., Ito, H., Tanaka, K., and Hirano, A. (1997). Immunocytochemical colocalization of the proteasome in ubiquitinated structures in neurodegenerative diseases and the elderly. *J Neuropathol Exp Neurol*, 56(2):125–31.

Jap, B., Puhler, G., Lucke, H., Typke, D., Lowe, J., Stock, D., Huber, R., and Baumeister, W. (1993). Preliminary X-ray crystallographic study of the proteasome from *Thermoplasma acidophilum*. *J Mol Biol*, 234(3):881–4.

Johnston, A., J., Ward, L., C., Kopito, and R., R. (1998). Aggresomes: a cellular response to misfolded proteins. *J Cell Biol*, 143(7):1883–98.

Kanayama, H., Tanaka, K., Aki, M., Kagawa, S., Miyaji, H., Satoh, M., Okada, F., Sato, S., Shimbara, N., and Ichihara, A. (1991). Changes in expressions of proteasome and ubiquitin genes in human renal cancer cells. *Cancer Res*, 51(24):6677–85.

Katchalsky, A. and Curran, P. (1946). *Non-Equilibrium Thermodynamics in Biophisics*. Harvard University Press, Cambridge, Massachssets.

Kim, B., K., Myung, J., Sin, N., Crews, and M., C. (1999). Proteasome inhibition by the natural products epoxomicin and dihydroeponemycin: insights into specificity and potency. *Bioorg Med Chem Lett*, 9(23):3335–40.

Kinoshita, M., Hamakubo, T., Fukui, I., Murachi, T., and Toyohara, H. (1990). Significant amount of multicatalytic proteinase identified on membrane from human erythrocyte. *J Biochem (Tokyo)*, 107(3):440–4.

Kisselev, F., A., Akopian, N., T., Castillo, V., Goldberg, and L., A. (1999a). Proteasome active sites allosterically regulate each other, suggesting a cyclical bite-chew mechanism for protein breakdown. *Mol Cell*, 4(3):395–402.

Kisselev, F., A., Akopian, N., T., Goldberg, and L., A. (1998a). Range of sizes of peptide products generated during degradation of different proteins by archaeal proteasomes. *J Biol Chem*, 273(4):1982–9.

Kisselev, F., A., Akopian, N., T., Goldberg, and L., A. (1998b). Range of sizes of peptide products generated during degradation of different proteins by archaeal proteasomes. *J Biol Chem*, 273(4):1982–9.

Kisselev, F., A., Akopian, N., T., Woo, M., K., Goldberg, and L., A. (1999b). The sizes of peptides generated from protein by mammalian 26 and 20 S proteasomes. Implications for understanding the degradative mechanism and antigen presentation. *J Biol Chem*, 274(6):3363–71.

Kopito, R., R., and Sitia, R. (2000). Aggresomes and Russell bodies. Symptoms of cellular indigestion? *EMBO rep*, 1(3):225–31.

Kruger, E., Kloetzel, P., and Enenkel, C. (2001). 20S proteasome biogenesis. *Biochimie*, 83(3-4):289–93.

Kuckelkorn, U., Frentzel, S., Kraft, R., Kostka, S., Groettrup, M., Kloetzel, and M., P. (1995). Incorporation of major histocompatibility complex–encoded subunits LMP2 and LMP7 changes the quality of the 20S proteasome polypeptide processing products independent of interferon-gamma. *Eur J Immunol*, 25(9):2605–11.

Kumamoto, T., Fujimoto, S., Ito, T., Horinouchi, H., Ueyama, H., and Tsuda, T. (2000). Proteasome expression in the skeletal muscles of patients with muscular dystrophy. *Acta Neuropathol (Berl)*, 100(6):595–602.

Kuramochi, H., Nakata, H., and Ishii, S. (1979). Mechanism of association of a specific aldehyde inhibitor, leupeptin, with bovine trypsin. *J Biochem (Tokyo)*, 86(5):1403–10.

Langworthy and A., T. (1977). Long-chain diglycerol tetraethers from *Thermoplasma acidophilum*. *Biochim Biophys Acta*, 487(1):37–50.

Langworthy, A., T., Smith, F., P., Mayberry, and R., W. (1972). Lipids of *Thermoplasma acidophilum*. *J Bacteriol*, 112(3):1193–200.

Lee, H., D., Goldberg, and L., A. (1998). Proteasome inhibitors: valuable new tools for cell biologists. *Trends Cell Biol*, 8(10):397–403.

Li, C., X., Gu, Z., M., Etlinger, and D., J. (1991). Isolation and characterization of a novel endogenous inhibitor of the proteasome. *Biochemistry*, 30(40):9709–15.

Loidl, G., Groll, M., Musiol, J., H., Ditzel, L., Huber, R., and Moroder, L. (1999). Bifunctional inhibitors of the trypsin-like activity of eukaryotic proteasomes. *Chem Biol*, 6(4):197–204.

Lowe, J., Stock, D., Jap, B., Zwickl, P., Baumeister, W., and Huber, R. (1995). Crystal structure of the 20S proteasome from the archaeon *T. acidophilum* at 3.4Å resolution. *Science*, 268(5210):533–9.

Lupas, A., Zwickl, P., Wenzel, T., Seemuller, E., and Baumeister, W. (1995). Structure and function of the 20S proteasome and of its regulatory complexes. *Cold Spring Harb Symp Quant Biol*, 60:515–24.

Magae, J., Illenye, S., Tejima, T., Chang, C., Y., Mitsui, Y., Tanaka, K., Omura, S., Heintz, and H., N. (1997). Transcriptional squelching by ectopic expression of E2F-1 and p53 is alleviated by proteasome inhibitors MG-132 and lactacystin. *Oncogene*, 15(7):759–69.

Matthews, W., Driscoll, J., Tanaka, k., Ichihara, A., Goldberg, and L., A. (1989). Involvement of the proteasome in various degradative processes in mammalian cells. *Proc Natl Acad Sci U S A*, 86(8):2597–601.

Mayr, J., Seemuller, E., Muller, A., S., Engel, A., and Baumeister, W. (1998). Late events in the assembly of 20S proteasomes. *J Struct Biol*, 124(2-3):179–88.

McCormack, A., T., Cruikshank, A., A., Grenier, L., Melandri, D., F., Nunes, L., S., Plamondon, L., Stein, L., R., Dick, and R., L. (1998). Kinetic studies of the branched chain amino acid preferring peptidase activity of the 20S proteasome: development of a continuous assay and inhibition by tripeptide aldehydes and clasto-lactacystin beta-lactone. *Biochemistry*, 37(21):7792–800.

McNaught, K.S., W., O. C., B., H., Isacson, O, Jenner, and P (2001). Failure of the ubiquitin-proteasome system in Parkinson's disease. *Nat Rev Neurosci*, 2:589–94.

Michalek, T., M., Grant, P., E., Gramm, C., Goldberg, L., A., Rock, and L., K. (1993). A role for the ubiquitin-dependent proteolytic pathway in MHC class I- restricted antigen presentation. *Nature*, 363(6429):552–4.

Miller, W., D., Dill, and A., K. (1997). Ligand binding to proteins: the binding landscape model. *Protein Sci*, 6(10):2166–79.

Mitch, E., W., Goldberg, and L., A. (1996). Mechanisms of muscle wasting. The role of the ubiquitin-proteasome pathway. *N Engl J Med*, 335(25):1897–905.

Miyake, S., Sellers, R., W., Safran, M., Li, X., Zhao, W., Grossman, R., S., Gan, J., DeCaprio, A., J., Adams, D., P., Kaelin, and G., W. (2000). Cells degrade a novel inhibitor of differentiation with E1A-like properties upon exiting the cell cycle. *Mol Cell Biol*, 20(23):8889–902.

Moretti, F., Nanni, S., Farsetti, A., Narducci, M., Crescenzi, M., Giuliacci, S., Sacchi, A., and Pontecorvi, A. (2000). Effects of exogenous p53 transduction in thyroid tumor cells with different p53 status. *J Clin Endocrinol Metab*, 85(1):302–8.

Morrison, F., J., Walsh, and T., C. (1988). The behavior and significance of slow-binding enzyme inhibitors. *Adv Enzymol Relat Areas Mol Biol*, 61:201–301.

Murray, Z., R., and Norbury, C. (2000). Proteasome inhibitors as anti-cancer agents. *Anticancer Drugs*, 11(6):407–17.

Muszkat, A., K., Weinstein, S., Khait, I., and Vered, M. (1983). Photo-CIDNP study of interactions of serine proteinases with their protein inhibitors. *Biopolymers*, 22(1):387–90.

Myung, J., Kim, B., K., Crews, and M., C. (2001a). The ubiquitin-proteasome pathway and proteasome inhibitors. *Med Res Rev*, 21(4):245–73.

Myung, J., Kim, B., K., Lindsten, K., Dantuma, P., N., Crews, and M., C. (2001b). Lack of proteasome active site allostery as revealed by subunit-specific inhibitors. *Mol Cell*, 7(2):411–20.

Navon, A. and Goldberg, A. L. (2001). Proteins are unfolded on the surface of the ATPase ring before transport into the proteasome. *Molecular Cell*, 8(6):1339–49.

Niedermann, G., Geier, E., Lucchiari-Hartz, M., Hitziger, N., Ramsperger, A., and Eichmann, K. (1999). The specificity of proteasomes: impact on MHC class I processing and presentation of antigens. *Immunol Rev*, 172:29–48.

Nussbaum, K., A., Dick, P., T., Keilholz, W., Schirle, M., Stevanovic, S., Dietz, K., Heinemeyer, W., Groll, M., Wolf, H., D., Huber, R., Rammensee,

G., H., and Schild, H. (1998). Cleavage motifs of the yeast 20S proteasome beta subunits deduced from digests of enolase 1. *Proc Natl Acad Sci U S A*, 95(21):12504–9.

Orlowski, M. (1990). The multicatalytic proteinase complex, a major extralysosomal proteolytic system. *Biochemistry*, 29(45):10289–97.

Orlowski, M. (1993). The multicatalytic proteinase complex (proteasome) and intracellular protein degradation: diverse functions of an intracellular particle. *J Lab Clin Med*, 121(2):187–9.

Orlowski, M. and Michaud, C. (1989). Pituitary multicatalytic proteinase complex. Specificity of components and aspects of proteolytic activity. *Biochemistry*, 28(24):9270–8.

Orlowski, M. and Wilk, S. (2000). Catalytic activities of the 20 S proteasome, a multicatalytic proteinase complex. *Arch Biochem Biophys*, 383(1):1–16.

Penefsky and S., H. (1977). Reversible binding of Pi by beef heart mitochondrial adenosine triphosphatase. *J Biol Chem*, 252(9):2891–9.

Pereira, E., M., Nguyen, T., Wagner, J., B., Margolis, W., J., Yu, B., and Wilk, S. (1992). 3,4-Dichloroisocoumarin-induced activation of the degradation of beta-casein by the bovine pituitary multicatalytic proteinase complex. *J Biol Chem*, 267(11):7949–55.

Piccinini, M., Tazartes, O., Mostert, M., Musso, A., DeMarchi, M., Rinaudo, and T., M. (2000). Structural and functional characterization of 20S and 26S proteasomes from bovine brain. *Brain Res Mol Brain Res*, 76(1):103–14.

Puhler, G., Weinkauf, S., Bachmann, L., Muller, S., Engel, A., Hegerl, R., and Baumeister, W. (1992). Subunit stoichiometry and three-dimensional arrangement in proteasomes from *Thermoplasma acidophilum*. *Embo J*, 11(4):1607–16.

Rivett, J., A., Gardner, and C., R. (2000). Proteasome inhibitors: from in vitro uses to clinical trials. *J Pept Sci*, 6(9):478–88.

Roche, D., E., Sauer, and T., R. (1999). SsrA-mediated peptide tagging caused by rare codons and tRNA scarcity. *Embo J*, 18(16):4579–89.

Rock, L., K., Gramm, C., Rothstein, L., Clark, K., Stein, R., Dick, L., Hwang, D., Goldberg, and L., A. (1994). Inhibitors of the proteasome block the degradation of most cell proteins and the generation of peptides presented on MHC class I molecules. *Cell*, 78(5):761–71.

Rose, A., I., Warms, V., J., Kuo, and J., D. (1992). Proton transfer in catalysis by fumarase. *Biochemistry*, 31(41):9993–9.

Rubin, M., D., Nocker, S., v., Glickman, M., Coux, O., Wefes, I., Sadis, S., Fu, H., Goldberg, A., Vierstra, R., and Finley, D. (1997). ATPase and ubiquitin-binding proteins of the yeast proteasome. *Mol Biol Rep*, 24(1-2):17–26.

Ruepp, A., Graml, W., Santos-Martinez, L., M., Koretke, K., K., Volker, C., Mewes, W., H., Frishman, D., Stocker, S., Lupas, N., A., and Baumeister, W. (2000). The genome sequence of the thermoacidophilic scavenger *Thermoplasma acidophilum*. *Nature*, 407(6803):508–13.

Sambrook, J. and Russell, D. W. (2001). *Molecular Cloning: A laboratory manual, 3rd ed.* Cold Spring Harbor Laboratory Press, Cold Spring Harbor, New York.

Schmidtke, G., Holzhutter, G., H., Bogyo, M., Kairies, N., Groll, M., Giuli, R., d., Emch, S., and Groettrup, M. (1999). How an inhibitor of the HIV-I protease modulates proteasome activity. *J Biol Chem*, 274(50):35734–40.

Schubert, U., Anton, C., L., Gibbs, J., Norbury, C., C., Yewdell, W., J.,

Bennink, and R., J. (2000). Rapid degradation of a large fraction of newly synthesized proteins by proteasomes. *Nature*, 404(6779):770–4.

Schwartz, L., A., and Ciechanover, A. (1999). The ubiquitin-proteasome pathway and pathogenesis of human diseases. *Annu Rev Med*, 50(9):57–74.

Schwarz, K., Giuli, R., d., Schmidtke, G., Kostka, S., den Broek, M., v., Kim, B., K., Crews, M., C., Kraft, R., and Groettrup, M. (2000). The selective proteasome inhibitors lactacystin and epoxomicin can be used to either up- or down-regulate antigen presentation at nontoxic doses. *J Immunol*, 164(12):6147–57.

Seemuller, E., Lupas, A., and Baumeister, W. (1996). Autocatalytic processing of the 20S proteasome. *Nature*, 382(6590):468–71.

Seemuller, E., Lupas, A., Stock, D., Lowe, J., Huber, R., and Baumeister, W. (1995a). Proteasome from *Thermoplasma acidophilum*: a threonine protease. *Science*, 268(5210):579–82.

Seemuller, E., Lupas, A., Zuhl, F., Zwickl, P., and Baumeister, W. (1995b). The proteasome from *Thermoplasma acidophilum* is neither a cysteine nor a serine protease. *FEBS Lett*, 359(2-3):173–8.

Seemuller, E., Lupas, A., Zuhl, F., Zwickl, P., and Baumeister, W. (1995c). The proteasome from *Thermoplasma acidophilum* is neither a cysteine nor a serine protease. *FEBS Lett*, 359(2-3):173–8.

Sherman, Y., M., Goldberg, and L., A. (1996). Involvement of molecular chaperones in intracellular protein breakdown. *Exs*, 77:57–78.

Shibatani, T., Ward, and F., W. (1995). Sodium dodecyl sulfate (SDS) activation of the 20S proteasome in rat liver. *Arch Biochem Biophys*, 321(1):160–6.

Shimada, H., Nemoto, N., Shida, Y., T., O., and Yamagishi, A. (2002). Complete polar lipid composition of thermoplasma acidophilum ho-62 determined by high-performance liquid chromatography with evaporative light-scattering detection. *J Bacteriology*, 184(2):556–63.

Shimbara, N., Ogawa, K., Hidaka, Y., Nakajima, H., Yamasaki, N., Niwa, S., Tanahashi, N., and Tanaka, K. (1998). Contribution of proline residue for efficient production of MHC class I ligands by proteasomes. *J Biol Chem*, 273(36):23062–71.

Smith, J. S. and Scholtz, J. M. (1996). Guanidine hydrochloride unfolding of peptide helices: separation of denaturant and salt effects. *Biochemistry*, 35(22):7292–7.

Stein, L., R., Melandri, F., and Dick, L. (1996). Kinetic characterization of the chymotryptic activity of the 20S proteasome. *Biochemistry*, 35(13):3899–908.

Tamura, N., Lottspeich, F., Baumeister, W., and Tamura, T. (1998). The role of tricorn protease and its aminopeptidase-interacting factors in cellular protein degradation. *Cell*, 95(5):637–48.

Tamura, T., Nagy, I., Lupas, A., Lottspeich, F., Cejka, Z., Schoofs, G., Tanaka, K., Mot, R., D., and Baumeister, W. (1995). The first characterization of a eubacterial proteasome: the 20S complex of *Rhodococcus*. *Curr Biol*, 5(7):766–74.

Tamura, T., Tamura, N., Cejka, Z., Hegerl, R., Lottspeich, F., and Baumeister, W. (1996). Tricorn protease–the core of a modular proteolytic system . *Science*, 274(5291):1385–9.

Tanahashi, N., Kawahara, H., Murakami, Y., and Tanaka, K. (1999). The proteasome-dependent proteolytic system. *Mol Biol Rep*, 26(1-2):3–9.

Tanahashi, N., Tsurumi, C., Tamura, T., and Tanaka, K. (1993). Molecular structure of 20S and 26S proteasomes. *Enzyme Protein*, 47(4-6):241–51.

Tanaka, K. and Ichihara, A. (1988). Involvement of proteasomes (multicatalytic proteinase) in ATP-dependent proteolysis in rat reticulocyte extracts. *FEBS Lett*, 236(1):159–62.

Tanaka, K., Tanahashi, N., and Shimbara, N. (1997). Molecular mechanisms for processing of endogenous antigens. *Tanpakushitsu Kakusan Koso*, 42(14 Suppl):2368–75.

Teicher, A., B., Ara, G., Herbst, R., Palombella, J., V., and Adams, J. (1999). The proteasome inhibitor PS-341 in cancer therapy. *Clin Cancer Res*, 5(9):2638–45.

Thompson, J. D., Higgins, D. G., and Gibson, T. J. (1994). CLUSTAL W: improving the sensitivity of progressive multiple sequence alignment through sequence weighting, position-specific gap penalties and weight matrix choice. *Nucleic Acids Res.*, 22:4673–80.

Tipton, F., K., Dixon, and F., B. (1979). Effects of pH on Enzymes. *Adv Enzymol Relat Areas Mol Biol*, 63:183–234.

Vinitsky, A., Cardozo, C., Sepp-Lorenzino, L., Michaud, C., and Orlowski, M. (1994). Inhibition of the proteolytic activity of the multicatalytic proteinase complex (proteasome) by substrate-related peptidyl aldehydes. *J Biol Chem*, 269(47):29860–6.

Vu, K., P., Sakamoto, and M., K. (2000). Ubiquitin-mediated proteolysis and human disease. *Mol Genet Metab*, 71(1-2):261–6.

Waldmann, T., Lupas, A., Kellermann, J., Peters, J., and Baumeister,

W. (1995). Primary structure of the thermosome from *Thermoplasma acidophilum*. *Biol Chem Hoppe Seyler*, 376(2):119–26.

Weissman, J., Sigler, P., and Haorwich, A. (1995). From the cradle to the grave: ring complexes in the life of a protein. *Science*, 268(5210):523–4.

Wenzel, T. and Baumeister, W. (1993). *Thermoplasma acidophilum* proteasomes degrade partially unfolded and ubiquitin-associated proteins. *FEBS Lett*, 326(1-3):215–8.

Wenzel, T. and Baumeister, W. (1995). Conformational constraints in protein degradation by the 20S proteasome. *Nat Struct Biol*, 2(3):199–204.

Wenzel, T., Eckerskorn, C., Lottspeich, F., and Baumeister, W. (1994). Existence of a molecular ruler in proteasomes suggested by analysis of degradation products. *FEBS Lett*, 349(2):205–9.

Whitby, G., F., Masters, I., E., Kramer, L., Knowlton, R., J., Yao, Y., Wang, C., C., Hill, and P., C. (2000). Structural basis for the activation of 20S proteasomes by 11S regulators. *Nature*, 408(6808):115–20.

Williams, W., J., Morrison, and F., J. (1979). The kinetics of reversible tight-binding inhibition. *Methods Enzymol*, 63:437–67.

Wlodawer, A. (1995). Proteasome: a complex protease with a new fold and a distinct mechanism. *Structure*, 3(5):417–20.

Wolf, S., Lottspeich, F., and Baumeister, W. (1993). Ubiquitin found in the archaebacterium *Thermoplasma acidophilum*. *FEBS Lett*, 326(1-3):42–4.

Yamada, S., Sato, K., Uritani, M., Tokumoto, T., and Ishikawa, K. (1998). Activation of the 20S proteasome of Xenopus oocytes by cardiolipin: blockage

of the activation of trypsin-like activity by the substrate. *Biosci Biotechnol Biochem*, 62(6):1264–6.

Yao, Y., Toth, R., C., Huang, L., Wong, L., M., Dias, P., Burlingame, L., A., Coffino, P., Wang, and C., C. (1999). alpha5 subunit in *Trypanosoma brucei* proteasome can self-assemble to form a cylinder of four stacked heptamer rings. *Biochem J*, 344 Pt 2:349–58.

York, I., Goldberg, A.L., Mo, X.Y., Rock, and K.L. (1999). Proteolysis and class I major histocompatibility complex antigen presentation. *Immunol Rev*, 172:49–66.

Yu, B., Pereira, E., M., and Wilk, S. (1993). Changes in the structure and catalytic activities of the bovine pituitary multicatalytic proteinase complex following dialysis. *J Biol Chem*, 268(3):2029–36.

Yu, E. W. and Koshland, D. E. (2001). Propagating conformational changes over long (and short) distances in proteins. *Proc Natl Acad Sci U S A*, 98(17):9517–20.

Zhou, P., Bogacki, R., McReynolds, L., Howley, and M., P. (2000). Harnessing the ubiquitination machinery to target the degradation of specific cellular proteins. *Mol Cell*, 6(3):751–6.

Zwickl, P., Kleinz, J., and Baumeister, W. (1994). Critical elements in proteasome assembly. *Nat Struct Biol*, 1(11):765–70.